UNIVERSIDAD EUROPEA DE MADRID

ESCUELA DE ARQUITECTURA, INGENIERÍA Y DISEÑO

DEGREE IN AEROSPACE ENGINEERING

FINAL PROJECT REPORT

LIFTING SURFACES PERFORMANCE AND MITIGATION OF VORTEX INDUCED VIBRATIONS (VIV)

Íñigo Azcona Sánchez-Arjona

YEAR 2022-2023

TITLE: Lifting Surface Performance & Mitigation of Vortex Induced Vibrations (VIV)

AUTHOR: Íñigo Azcona Sánchez-Arjona

SUPERVISOR: Dra. Almudena Vega Coso

DEGREE OR COURSE: Degree in Aerospace Engineering and Aircraft

DATE: 08/06/2023

ABSTRACT

In this project, the main idea is to study the advantages and disadvantages of adding a high-lift device to a wing. And, to study the risk of Vortex Induced Vibrations (VIV) formation in both structures. For it we will perform a performance analysis of an airfoil wing and compare it with the performances obtained when adding a high-lift device. Before starting to analyze the impact of adding a high-lift device, we will first analyze the wing by itself, and we will observe the different performance values. So then, we can compare them to the results of the analysis of adding a high-lift device, where we can observe how the high-lift device affects the overall aerodynamics of the set. Making a conclusion on the advantages or disadvantages of adding a high-lift device.

The profile of the wing we will be analyzing is a cambered NACA 4412 profile, while in the high-lift device, we will use a cambered NACA 2412.

To perform this analysis, we will use the ANSYS Fluent software to perform a CFD study. The analysis will be conducted in a turbulence flow condition, so a high Reynolds number fluid will be used.

After performing the CFD analysis of the wing, and the wing+high-lift device, we will perform an aeroelastic analysis of the wing and the high-lift device in 3D, where we will study the risk of Vortex Induced Vibrations (VIV) in both structures. For this we will perform a modal analysis of the structures, a time dependent CFD analysis to observe the generation of Karman vortices related to the Strouhal number; analyzing buffeting risk. After that, we will perform a redesign of the structures to eliminate the risk of Vortex Induced Vibrations(VIV).

Keywords: NACA airfoil
ANSYS Fluent
CFD (Computational Fluid Dynamics)
Reynolds Number
Strouhal Number

RESUMEN

En este proyecto, la idea principal es estudiar las ventajas e inconvenientes de añadir un dispositivo hipersustentador a un ala. Y, estudiar el riesgo de formación de Vibraciones Inducidas por Vórtices en ambas estructuras. Para ello realizaremos un análisis de las prestaciones aerodinámicas de un ala y las compararemos con las prestaciones obtenidas al añadir un dispositivo hipersustentador. Antes de comenzar a analizar el impacto de añadir un dispositivo hipersustentador, primero analizaremos el ala por sí misma, y observaremos los diferentes valores de rendimiento. A continuación, podremos compararlos con los resultados del análisis de la adición de un dispositivo hipersustentador, donde podremos observar cómo afecta el dispositivo hipersustentador a la aerodinámica general del conjunto. Llegando a una conclusión sobre las ventajas o desventajas de añadir un dispositivo hipersustentador.

El perfil del ala que vamos a analizar es un perfil NACA 4412 curvado, mientras que en el dispositivo hipersustentador, utilizaremos un NACA 2412 curvado.

Para realizar este análisis, utilizaremos el software ANSYS Fluent para realizar un estudio CFD. El análisis se realizará en condiciones de flujo turbulento, por lo que se utilizará un fluido con alto número de Reynolds.

Tras realizar el análisis CFD del ala, y de la sección ala+dispositivo hipersustentador, realizaremos un análisis aeroelástico del ala y del dispositivo hipersustentador en 3D, donde estudiaremos el riesgo de Vibración Inducida por Vórtices en ambas estructuras. Para ello realizaremos un análisis modal de las estructuras, un análisis CFD dependiente del tiempo para observar la generación de vórtices de Karman relacionados con el número de Strouhal, analizando el riesgo de bataneo. A continuación, realizaremos un rediseño de las estructuras para eliminar el riesgo de Vibración Inducida por Vórtices.

Palabras clave: Perfil NACA
ANSYS Fluent
CFD (Dinámica de Fluidos Computacional)
Número de Reynolds
Número de Strouhal

ACKNOWLEDGEMENTS

I would like to thank the European University of Madrid for allowing me to study Aerospace Engineering at their institution, and to all the professors who have accompanied me throughout these years and made it possible for this goal to be achieved.

I would also like to thank my tutor Almudena Vega Coso for her help. I would also like to thank my co-workers Gustavo Rodriguez and Jeronimo Fernandez who helped me with some difficult decisions during the project.

And finally, I would like to thank my parents, my sister and my aunt for their support at difficult stages of the project.

Contents

Figures

Tables

Equations

Chapter 1. INTRODUCTION

The objective of the project is to analyze the advantages or disadvantages of adding a high-lift device to a wing. Justifying the implementation of high-lift devices. And analyze risk of Vortex Induced Vibrations (VIV) formation in the wing and in the high-lift device. For it, CFD (steady), CFD (transient) and Modal analysis will be performed.

1.1 Problem Approach or Statement.

For many years, the implementation of high-lift devices on aircrafts has been very common on aerospace industry, to the point where every aircraft nowadays has implemented these high-lift devices. And so, the objective of this project is to study the influence of adding these high-lift devices in terms of performance and so understanding how they work and how they improve the overall performance of the aircraft, justifying the implementation of them. After having performed this analysis, we will focus on a main aeroelastic phenomena, such as the risk of buffeting formation in the wing and in the high-lift device, where we will focus on redesigning for mitigating this phenomenon.

For achieving these objectives, a CFD analysis will be performed for analyzing the implementation of the high-lift device. And for the aeroelastic phenomena, we will carry out the risk formation of VIV on the wing, performing CFD (Transient) and modal analysis.

1.2 Project Objectives.

We can divide this project in the following objectives:

- Build wing & flap geometry.
- Perform CFD (Steady) Analysis.
- Perform CFD (Transient) Analysis.
- Perform Modal Analysis.
- Perform Aeroelastic Analysis.

Chapter 2. High-Lift Devices.

2.1 History of High-Lift Devices.

The first high-lift device was developed by Gustav Lachmann in 1918 and simultaneously by Handley-Page taking a patent in 1919. These first high-lift devices were leading edge high-lift devices, better known as slots or slats. These first high-lift devices were not automatically activated, but instead they were activated by the airflow pressure, when flying at low speeds, the springs opened the slat, and when flying at higher speeds, they were closed due to the dynamic pressure force. And it wasn't until 1930 when they became automatically activated, which could be open or closed based on the demanding of the flight. [28]

High-Lift devices took an important role in World War II, since it let aircrafts to takeoff from shorter runways, letting them to take off from aircraft carriers, and also to takeoff with more weight, in terms of machinery and fuel.

The first high-lift trailing edge devices didn't appear until the 1930s where they appear along with the arrival of faster moder monoplanes.

The first commercial aircraft that implemented the use of high-lift devices was the Vickers Viscount, developed by the Vickers-Armstrong company. Making its first flight in 1948. The Vickers Viscount not only implemented leading edge devices, but also implemented trailing edge high lift devices such as the flaps.

Figure 1. Vickers Viscount [14]

2.2 How High-Lift Devices Work.

Once explained the history of high-lift devices, we will explain how these devices work and their aerodynamic principle. High lift devices are fixed or movable surfaces which are attached to the aircraft's wing, at the trailing edge or at the leading edge of the wing, and their purpose is to increase the overall lift of the aircraft at different stages of the flight. Even though they are used for creating lift, they also increase the overall drag of the aircraft, since more surfaces are placed along the airflow, increasing resistance. This, in terms of performance, is not efficient, but this increase of drag helps the aircraft to reduce the speed of it, and so allowing aircraft to land at shorter runways and perform a wider variety types of missions. These devices are essential for the improvement in takeoff and landing performance, usually for short runways, but also by delaying the stalling angle of the aircraft, allowing them to fly at higher angles of attack which leads to higher lifting force.

The way high lift devices work, is by modifying the wing's geometry, increasing the effective camber and surface of the wing. And, as we can observe at the lift and drag equations $\boxed{L = C_L \, {}^1\!/_2 \, \rho U^2 S; \; D = C_D \, {}^1\!/_2 \, \rho U^2 S}$, the increase of wing surface is directly proportional to the lift created by the wing, and also to the drag created by the wing. [15]

- $\mathbf{C_L}$: lift coefficient, affected by the angle of attack and wing shape.
- $\mathbf{C_D}$: drag coefficient, affected by the angle of attack and wing shape.
- $\boldsymbol{\rho}$: density of air at flight conditions(altitude).
- **U**: airspeed.
- **S**: wing surface.

Different types of high-lift devices exist, which are: flaps, slats, and blown flaps.

2.3 Flaps.

Flaps are high-lift devices placed at the trailing edge of the wing. The flaps when extended increase the chord of the wing, and so it's surface. This increase in the surface will lead to an increase in lift and drag. Allowing the aircraft to fly at lower speeds, meaning that the stall speed of the aircraft will decrease.

There are many different types of flaps, the most common ones are the followings: plain flap, split flap, slotted flap, double-slotted fowler flap, Junkers flap, and Krueger flap. [8]

2.3.1 Plain Flap.

The plain flap is one of the simplest flaps that are in use, these flaps are attached at the trailing edge of the wing, even though these flaps are not the most efficient to use since they are very limited to the amount of lift they can produce. The reason these flaps are not very efficient is that are attached at the trailing edge, so there is any airflow flowing in between the trailing edge of the wing, and the leading edge of the flap, and so there is no way to reenergize the flow employing the flap. And so, as we extend more the plain flaps, the increase of drag is huge, since it leaves a large wake behind, affecting the performance. [9]

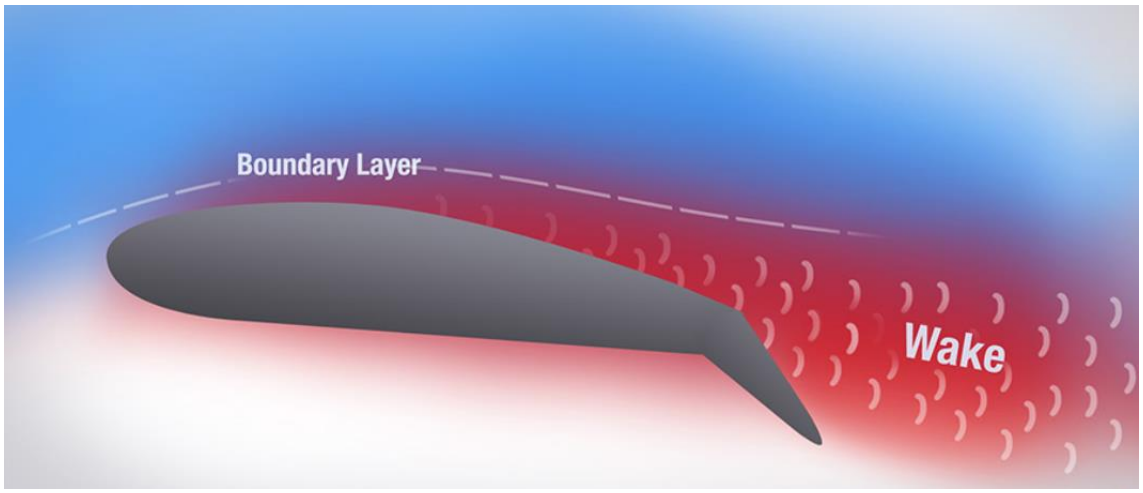

Figure 2. Plain Flap Extended [9]

2.3.2 Split Flap.

The split flap is very similar to the plain flap, but, instead of moving the whole flap, it only moves the lower surface of it, while leaving the upper surface in its original position. The split flap consists of a hinged section located at the trailing edge of the wing. When extended, it deploys downward and backwards, increasing the effective camber of the wing, and so increasing the lift coefficient. This flap is also used when achieving critical angles of attack, since when deployed at high angles of attack it redirects the flow, delaying the stalling. [9]

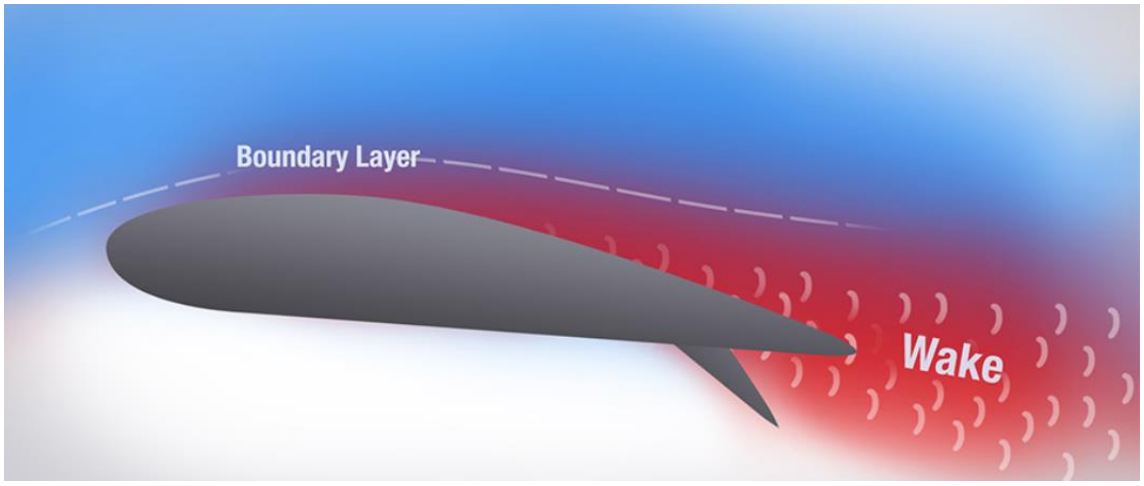

Figure 3. Split Flap Extended.[9]

2.3.3 Slotted Flap.

The slotted flap is an improved version of the plain flap since in this case, we reenergize the boundary layer. The way we reenergize the boundary layer is by adding a slot between the leading edge of the flap, and the trailing edge of the wing. By means of this slot, the high-pressure flow that comes from the lower surface of the wing, channels through the slot, into the upper surface of the flap, this reenergizes the boundary layer, and so being able to increase the overall lift, but not that much the drag as with the previous flaps. It is one of the most widely configurations of flaps used. [9]

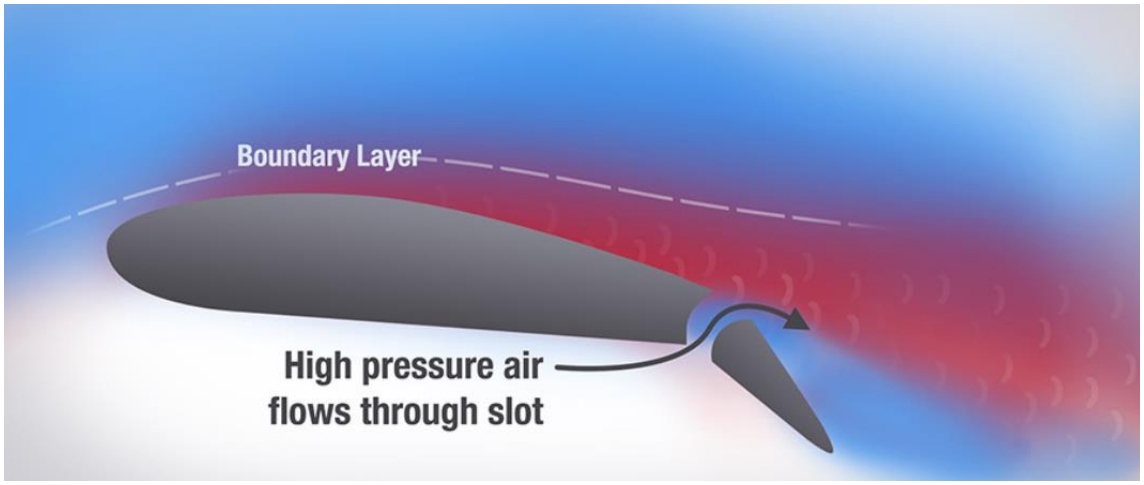

Figure 4. Slotted Flap Extended.[9]

2.3.4 Double-Slotted Fowler Flap.

The double-slotted flap follows the same principle as the one-slotted flap, but in this case, instead of having one slot, it has two slots. The principle of reenergizing the boundary layer is the same as in the one-slotted flap, but the main difference is that the double-slotted flap, allows the pilot to extend to its needs the flaps. Varying from a fully extended configuration to a partially extended configuration based on the actual needs of the flight, such as short landings or short take-offs where a fully deployed configuration will be used since a substantial increase of lift and drag is needed. Or in a landing approach, where a slight increase of drag and lift is needed.[9]

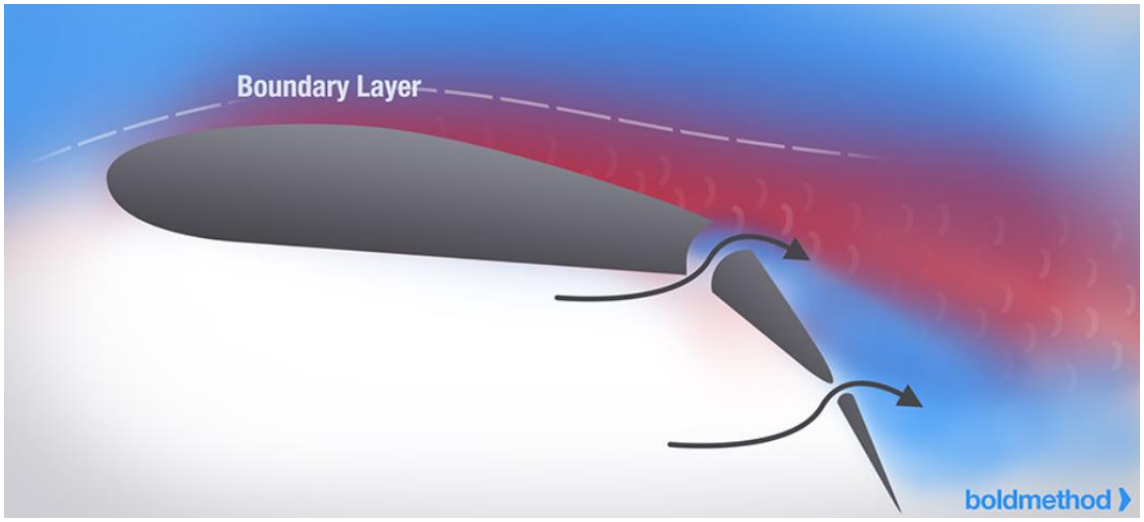

Figure 5. Double-Slotted Flaps Extended.[9]

2.3.5 Junkers Flap.

The Junkers flap is a combination of the slotted flap and the plain flap. In this configuration, the flap is fixed below the trailing edge of the wing, this has some benefits and advantages. In terms of advantages, the flap is constantly creating lift since there is no way to retract it. But in terms of disadvantages, it creates a lot more parasitic and induced drag than other flap configurations, since as they cannot be retracted, they create a huge amount of adverse yaw. This type of flap configuration is very beneficial for low-speed flights, and short takeoff and landing (STOL). [21]

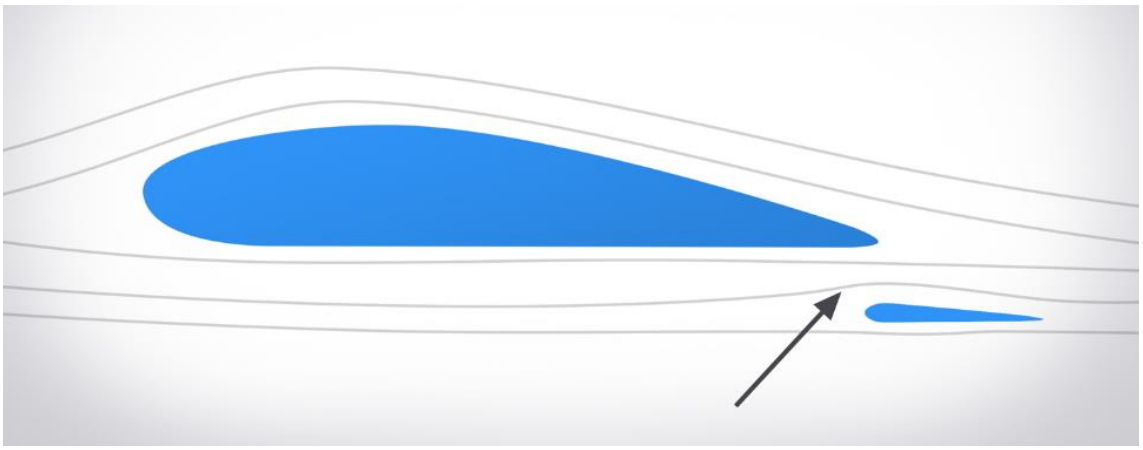

Figure 6. Junkers Flap Retracted.[21]

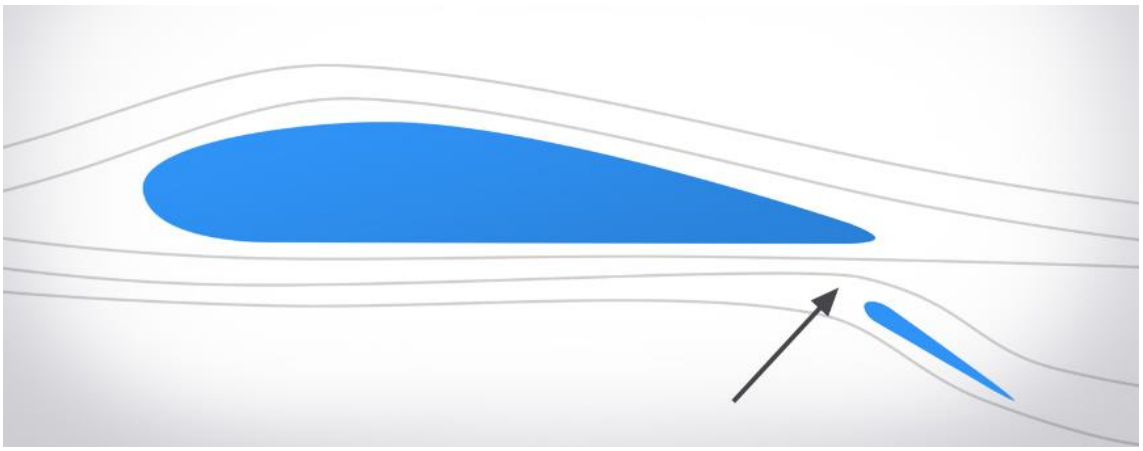

Figure 7. Junkers Flap Extended.[21]

2.3.6 Krueger Flap.

Krueger flaps are high lift devices, but in this case, they are fitted onto the leading edge of the wing, they are very similar to the slats, but instead of moving the upper surface of the wing, a section of the lower surface of the wing is extended in front of the main wing leading edge. The aerodynamic effect that the Krueger flap has on the wing, is the same as in other flap configurations, it creates an increase in the wing camber, and so increasing the coefficient of lift. [29]

Figure 8. Krueger Flap Extended.[29]

2.4 Slats.

Slats are the same as flaps, but instead of being at the trailing edge of the wing, they are implemented at the leading edge of the wing. The slats when extended increase the chord of the wing, and so it's surface. This increase in the surface will lead to an increase in lift and drag. Allowing the aircraft to fly at lower speeds, meaning that the stall speed of the aircraft will decrease. [7]

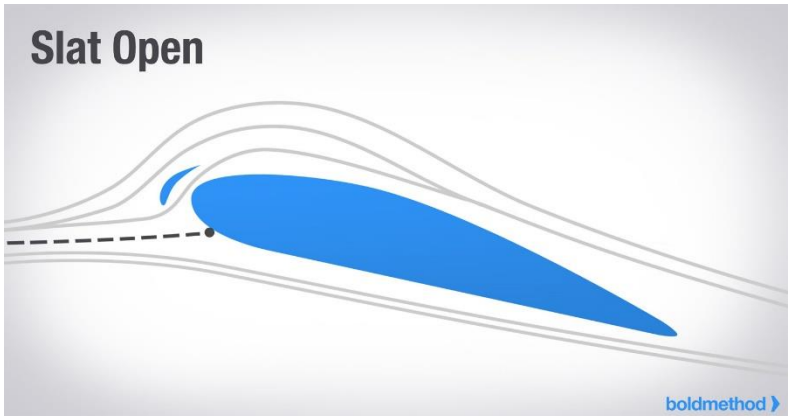

Figure 9. Slat Open [7]

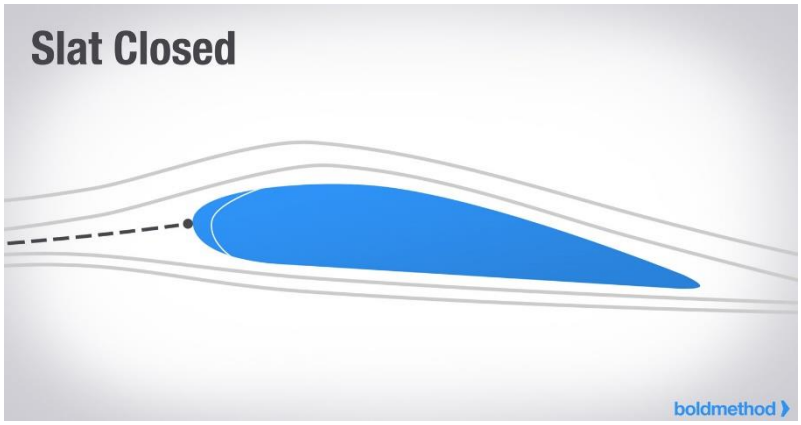

Figure 10. Slat Closed [7]

2.5 Blown Flaps.

Blown flaps are another type of high-lift device, which are not as common as the other ones. The way these blown flaps work is by as it names says, blowing air from the nozzle to the wing and the flap, directing the flow downwards to increase the lift coefficient. The way this is achieved is by using internal ductwork thought the wing to redirect that blown air form the engine into the wing shape. This air blown is compressed air from the engine. By blowing this air the boundary layer re-energizes and so delays boundary layer separation, increasing aerodynamic performance of the aircraft. [26]

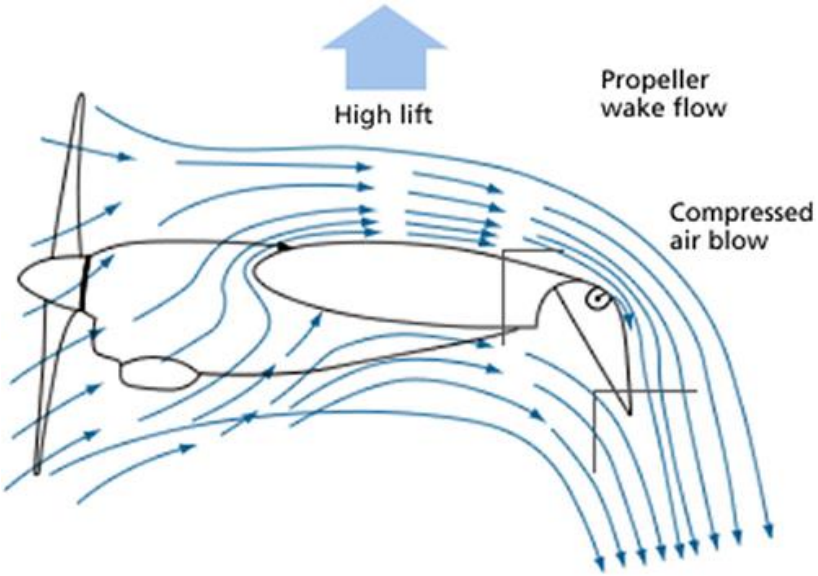

Figure 11. Blown Flap [32]

2.6 High-Lift Device Selection.

Of all the devices I have discussed above, I have decided to choose the Junkers flap for the study. The decision to choose this high-lift device is because it is one of the first devices that were used to increase the performance on wings, and therefore I find it very curious to study the justifications of why it was implemented at that time. It is true that there are more efficient high-lift devices, however, at the level of geometric design they would be very complex, and therefore would divert the main objective of the project, which is not the design of such high-lift device, which would be very complex, consuming project time. In addition, at the aeroelastic analysis level, it would be very complex to analyze its behavior at different extensions of the same. That is why I have decided to analyze the Junkers flap as it allows a better analysis of the conclusions.

Chapter 3. CFD-Based Performance Analysis.

3.1 CFD, Computational Fluid Dynamics.

CFD stands for "Computational Fluid Dynamics", and it is widely used in the aerospace sector. It is a well-known tool that combines fluid dynamics with numeric methods for solving analysis of different scenarios, such as fluid flows, heat flows, mass flows, or more complex iterations such as combustion, chemical reactions, and aeroacoustics.

There are three key aspects needed for performing a good CFD simulation, these are turbulent modeling selection, the mesh generation, and the development of algorithms. [31]

3.2 CFD, how it works?

The Navier Stokes equations together with the continuity equations, are used for describing the behavior of a fluid flow. Once they are solved, they provide the pressure and velocity values for all the fluid flow regime of study. In cases where there are heat transfers or the flow is compressible, we also must add the energy equation, and so obtaining the density and temperature distribution along the fluid regime.

Since the Navier Stokes equations are differential equations with very complex solutions, this is the reason why numeric methods are needed to solve the distribution of pressures and velocities along the flow regime.

For an incompressible flow, which is the case of our analysis, the Navier Stokes equations and the Continuity equation are the following.

- **X-Component Navier-Stokes for Incompressible Flow:**

$$\rho \cdot \left(\frac{\partial u}{\partial t} + u\frac{\partial u}{\partial x} + v\frac{\partial u}{\partial y} + w\frac{\partial u}{\partial z} \right) = -\frac{\partial P}{\partial x} + \rho g_x + \mu \left(\frac{\partial^2 u}{\partial x^2} + \frac{\partial^2 u}{\partial y^2} + \frac{\partial^2 u}{\partial z^2} \right)$$

Equation 1. Navier-Stokes Equation X-Component [13]

- **Y-Component Navier-Stokes for Incompressible Flow:**

$$\rho \cdot \left(\frac{\partial v}{\partial t} + u\frac{\partial v}{\partial x} + v\frac{\partial v}{\partial y} + w\frac{\partial v}{\partial z}\right) = -\frac{\partial P}{\partial y} + \rho g_y + \mu\left(\frac{\partial^2 v}{\partial x^2} + \frac{\partial^2 v}{\partial y^2} + \frac{\partial^2 v}{\partial z^2}\right)$$

Equation 2. Navier-Stokes Equation Y-component [13]

- **Z-Component Navier-Stokes for Incompressible Flow:**

$$\rho \cdot \left(\frac{\partial w}{\partial t} + u\frac{\partial w}{\partial x} + v\frac{\partial w}{\partial y} + w\frac{\partial w}{\partial z}\right) = -\frac{\partial P}{\partial z} + \rho g_z + \mu\left(\frac{\partial^2 w}{\partial x^2} + \frac{\partial^2 w}{\partial y^2} + \frac{\partial^2 w}{\partial z^2}\right)$$

Equation 3. Navier-Stokes Equation Z-component [13]

- **Continuity Equation for Incompressible Flow:**

$$\frac{\partial u}{\partial x} + \frac{\partial v}{\partial y} + \frac{\partial w}{\partial z} = 0$$

Equation 4. Continuity Equation Incompressible Flow [13]

3.3 General Equations.

Before proceeding with the analysis, we must first understand the conservation laws of physics that are considered, and also the equations needed for performing the analysis.

3.3.1 Energy Equation.

The energy equation represents the first law of thermodynamics, relating the increment of energy of a system with the increment of heat and work on it. The first law of thermodynamics establishes that the increment of energy in a system is equal to the sum of increments of heat and work done by the system.

$$dE_t = dQ + dW$$

Figure 12. First Law of Thermodynamics

- dE → total increment of energy during the local change with time.
- dQ → total heat added to the system.
- dW → total work done by the system.

$$\rho\left[\frac{\partial h}{\partial t}+\nabla\cdot(h\overrightarrow{v})\right]=-\frac{\partial p}{\partial t}+\nabla\cdot(k\nabla T)+\Phi$$

Equation 5. Energy Equation [13]

3.3.2 Conservation of Momentum.

The conservation of momentum formula is based on the well-known Newton's second law, $F = m \cdot a$, which tells that any particle that is accelerated, then a force is acting on it. In terms of momentum, this formula tells that the rate of change of a particle's momentum $\boldsymbol{p}$ is related to the force acting on the particle, $F = {}^{\partial p}/_{\partial t}$. In the case where there is no force acting on the particle ${}^{\partial p}/_{\partial t} = 0$, then the momentum $\boldsymbol{p}$ must be constant, or conserved.

$$\rho\left(\frac{\partial v_x}{\partial t}+v_x\frac{\partial v_x}{\partial x}+v_y\frac{\partial v_x}{\partial y}+v_z\frac{\partial v_x}{\partial z}\right)=-\frac{\partial p}{\partial x}=\mu\left[\frac{\partial^2 v_x}{\partial x^2}+\frac{\partial^2 v_x}{\partial y^2}+\frac{\partial^2 v_x}{\partial z^2}\right]+\rho g$$

Equation 6. Conservation of Momentum Equation

The following equation establish that in an isolated region, the total momentum of the two particles after the collision must be equal to the momentum of the two particles after the collision.

3.3.3 Conservation of Mass.

The mass conservation equation states that the mass of any closed system must remain constant over time. Since the flow is incompressible, then the density cannot change over time, and so keeping the mass of the system always constant. The mass conservation equation taking the flow incompressible is the following.

$$\frac{\partial p}{\partial t}+\frac{\partial}{\partial x}(\rho v_x)+\frac{\partial}{\partial y}(\rho v_y)+\frac{\partial}{\partial z}(\rho v_z)=0$$

Equation 7. Conservation of Mass Equation

3.3.4 Reynolds Equation.

The Reynolds equation is essential for this analysis since it allows to predict the type of flow it will be. By taking into account the air velocity, air density, the length of the wing chord, and the dynamic viscosity of the air. Reynolds number is a dimensionless number.

$$Re = \frac{inertial\ forces}{viscous\ forces} = \frac{\rho v L}{\mu}$$

Equation 8. Reynolds Number Equation

There are three different stages of the flow depending on the value of the Reynolds number. This criterion only applies for external flow.

- **Laminar Flow→** $Re < 5 \cdot 10^5$. Laminar flow occurs when the fluid flows in infinitesimal parallel layers with no disturbance between them. In laminar flows, there are no eddies, currents or swirls flowing normal to the flow.

- **Transitional Flow→** $5 \cdot 10^5 < Re < 3 \cdot 10^6$. Transitional flow is a flow which has both laminar and turbulent characteristics. It is the intermediate step between going from a purely laminar flow to a purely turbulent flow.

- **Turbulent Flow→** $Re > 3 \cdot 10^6$. Turbulent flow is characterized by the chaotic motion of fluid particles. It is more predominant to occur at higher velocities and lower viscosity.

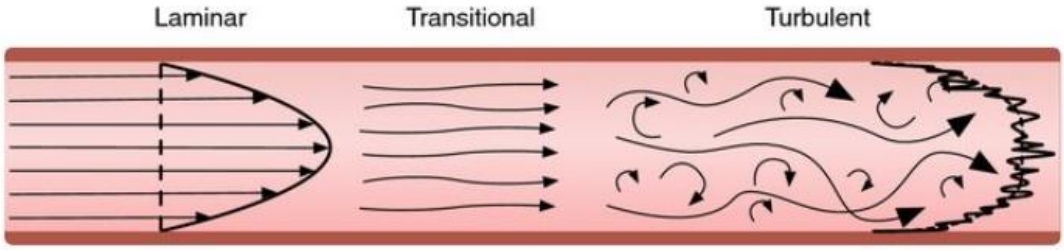

Figure 13. Laminar Flow vs Transitional Flow vs Turbulent Flow [13]

3.4 Turbulence Models.

Turbulence models are used in Computational Fluid Dynamics for performing an analysis of turbulent flows. The method for choosing the appropriate turbulent model follows the following scheme:

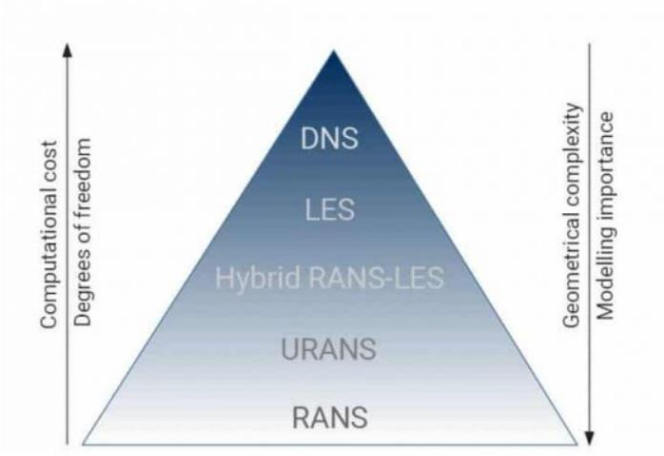

Figure 14. Turbulence Models in CFD from RANS to DNS [23]

The way this scheme works, is, as we increase the computational cost of CFD, and the degrees of freedom, we move from a RANS model to a DNS model. And, as we increase the geometrical complexity and the modelling importance, we move from a DNS model to a RANS model. Normally, Hybrid RANS-LES; URANS; and RANS, are widely used for complex industrial problems. While DNS and LES are usually used for simple geometries and academic approaches.

- **RANS Model:** RANS stands for Reynolds Averaged Navier-Stokes (RANS) equations. These equations are pretty much the same as the original equations of the Navier-Stokes, but they contain additional terms called Reynold stress terms, which need to be modeled. RANS modelling is the most widely used model approach in aerospace industrial application. [15]

- **URANS Model:** URANS stands for Unsteady Reynolds Averaged Navier-Stokes equations. This model is used when the equations are averaged over a short time, and so the time derivative remains in the equation and so the variables in the equation represent the average results during the small, averaged time. [12]

- **Hybrid RANS-LES:** many Hybrid RANS-LES methods, have been developed during the last years, based on the Spalart model. This model is based in an unification between the RANS and LES methods. The hybrid RANS-Les model can perform a RANS-type behavior in the surroundings of a solid boundary, while performing a LES-type behavior far away from the boundary. [23]

- **LES Model:** LES stands for Large Eddy Simulations. LES is used in turbulence models for ignoring the smaller scale phenomena in a CFD simulation while focusing on lager length scales. Even though for obtaining accurate results with this model, it must be done with a sufficiently fine meshing and time resolution.[23]

- **DNS Model:** DNS stands for Direct Numerical Simulation. DNS models are used for solving the smallest eddies and time scales of turbulence within a flow. For obtaining accurate results with this model, very fine mesh and extremely small-time steps need to be used. DNS is limited to solving low Reynolds flows.[23]

Out of all the turbulence models there are, I have chosen to study for my analysis the following ones: SST K-omega, Scale Adaptive Simulation (SAS), and Detached Eddy Simulation (DES). Based on the needs and constraints of the analysis.

3.4.1 SST K-omega Model.

The SST K-omega turbulence model is a two-equation eddy-viscosity model that is widely used in aerospace applications. The SST K-omega model belongs to the Hybrid RANS-LES model combining the Wilcox k-omega and the k-epsilon model in the analysis. This combination of these two models is used since the k-omega model is ideal for simulations of flow in the viscous sub-layer. While the k-epsilon is well suited for simulating the flow regimes away from the wall. The way this model works is by predicting the turbulence by means of two partial differential equations of two variables, k and ω. Being k the kinetic energy of turbulence; and ω the specific dissipation of turbulence. [2]

3.4.2 Scale Adaptive Simulation, SAS.

SAS, which stands for Scale Adaptive Simulation, is an unsteady RANS based model where a von Karman length scales is introduced into the turbulence scale equation. This allows the software to give results like LES in some flows. But even thought, SAS will not always work properly and will produce a steady state flow. [2]

3.4.3 Detached Eddy Simulation, DES.

The Detached Eddy Simulation model was originally implanted by Philipe Spalart in 1997. And it is one of the most used hybrid RANS-LES models. The DES model uses the RANS model for regions of the boundary layer or near solid surfaces where the flow is attached, while the LES model is used for taking values of separated regions from the boundary layer. [2]

3.5 2D Airfoils Selection, Initial Conditions.

For the performance of my 2D analysis I have chosen the following NACA airfoils and the following properties of flow. This approach on the properties of the flow, has been made based on the conditions in flight of a small aircraft.

Initial Conditions:

- **Altitude:** 8000 m
- **Temperature (h=8000 m):** 236.15 K
- **Air Density (h=8000 m):** 0.526 Kg/m3 [20]
- **Speed of Sound (h=8000 m):** 308.01 m/s
- **Air Velocity:** 270 Km/h→ 75 m/s
- **Flying Mach:** 0.2435
- **Air Dynamic Viscosity:** $1.526 \cdot 10^{-5}\ N \cdot s/m^2$
- **Reynolds Number:** $2.583 \cdot 10^{6}$ (turbulent flow)

Wing NACA Airfoil:

- **Chord:** 1 m
- **NACA Profile:** NACA 4412
- **Max. Thickness:** 12% at 30% chord

- **Max. Camber:** 4% at 40% chord [17]

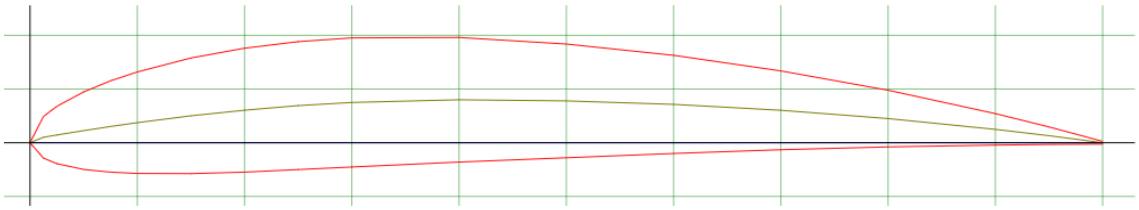

Figure 15. NACA 4412 Airfoil [17]

Junkers Flap NACA Airfoil:

- **Chord:** 0.325 m
- **NACA Profile:** NACA 2312
- **Max. Thickness:** 12% at 30.9% chord
- **Max. Camber:** 2% at 30.9% chord [18]

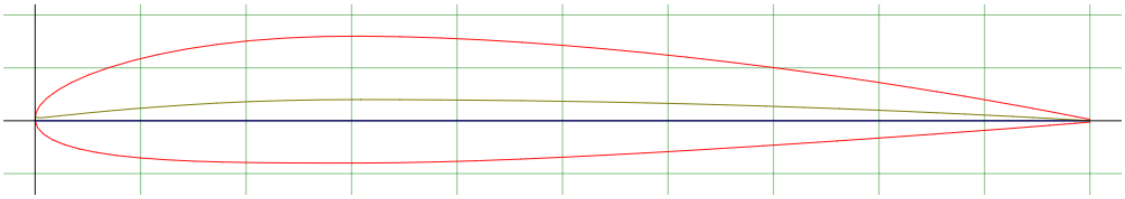

Figure 16. NACA 2312 Airfoil [11]

3.6 CFD Analysis.

Once we have set up the initial conditions of the analysis, we proceed with the calculation of the results. For performing this analysis, we will first analyze the performance of the wing by itself, in terms of CL vs angle of attack (for analyzing the stalling point); CD vs angle of attack; and CL vs CD (for analyzing its aerodynamic efficiency), and once obtained its performance we will proceed with the analysis of the performance of the wing+Junkers flap together, comparing the same performance data as the graphs taken for the wing itself. After obtaining the results we can make a conclusion of the advantages and disadvantages of the implementation of a high lift device on an aircraft's wing. For performing the CFD analysis we will be using the ANSYS Fluent Software, with a student version, which limits the number of elements when performing

the meshing of the geometry, limiting the accuracy of our analysis, but sufficiently precise to be able to rely on the results obtained to make the performance comparison.

3.6.1 ANSYS Analysis.

To be able to compare the results between the wing itself and the set of wing+Junkers flap, and obtain the increase of performance provided by the high-lift device, we will perform the CFD analysis with the same initial conditions otherwise the results of the comparison could not be used for an accurate performance comparison as the boundary conditions affect all performance parameters. The steps followed for setting the analysis are shown in Appendix 3.

3.6.1.1 ANSYS Fluent Turbulence Model Selection.

For performing the analysis, I have chosen the SST K-omega turbulence model, since it is the one that best fits for our type of analysis. The SST K-omega turbulence model gives better results than the other turbulence models I have studied. The justification of the choice is based on the reason that SST K-omega model is specially designed to deal with flow separations, which in our case is a very important fact to be able to analyze, since flow separations make a difference in terms of aerodynamic performance. Also, SST K-omega has high computational efficiency. Based on this and the results obtained when running the other turbulence models, I chosen this turbulence model.

3.7 CFD Results.

On this CFD results section, we will have the CL vs alpha, CD vs Alpha, and the CL vs CD graphs results obtained from the Ansys analysis. It is divided into an only wing analysis, and the wing+Junkers flap analysis to be able to compare the increase in performance when adding a flap, compared to the results in performance obtained by the wing itself.

3.7.1 Only Wing Analysis Results.

Performance graphs obtained from analyzing wing profile NACA 4412 at different angles of attack.

- ***CL vs Alpha. Wing***

Figure 17. CL vs AoA (Wing)

- ***CD vs Alpha. Wing***

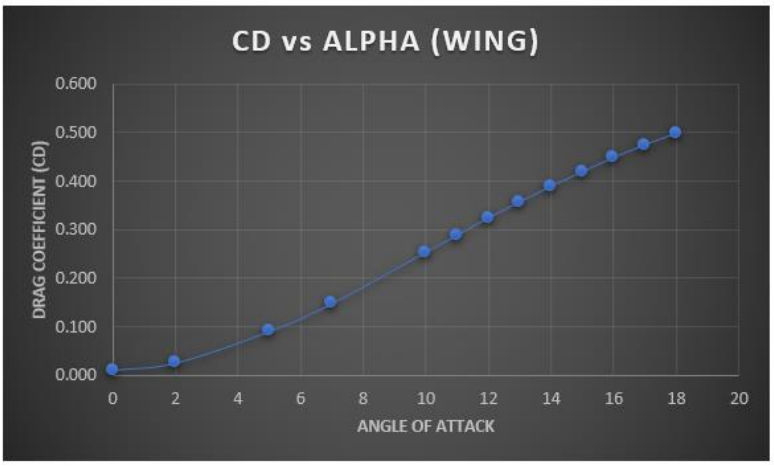

Figure 18. CD vs AoA (Wing)

- ***CL vs CD. Wing***

Figure 19. CL vs CD (Wing)

3.7.2 WING+Junkers FLAP Analysis Results.

For the analysis of the Wing+Junkers flap set, I will be fixing the angle of attack of the flap, while varying the angle of attack of the wing, in this manner, we can compare how the aerodynamic performance of the wing is influenced by the addition of a Junker's flap, since we can observe if the stalling angle point is delayed and at different angles of attack of the wing what the overall performance is.

We will be analyzing for the following angles of attack of the flap: 0º(full retracted), 10º, 12º, 15º, 18º. The angles in between are not very useful for the analysis of the performance of the flap, since normally flaps are used for stages in the flight for obtaining maximum lift, or maximum drag. Even though, we cannot bypass the configuration of the full retracted flap, since as it is a Junkers flap, in the fully retracted position it still affects the aerodynamics, since in its fully retracted position it is still in the flow direction.

3.7.2.1 Flap 0º.

Performance graphs obtained from placing the flap at an angle of attack of 0º while varying the AoA of the wing.

- ***CL vs AoA Wing.***

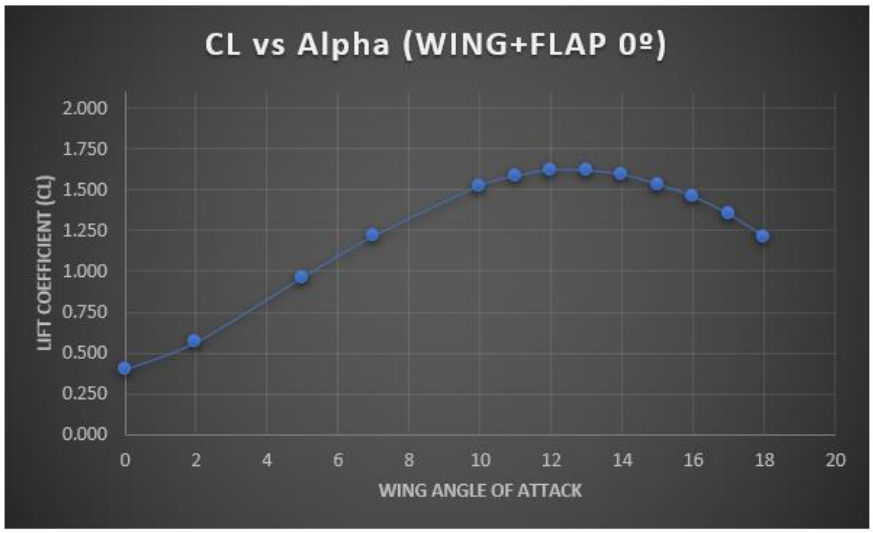

Figure 20. CL vs AoA Wing. Flap 0º

- ***CL vs CD.***

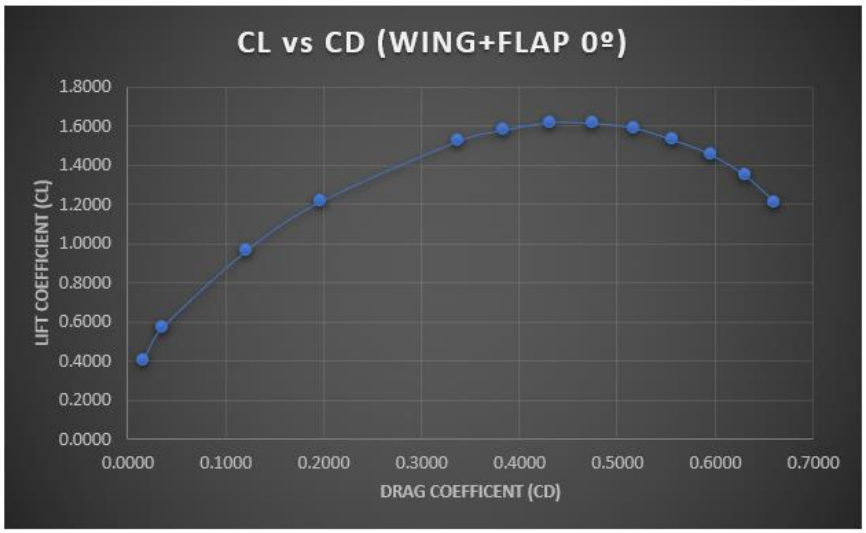

Figure 21. CL vs CD. Flap 0º

- ***CD vs AoA Wing.***

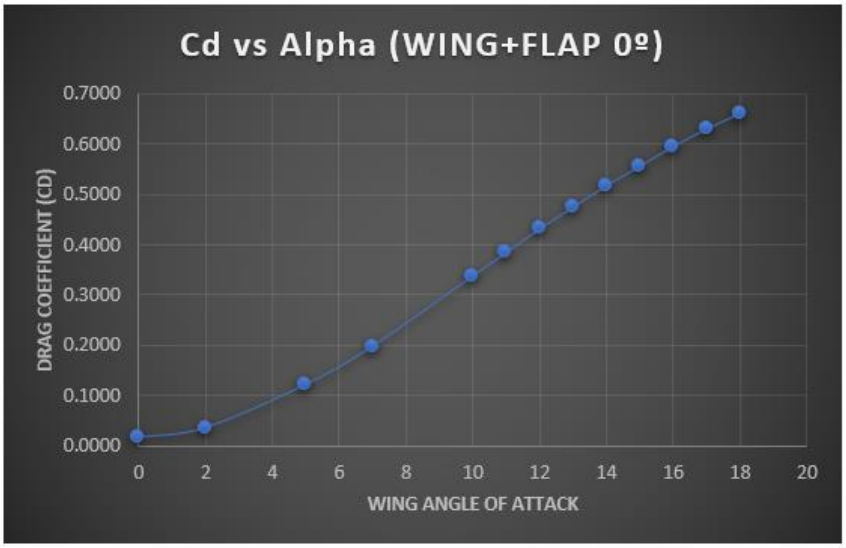

Figure 22. CD vs AoA Wing. Flap 0º

3.7.2.2 Flap 10º.

Performance graphs obtained from placing the flap at an angle of attack of 10º while varying the AoA of the wing.

- ***CL vs AoA Wing.***

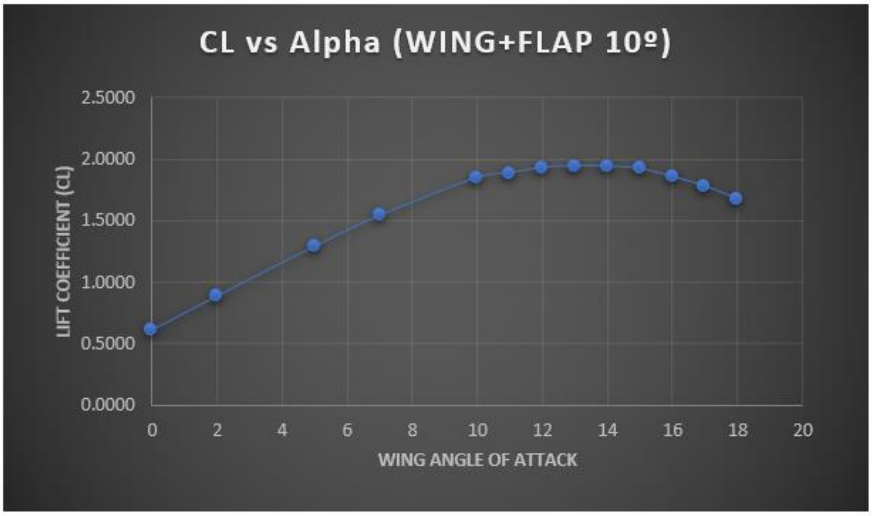

Figure 23. CL vs AoA Wing. Flap 10º

- ***CD vs AoA Wing.***

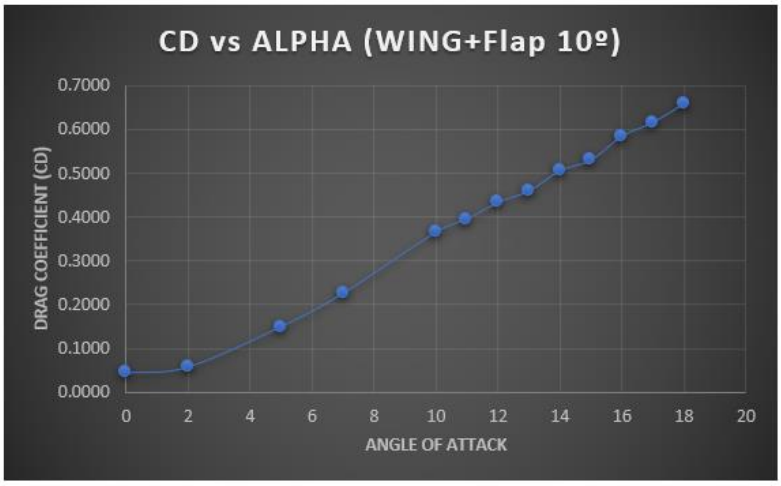

Figure 24. CD vs AoA Wing. Flap 12º

- ***CL vs CD.***

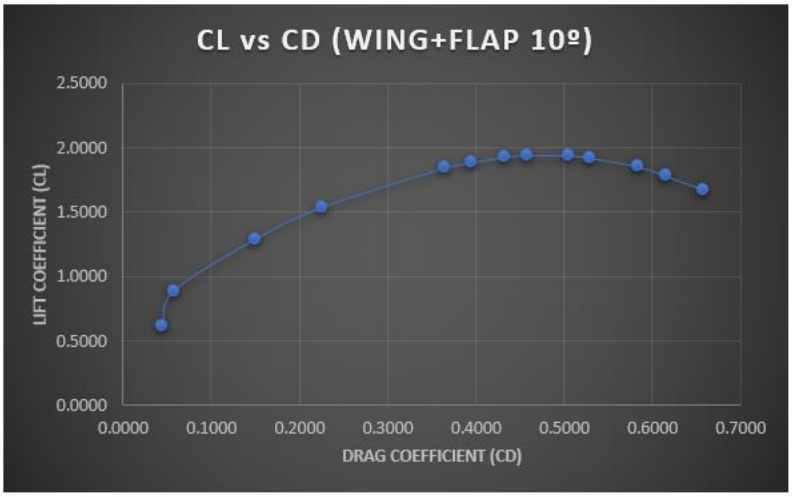

Figure 25. CL vs CD. Flap 10º

3.7.2.3 Flap 12º.

Performance graphs obtained from placing the flap at an angle of attack of 12º while varying the AoA of the wing.

- ***CL vs AoA Wing.***

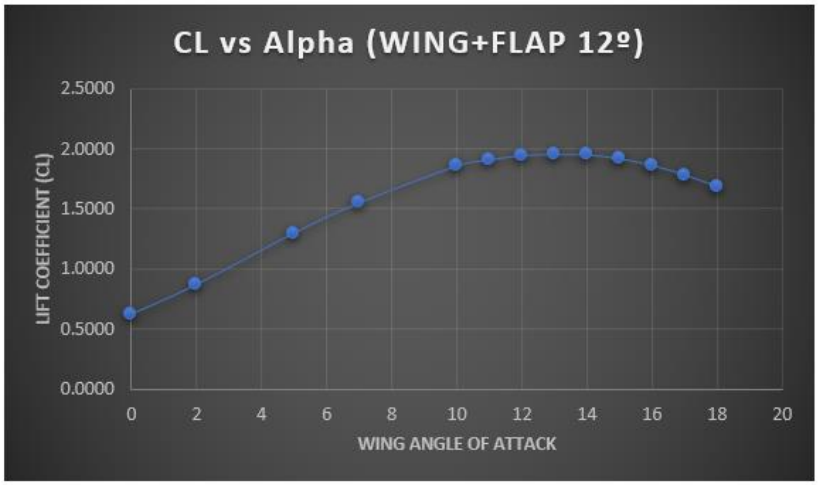

Figure 26. CL vs AoA Wing. Flap 12º

- ***CD vs AoA Wing.***

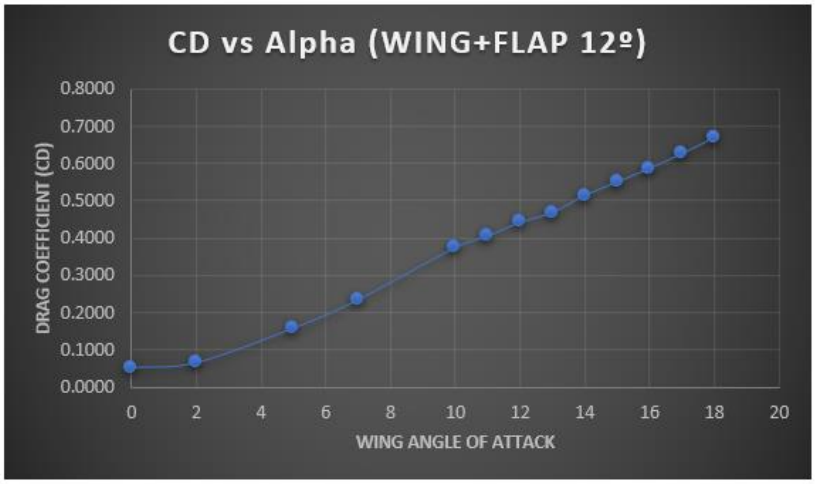

Figure 27. CD vs AoA Wing. Flap 12º

- ***CL vs CD.***

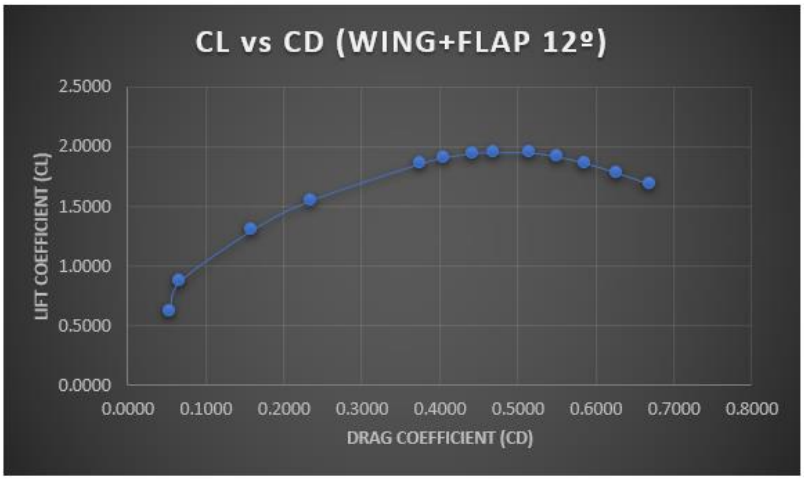

Figure 28. CL vs CD. Flap 12º

3.7.2.4 Flap 15º.

Performance graphs obtained from placing the flap at an angle of attack of 15º while varying the AoA of the wing.

- ***CL vs AoA Wing.***

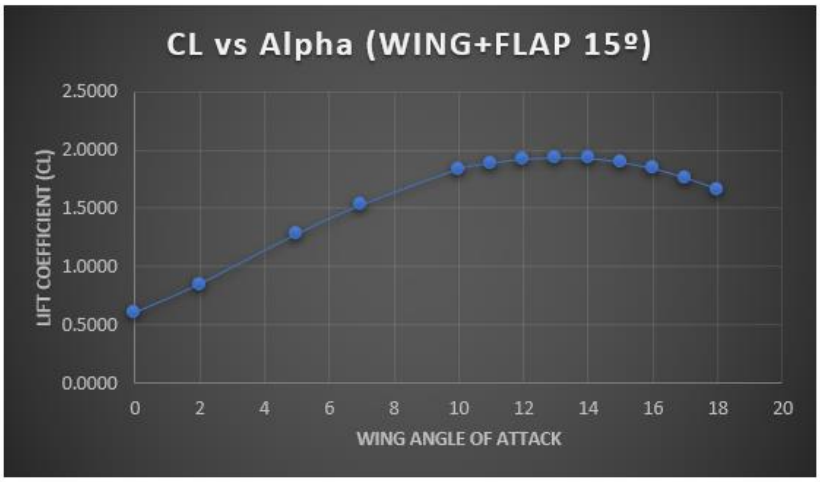

Figure 29. CL vs AoA Wing. Flap 15º

- ***CD vs AoA Wing.***

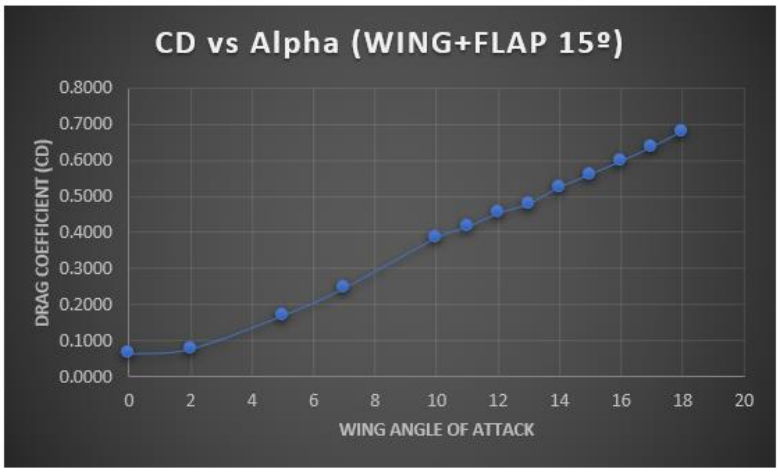

Figure 30. CD vs AoA Wing. Flap 15º

- ***CL vs CD.***

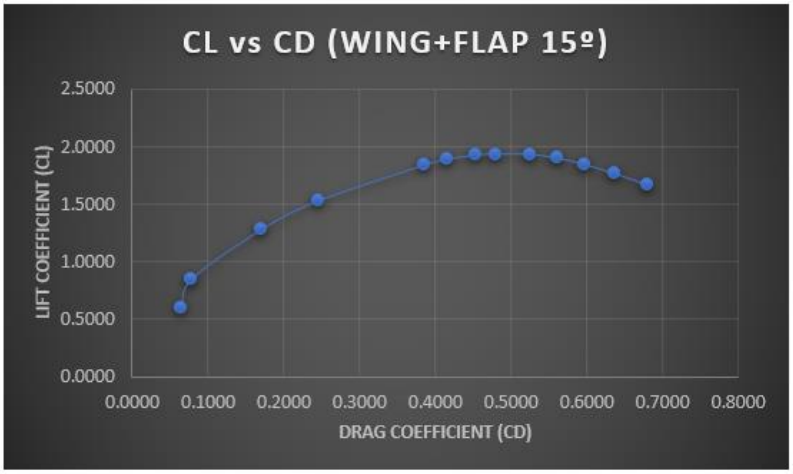

Figure 31. CL vs CD. Flap 15º

3.7.2.5 Flap 18º.

Performance graphs obtained from placing the flap at an angle of attack of 18º while varying the AoA of the wing.

- ***CL vs AoA Wing.***

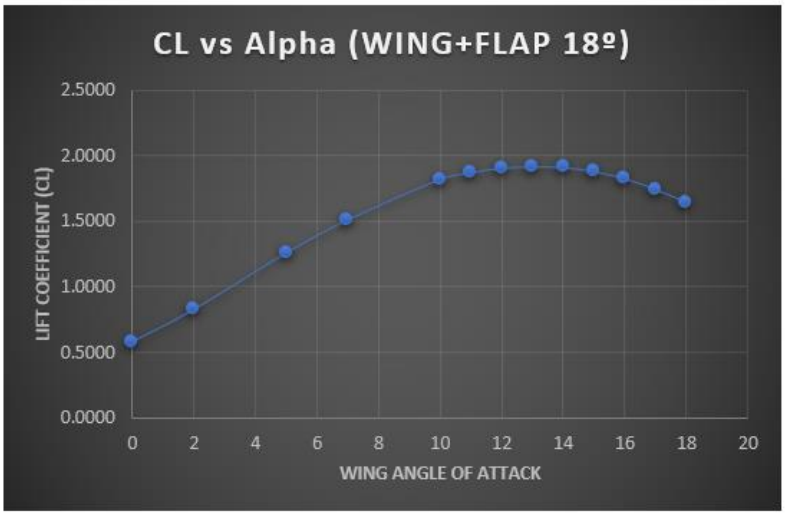

Figure 32. CL vs AoA Wing. Flap 18º

- ***CD vs AoA Wing.***

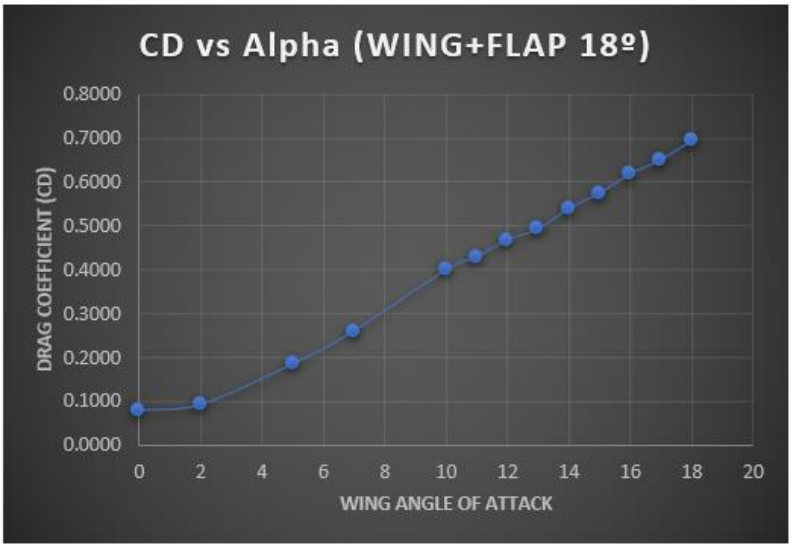

Figure 33. CD vs AoA Wing. Flap 18º

- ***CL vs CD.***

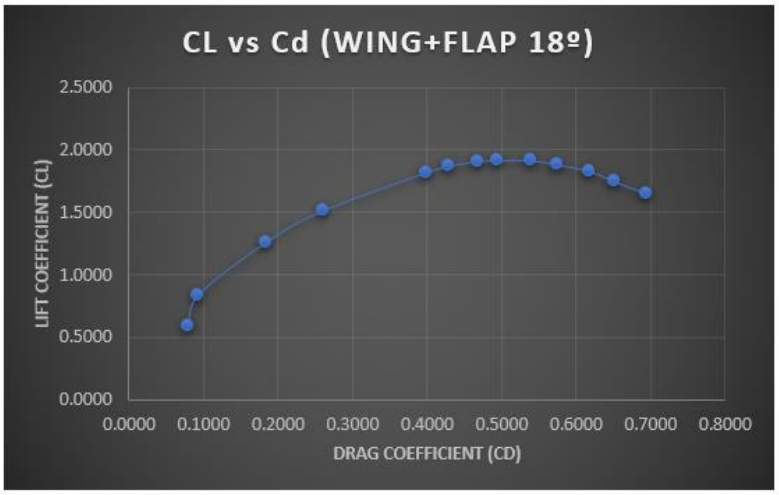

Figure 34. CL vs CD. Flap 18º

3.7.3 Table Results Analysis.

- ***Only Wing Results.***

AoA Wing	CL Wing	CD Wing
0	0.352	0.011
2	0.533	0.026
5	0.863	0.091
7	1.052	0.148
10	1.285	0.254
11	1.327	0.289
12	1.357	0.324
13	1.354	0.357
14	1.336	0.389
15	1.291	0.419
16	1.235	0.448
17	1.154	0.475
18	1.047	0.498

Table 1. Analysis Results Only Wing

- ***Flap 0º Results.***

AoA Flap	AoA Wing	CL (Wing+Flap)	CD (Wing+Flap)
0	0	0.400	0.017
0	2	0.568	0.036
0	5	0.963	0.122
0	7	1.214	0.198
0	10	1.522	0.338
0	11	1.579	0.384
0	12	1.617	0.432
0	13	1.614	0.475
0	14	1.590	0.518
0	15	1.530	0.556
0	16	1.455	0.596
0	17	1.349	0.631
0	18	1.212	0.661

Table 2. Analysis Results Flap 0º

- ***Flap 10º Results***

AoA Flap	AoA Wing [deg]	CL (Wing+Flap)	CD (Wing+Flap)
10	0	0.610	0.044
10	2	0.886	0.058
10	5	1.288	0.150
10	7	1.539	0.226
10	10	1.847	0.366
10	11	1.885	0.396
10	12	1.929	0.433
10	13	1.942	0.459
10	14	1.940	0.505
10	15	1.921	0.530
10	16	1.855	0.584
10	17	1.781	0.616
10	18	1.673	0.659

Table 3. Analysis Results Flap 10

- ***Flap 12º.***

AoA Flap	AoA Wing [deg]	CL (Wing+Flap)	CD (Wing+Flap)
12	0	0.620	0.054
12	2	0.868	0.067
12	5	1.297	0.159
12	7	1.548	0.235
12	10	1.857	0.375
12	11	1.907	0.405
12	12	1.944	0.443
12	13	1.952	0.469
12	14	1.950	0.515
12	15	1.917	0.550
12	16	1.861	0.587
12	17	1.783	0.626
12	18	1.684	0.670

Table 4. Analysis Results Flap 12º

- ***Flap 15º.***

AoA Flap	AoA Wing	CL (Wing+Flap)	CD (Wing+Flap)
15	0	0.599	0.065
15	2	0.847	0.079
15	5	1.276	0.171
15	7	1.527	0.247
15	10	1.836	0.387
15	11	1.886	0.417
15	12	1.923	0.454
15	13	1.931	0.480
15	14	1.928	0.526
15	15	1.896	0.562
15	16	1.840	0.599
15	17	1.762	0.638
15	18	1.663	0.682

Table 5. Analysis Results Flap 15º

- ***Flap 18º.***

AoA Flap	AoA Wing	CL (Wing+Flap)	CD (Wing+Flap)
18	0	0.583	0.079
18	2	0.831	0.092
18	5	1.260	0.184
18	7	1.511	0.260
18	10	1.820	0.400
18	11	1.870	0.430
18	12	1.907	0.468
18	13	1.915	0.494
18	14	1.913	0.540
18	15	1.880	0.576
18	16	1.828	0.619
18	17	1.746	0.652
18	18	1.647	0.695

Table 6. Analysis Results Flap 18º

3.7.4 Wing vs Wing+Flap Comparison Graphs Analysis Results.

From these graphs, we can observe how the lift coefficient increases as we implement the high lift device or flap. Out of all the angles of attack of flaps we analyzed, the one that gave the best performances in terms of lift coefficient, is the flap at 12º of angle of attack. We could think that the flap at 18º will give better lift performances, but, at that angle, the flap is stalling. And so, the configuration of the flap at 12º is the best in terms of climbing, while the flap at an angle of attack of 18º gives us a better performance in terms of landing approach, since it is the one that gives us the higher drag coefficient. Obtaining from these graphs the stalling point of the flap, which once increases the angle over 12º, the lift coefficient starts decreasing.

- ***Wing vs Wing+Flap, CL vs AoA Wing***.

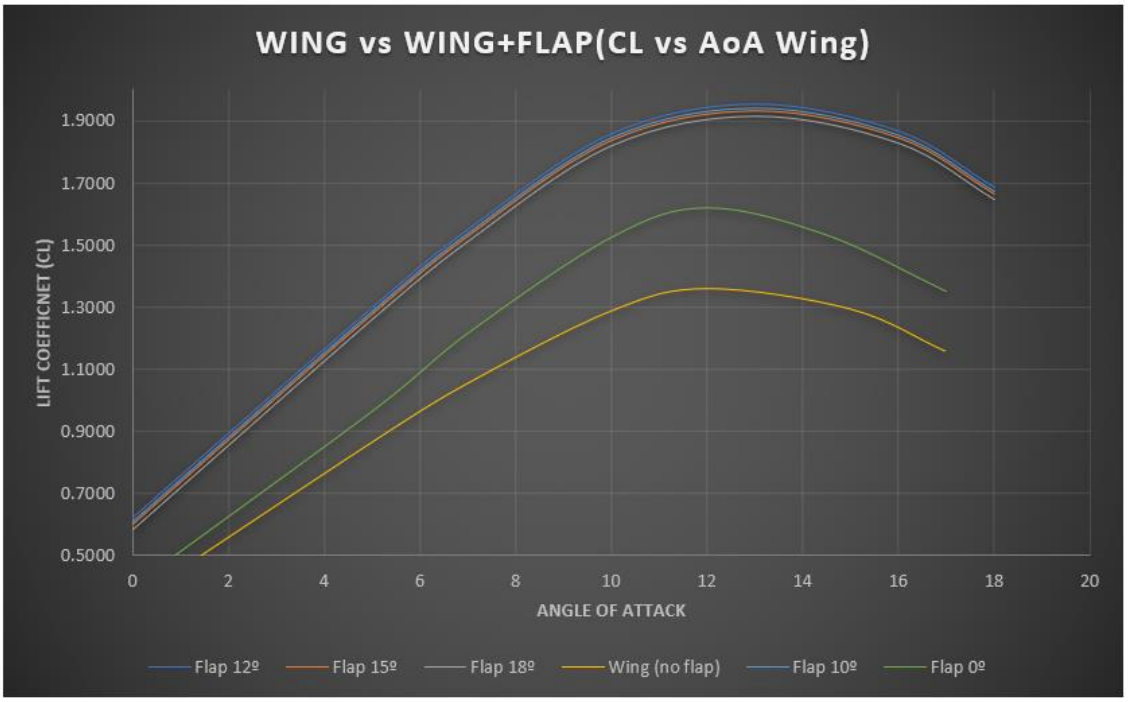

Figure 35. Wing vs Wing+Flap Performance Comparison

- ***Wing vs Wing+Flap, CL vs CD.***

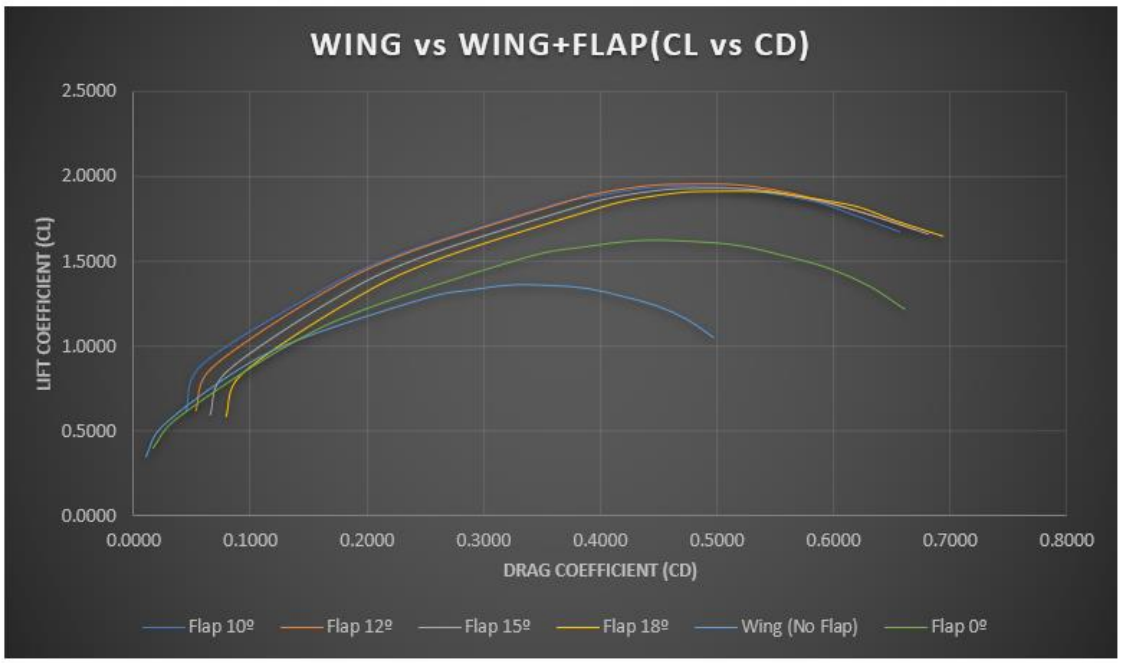

Figure 36. Wing vs Wing+Flap Performance Comparison. CL vs CD

- ***Wing vs Wing+Flap, CD vs AoA Wing***.

Figure 37. Wing vs Wing+Flap Performance Comparison. CD vs AoA Wing

3.7.5 Analytical Comparison of Performance.

The last comparison I will make is in terms of an analytical comparison between implementing or not a high-lift device is by a comparison in lift force and drag force produce with the flap at an angle of attack of 12º (highest lift coefficient) with the wing at 13º; and the wing without high-lift implemented. In this way we can observe a numerical comparison in terms of performance of the high-lift device.

For performing this analysis, we have taken as references the geometrical parameters of the Cessna 172 wing:

- **Wingspan**: 11m
- **Wing Chord**: 1.47m
- **Wing Surface→** S=16.2 m2

Now we will take the data collected from our performance analysis, in the case for the drag force calculation, we will use the comparison between the flap fully retracted and the wing without flap, both cases the wing at 5º(normal value of flying angle), since in this case this is the

values analysis that we are interested in; this lets us see the impact of the high-lift device in the drag performance:

- **Lift Coefficient (Wing 12º; No Flap)→** $\boldsymbol{CLmax_{No\ Flap}}$=1.3567
- **Lift Coefficient (Wing 13º; Flap 12º)→** $\boldsymbol{CL_{Wing\ 13º;Flap\ 12º}}$=1.9518
- **Drag Coefficient(Wing5º;No Flap)→** $\boldsymbol{CD_{No\ Flap}}$=0.09076
- **Drag Coefficient (Wing5º; Flap 0º)→** $\boldsymbol{CD_{Wing5º;Flap0º}}$=0.1220

3.7.5.1 Lift Force and Drag Force Calculation.

For this calculation the flight conditions will be the same as the ones used for the initial conditions for the CFD analysis.

- ***Lift Force.***

These equations will be used for obtaining the lift force:

$$L_{No\ Flap} = \frac{1}{2} \cdot \rho \cdot V^2 \cdot CLmax_{No\ Flap} \cdot S$$

Equation 9. Lift Equation No Flap

$$L_{Wing13º;Flap12º} = \frac{1}{2} \cdot \rho \cdot V^2 \cdot CL_{Wing13º;Flap12º} \cdot S$$

Equation 10. Lift Equation. Wing 13º, Flap 12º

- Lift Force (No Flap) → $\boldsymbol{L_{No\ flap}}$=32514.50N
- Lift Force (Wing13º; Flap 12º)→ $\boldsymbol{L_{Wing13º;Flap12º}}$=46776.59N
- Percentage Gain of Lift→ **%Lift Gain**= 43.86%

- ***Drag Force.***

These equations will be used for obtaining the drag force:

$$D_{No\ Flap} = \frac{1}{2} \cdot \rho \cdot V^2 \cdot CD_{No\ Flap} \cdot S$$

Equation 11. Drag Equation. No Flap

$$D_{Wing5º;Flap0º} = \frac{1}{2} \cdot \rho \cdot V^2 \cdot CD_{Wing5º;Flap0º} \cdot S$$

Equation 12. Drag Equation. Wing 5º; Flap 0º

- Drag Force (No Flap)→ → $\boldsymbol{D_{No\ flap}}$= 2175.14N
- Lift Force (Wing5º; Flap 0º)→ $\boldsymbol{D_{Wing5º;Flap0º}}$= 2923.83N
- Percentage Gain of Drag→ **%Drag Gain**= 34.42%

3.7.6 Conclusions of Implementing a High-Lift Device.

As a conclusion for the results obtained in the analysis, we can tell that we have advantages when implementing a high lift device, but also, we get disadvantages when implementing it.

First of all, on the only wing analysis we can observe the performance of the 2D profile NACA 4412 where we can see the angle of attack at which the airfoil starts getting to a stalling point, which is at the angle of attck of 12º since we can see how when it reaches that value of angle of attck the CL of the wing starts decreasing, meaning it has entered in stalling, due to the separation of the boundary layer.

After seeing the aerodynamic performance of the wing without high-lift device, we will focus on the fully retracted position of the flap, where we can observe and coclude how the decision to have used a non-symmetrical profile for the junkers flap is a great advantage, since, being a Junkers flap and not being able to fully retract it, it does affects our aerodynamics, that is why in the 0º position (fully retracted) the Junkers provides us with an increase in lift and therefore, being able to compensate the increase in drag. On the other hand, if we had opted for a symmetrical airfoil for the Junkers flap, we would have a drop in the overall aerodynamic performance of the aircraft, due to the increase in parasitic drag, but in this case without increasing the lift of the aircraft since the usage of a symmetrical airfoil.

Some of the advantages of implementing a high-lift device is the increase of the overall lift coefficient of the aircraft, which were the results expected before the analysis. This increase in the overall lift is essential not only because it increases the performance of the aircraft when flying at low speeds, but it also increases the efficiency of the flight during a period, since, with the same thrust propulsion, we can obtain better performances and so better efficiency of the

aircraft. Although it also increases the overall drag of the aircraft, which in fact is a disadvantage, we can turn over this disadvantage and convert it into an advantage. Since normally, light weight aircraft usually land in short runways, and so, being able to increase the overall drag coefficient of the aircraft, lets the aircraft to be more usable for other types of missions, such as landing at places where the runway wouldn't be long enough for the same aircraft to land without the high lift device. This leads to a wider range of missions, and so a better economic remuneration than the same aircraft without those high lift devices.

Also, another main advantage that we obtain is the delaying of the stalling point, where in the case of the only wing performance, the stalling point is located at an angle of attack of 12º, but when deploying the high-lift device, we get an increase of 1º stalling angle, delaying the stalling angle to 13º angle of attack of the wing.

Another advantage of implementing a Junkers flap as a high-lift device is that as we cannot fully retract the Junkers flap into the wing, the Junkers flap can be used also as an aileron, this reduces the amount of control devices, being able to use a high-lift device as an aileron. Converting the flap into a flaperon. Reducing weight of control surfaces in the aircraft.

And to conclude the advantages of why implementing a high-lift device as a Junkers is a good idea, we can observe the analytical comparison we made, where we obtained an increase in lift of 44%, due to the implementation of the Junkers flap. And in terms of drag, we get an increase in drag of only 34% due to implementing it. This ratio makes our decision stronger as to why it is a good idea to implement it.

On the other hand, every implementation has its disadvantages in terms of performance. From the graphs we can tell that the overall drag coefficient of the aircraft increases, and so leading to a draggier aircraft, but this increase in drag is compensated by the increase in lift of the aircraft. But even though this can be compensated, the only parameter that really affects the implementation of high lift devices is the increase of the momentum of the aircraft affecting the longitudinal stability of the aircraft when appearance of gusts. Which is not a critical disadvantage, since it can be counteracted by the horizontal stabilizer, but it must be considered for the performance of the flight and the aircraft's stability.

Chapter 4. AEROELASTIC ANALYSIS.

4.1 Theory Introduction, Aeroelastic Analysis.

Before starting to explain what an aeroelastic analysis cover, and what an aeroelastic analysis is. First, we must first talk about the structural analysis. Well, structural analysis is an essential point in the design of an aircraft, since it lets to understand how capable is the structure we are designing of withstanding several loads that may occur during flight. One of the most important parts of the aircraft to which an structural analysis is essential of doing, are the wings, since wings are one of the main components of aircrafts that have to withstand several forces coming from the production of lift, drag resultant forces, and also, it has to withstand the overall weight of the aircraft during flying operation. Even though, structural analysis are not very accurate when analyzing what loads and vibrations will the structure withstand during the fight, since structural analysis doesn't take into account the interaction of the fluid with the structure, which is an essential point to take into account, since the perturbation of the flow along the structure also affect its structural behavior, and this is the reason why we have to perform an analysis that take into account the interaction of the fluid with the structure, better known as an Aeroelastic Analysis.

Once understanded why an Aeroelastic Analysis is crucial to be performed for an aircraft, we will explain what an aeroelastic analysis is, and what type of aeroelastic analysis exists.

Aeroelasticity is the branch of physics and engineering studying the interactions between the inertial, elastic, and aerodynamic forces occurring while an elastic body is exposed to a fluid flow. Or, in other words, is the analysis of the effect that occurs to an elastic structure of being put under the interaction of a flow, in this case air. This analysis is essential for designing an aircraft, since it les the designers to understand how the structure will react to an incoming flow, such as perturbations, vibrations, etc. Also, this helps the designers and the engineers to achieve the best balance between elastic properties and strength properties in the structure, while being able to reduce as much as possible the weight of the structure while not compromising the overall performance of the structure. [27]

Inside aeroelasticity, there are two different types of aeroelastic analysis: Static Aeroelasticity, and Dynamic Aeroelasticity.

- Static Aeroelasticity: static aeroelasticity is the study that treat the interaction of aerodynamic and structural forces on a flexible structure. The reason that it is a static aeroelasticity is because the forces and motions are independent of time. And so, no inertial forces are considered when performing the static aeroelastic analysis. In simple words, it is an interaction of Steady Fluids with Solid Mechanics.
- Dynamic Aeroelasticity: dynamic aeroelasticity unlike static aeroelasticity, is the branch of the aeroelasticity that takes forces and motions that are dependent of time. And so, it considers the aerodynamic forces, elastic forces, and inertial forces.

On the following picture we can observe a scheme of what static aeroelasticity and dynamic aeroelasticity are dependent of, in a more visual way.

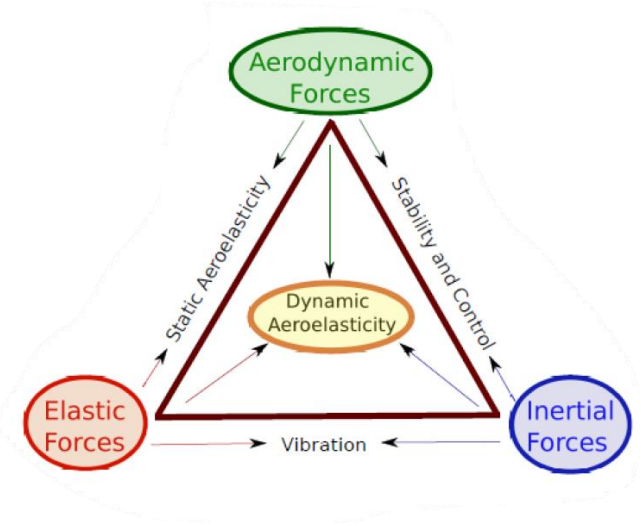

Figure 38. Dynamic Aeroelasticity and Static Aeroelasticity Scheme

Once explained the types of aeroelasticity there are, we will be talking about the different phenomena's there are in dynamic and static aeroelasticity:

4.1.1 **Static Aeroelasticity Phenomena:**

In an aircraft there exists two mains static aeroelastic phenomena, which are divergence and control reversal.

- **Divergence:** divergence is a static aeroelastic phenomena that appears in an airplane due to the combination of the elastic forces and the aerodynamic forces that occur at the

wing, due to the flow over the wing. The way divergence appears on an aircraft's wing is due to the deformation of the elastic forces in the structure that concludes into a change on the effective angle of the attack, and so, due to the increase in that effective angle of attack it creates an additional lift, that produces the divergence phenomena on the wing. There are two outcomes to these phenomena, it can either continue the increase in lift and the angle of attack decreases until a state of equilibrium, where the elastic forces are able to overcome the aerodynamic forces; or it can self-feed the phenomena, where no equilibrium is reached and so, the phenomena grow during time. Divergence occurs if the elastic center lies behind the aerodynamic center. [27]

- **Control Reversal:** control reversal is a static aeroelastic phenomena that affects the controllability of the aircraft. It causes headache in pilots since the flight controls reverse itself, and the become not intuitive. There are several factors that can cause this type of phenomena, but in terms of structural failure, the one that creates this phenomenon is the twisting of the wing. Wing twisting occurs due to the ailerons to generate more force than predicted, and so it twists the wing, due to the insufficient torsional stiffness of the wing. [27]

4.1.2 **Dynamic Aeroelasticity Phenomena:**

In aircraft's there are three different types of main dynamic aeroelastic phenomena: forced-response, flutter, non-synchronous vibrations and buffeting.

- **Forced-Response:** forced-response is dynamic aeroelasticity phenomena that is caused by the interaction of the aerodynamic forces, elastic forces, and inertial forces. These forces can generate aerodynamic loads, turbulence, or mechanical disturbances, and can cause the aircraft to experience malicious vibrations or oscillations. These vibrations can be very dangerous, since they can cause the failure of the structure or damage the structure. And so, forced response phenomenon has to be seriously taking care of when designing an aircraft, by stiffening the structure so they can resist the vibrations and oscillations. [27]

- **Flutter:** flutter consists of a self-excited vibration phenomenon caused by the interaction of the aerodynamic forces, elastic forces, and inertial forces every time the wing is subjected to an airflow, it is the highest and more predominant aeroelastic

problem. Flutter can be mitigated based on the response the structure has to the vibrations. Normally if the aircraft is flying at low speeds, the vibration is gradually attenuated after being disturbed. But there is a critical value in terms of flutter, that is called critical flutter speed, which is the speed at which flutter will occur, and it will be self-excited until the structure breaks, meaning that the system is unstable, since flutter increases as it goes in time. The reason why flutter must be mitigated before it appears, is because it consists of a self-excited vibration, which without any additional external force, it can be self-excited until the structure breaks. And usually, flutter appears at low-moderate reduced frequencies. [3]

- **Non-Synchronous Vibrations:** non-synchronous vibrations are a type of vibration that can occur in aircrafts while flying operations. These vibrations are different form the other vibrations phenomenon, since they are no attached or synchronized to any aircraft's engine or rotor speed. Non-synchronous vibrations can be caused by different factors that can include unbalanced components during the designing of the aircraft, aerodynamic forces caused while flying, and structural resonances. The way to prevent these non-synchronous vibrations are by making an analysis, from where it can be observed the root cause of the vibration and so, make a design or structural correction for preventing it to happen.

- **Buffeting**: buffeting is a type of aeroelastic phenomenon that occurs on aerodynamic structures, this aeroelastic phenomenon occurs due to the interaction of the flow and the structure. When a structure is flowing through air, it creates differences of pressures and so leading to vortex generators, these vortices are known as Karman vortices, these generation of vortices and differences of pressures lead to fluctuations generating oscillatory forces and excitations in the structure. These oscillatory forces don't constitute in fact any problem to the structure, until the frequency of these vortices (vortex shedding) match the natural frequency of the structure. When the natural frequency of the structure and the frequencies of these vortices (vortex shedding) match, they produced what is known as Vortex Induced Vibration (VIV), giving arise to the buffeting phenomenon. This phenomenon is very risky, since if it is not mitigated by aerodynamic damping or redesigning of the structure it can lead to structural failure during flight, which will be catastrophic. This phenomenon not only affects the structures of an aircraft, but it affects any structure which has associated natural

frequencies, and which are found in interaction with a fluid. Such as bridges, towers, cables, pipelines, and others. [20]

4.2 Aeroelastic Phenomenon to Analyze.

In this part of the project, where we will perform an aeroelastic analysis, we will focus on the **buffeting** phenomenon. For it, we will calculate the risk of buffeting formation in the wing and in the Junkers flap, the study must be performed for both structures since the flap as it cannot be fully retracted into the wing, it also has its natural frequencies an its risks of buffeting formation. The reasons I focus on studying the buffeting phenomenon are the following:

- Ensure structural integrity of the airplane, buffeting as we know implies vibrations and oscillations, this vibrations after long cycles imparts deformation forces on the structure, subjecting it to high levels of fatigue and stress. And so, if buffeting is not controlled or mitigated, it can be a serious problem for the structural safety of the aircraft.

- Aircraft efficiency, since buffeting imparts generation of vortices, it also affects the aircraft efficiency, since it generates an increase in the overall drag of the aircraft. And so, being able to mitigate buffeting also helps to increase aircraft efficiency, which leads to a reduction in fuel consumption.

- Contribute to better comfort in flight, since buffeting imparts a frequency of oscillation on the wing, this is reflected in the overall vibration of the aircraft, affecting the comfort of the passengers, that is why being able to mitigate this phenomenon, also helps the comfort of the passengers, making them feel safer during the flight, and therefore, this is not reflected in a decrease in the number of people flying.

- And one of the most important reasons, is related to the certification of the aircraft. Since there are many standards regulations that focus on buffeting mitigation, therefore being able to mitigate buffeting will help facilitate the aircraft certification process, as well as regulations.

For analyzing the risk of buffeting in the wing and in the Junkers flap, we will calculate the frequencies of the vortex shedding in the wing and in the flap, at different flight speeds. As we

explained before in the theory of dynamic aeroelasticity phenomenon's, buffeting can be determined by calculating the natural frequency modes of the structures that we want to analyze, and seeing where the vortex shedding frequency of the structure reaches the same value as the natural mode frequency.

4.3 Karman Vortex.

For understanding how Vortex Induced Vibrations (VIV) are produced we must first understand what Karman vortex are.

Karman vortices or better known as Karman Vortex Street, is a repeating pattern of swirling vortices, caused by a process known as vortex shedding, which occurs due to the unsteady separation of flow of a fluid around a body.

This repeating pattern of swirling vortices is caused by the interaction of the boundary layer of the flow with the wake of the flow caused by the production of lift or the interaction of the flow with the structure. This occurs due that the flow when in this case flowing through an airfoil causes difference of pressure in the structure, in this case between the upper and lower surface. And so, when the flow leaves the airfoil through the trailing edge, this differences of pressure and difference in velocities interact with the wake of the flow and so creating swirling vortices behind, which follows a trail, known as Karman Vortex Street. These swirling vortices don't happen instantaneously, but they are formed over time, while the flow leaves the trailing edge, and the vortices are energized by this separation. These vortices can also be known as shedding vortices. [30]

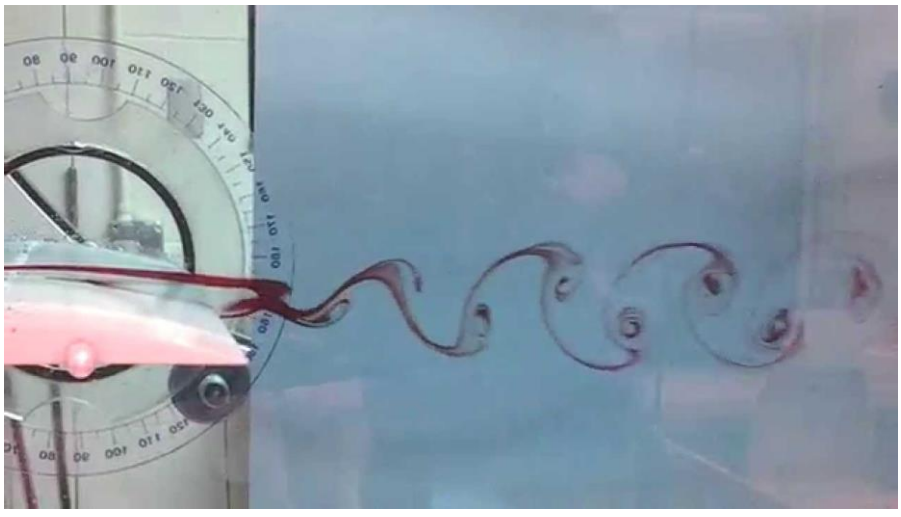

Figure 39. Karman Vortex NACA 4412 [22]

4.3.1 Strouhal Number.

To describe the Karman vortex frequency in relation with the velocity flow and the longitudinal characteristic of the structure, we can use a dimensionless parameter known as Strouhal number, St.

Strouhal number, St, is a dimensionless parameter that relates the ratio of inertial forces due to unsteadiness of the flow, to the inertial forces due to changes in the velocity at different points of the flow field. Also, it has been found that the Strouhal number, St, is a function of the Reynolds number, this is because the influence of viscous effects and inertial effects influence the Strouhal number, since as the Reynolds number increases, also the frequency at which these swirling vortices tend to become detached also increases, making the relation between the Strouhal number and the Reynolds number. [5]

Strouhal number can be calculated by the following equation:

$$St = \frac{f \cdot L}{U_\infty}$$

Equation 13. Strouhal Number Equation [5]

where:

- f= frequency of the vortex shedding [f=1/T]
- L= characteristic length on the body, normally stands for chord length in airfoils
- U_∞= flow velocity.

And here we can observe the relationship between the Strouhal number, St and the Reynolds number. Typically for turbulence flows, St is between 0.18 and 0.21.

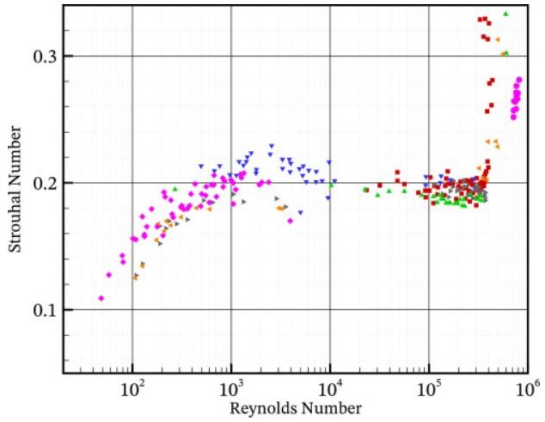

Figure 40. Strouhal Number vs Reynolds Number Graph [5]

4.4 Vortex Induced Vibrations, VIV.

Once we have understood the parameters that affect the appearance of Vortex Induced Vibrations, VIV. We must understand what they are.

Vortex Induced Vibrations is the vibration induced to the structure due to the matching of the Karman vortex frequency with the natural mode frequencies of the structure, in this case, the wing and the Junkers flap. Vortex Induced Vibrations are very dangerous for the structure since it subjects the structure to high cycles of fatigue and stress. When being subjected to this high number cycles of stress and fatigue it arises to the structural failure, where the wing structure can break, and so as explained before, this is why analyzing risk of buffeting is very important in aircrafts structures. [24]

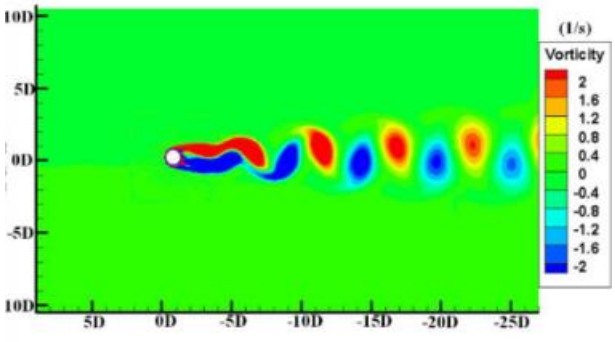

Figure 42. VIV contour at time t=x [25]

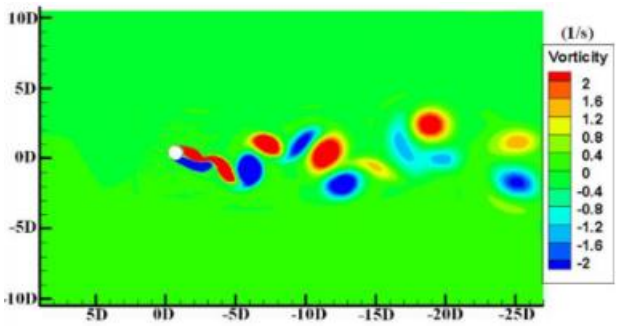

Figure 41. VIV at time t=x+1 [25]

For calculating the VIV on structures there are different methods or approaches:

- Experimental Methods: these experimental methods consist of wind tunnel testing, or experimental procedures made at laboratories with detailed equipment. This type of analysis is the more accurate one for obtaining results, since at an experimental method you can control all the variables and take out those that you don't want to affect.
- Numerical Methods: numerical methods are also very useful and constitute the obtaining of results using CFD computation analysis. This analysis is less accurate than the experimental methods, but also much less expensive in terms of costs related, and so in balance, normally it is the type of analysis that usually are taken as. Even though, it requires great computational power to make an analysis where it is taken as a time-dependent flow, this is a very limiting factor, because to perform a time-dependent flow-structure interaction analysis, it requires a huge amount of computational power.

Also, this type of method doesn't let you understand the influence of the different parameter that affect the analysis.

- Analytical Methods: analytical method uses the theoretical approximation based on mathematical equations and physical principles to obtain exact or approximate solutions of a given problem. This type of method is very flexible, since it lets you apply it to several type of analysis. Also, experimental methods lets you see the influence on the several parameters that affect the analysis and see how they affect the analysis. Being able to make comparison results in a more fast and less demanding way of the changes on those parameters that affect the analysis.

4.5 Modal Analysis, ANSYS.

To perform the analysis of risk of buffeting in the wing and in the flap, modal analysis is essential to be performed due to the necessity to obtain the natural vibration frequencies of the structure for performing this risk analysis.

Modal Analysis can be defined as the study of dynamic properties of the vibrating structures which leads either to eigenvalues (natural frequencies) or eigenvectors (vibration natural mode shapes). [6]

A complete modal analysis includes both data acquisition and subsequent parameter identifications. From its invention to today, modal analysis has been used for mechanical and structural engineering for designing and validating purposes. Also, in aerospace engineer is a very widely used analysis, used for determining limit frequencies of oscillation.

The results obtained from a modal analysis are the natural frequencies of vibrations of the structure, these frequencies are the ones at which the structure tends to oscillate without being subjected to any driving force or damping force.

Also, from the modal analysis we obtain the mode shapes, which are the deformation shown in the structure when vibrating at its natural vibration frequency, each natural vibration frequency is associated to a mode shape frequency.

Regarding the material, we used aluminum alloy for both analyses. Properties of the material are shown in the appendix.

Modal analysis is essential to perform our aeroelastic analysis since we must obtain the natural frequency vibrations of our wing and flap. To see the risk of buffeting appearance.

4.5.1 Analytical Calculation, Modal Analysis.

Even though we will not be using the analytical way to obtain the natural mode frequencies. It is important to understand the different parameters that affect the natural vibration frequencies.

The equation of motion for the modal analysis, where we obtain the mode shapes of a cantilever beam, is given by the following equation:

$$\frac{d^2}{dx^2}\left\{EI(x)\frac{d^2\delta Y(x)}{dx^2}\right\} = w^2 m(x)\delta Y(x)$$

Equation 14. Modal Analysis Equation

where:

- δY=displacement in y-direction at distance "x" from fixed support
- E=Young's modulus of the material
- I=moment of inertia of the beam cross section
- w= natural frequency
- m=ρA(x)=mass per unit length

Boundary Conditions:

- x=o ; Y(x) =0 ; $\frac{dY(x)}{dx}$ =0
- x=L ; $\frac{d^2Y(x)}{dx^2}$ =0 ; $\frac{d^3Y(x)}{dx^3}$ =0

Mode shapes of a cantilever beam are given by the following equation:

$$\emptyset_n(x) = A_n[(\sin\beta_n L - \sinh\beta_n L)(\sin\beta_n x - \sinh\beta_n x) + (\cos\beta_n L + \cosh\beta_n L)(\cos\beta_n x - \cosh\beta_n x)]$$

Equation 15. Mode Shapes Equation

Where:

- An= amplitude vibration of the structure.
- L= length of the structure.
- βn= parameter used for obtaining natural vibration frequencies from the structure. The equation of this parameter is the following: $\beta n = (\frac{W(i)^2 \cdot m}{E \cdot I})^{1/4}$
- w(i)= angular frequency of the vibration

- m= mass of the structure
- E= Young's modulus of the material
- I= moment of inertia of beam cross section

Natural Frequency Modes are given by the following equation:

$$w_n = {\alpha_n}^2 \sqrt{\frac{EI}{mL^4}} \rightarrow w_n = {\alpha_n}^2 \sqrt{\frac{EI}{\rho AL^4}}$$

Equation 16. Natural Vibration Frequency Equation

4.6 Aeroelastic Analysis Hypothesis.

For performing the aeroelastic analysis we make some hypothesis to be able to make some conclusions about the results obtained.

Some of the hypothesis made are:

- The wing natural frequency modes are not affected by the presence of the Junkers flap joints to the wing.
- The Junkers flap is attached to the wing through joints, and therefore these affect the natural frequency of the flap.
- Flow velocity is constant, meaning that the inlet velocity in the analysis doesn't change.
- It is assumed that the structural deformations due to the flow are minimal or equal to zero, which implies that no significant changes in the geometry of the aerodynamic surfaces occur.

4.7 Aeroelastic Analysis Calculation.

Once explained the different factors that affect our aeroelastic analysis for obtaining the risk of Vortex Induced Vibrations (VIV) formation in the wing and in the Junkers flap. We will go through the different steps taken to obtain the desire results. As said at the beginning, the objective of this aeroelastic analysis is to obtain the risk of buffeting in the wing and in the Junkers flap and see how by modifying some parameters of the analysis, such as velocity inlet, geometry dimensions, and geometry shapes; we can decrease the risk of buffeting.

4.7.1 Modal Analysis Calculation.

Before starting to calculate the risk of buffeting in the wing and in the Junkers flap, we have to obtain the natural mode frequencies of the structures. The modal analysis will be performed for half span of the entire wing, since wings are embedded in the fuselage. For it, we make use of the hypothesis made before, for the wing and for the flap.

In the case of the wing, it is assumed that its modal frequency is not affected by the joints between the wing and the Junkers flap, because the density and mass of the wing structure are much higher than those of the flap, and the joints are made to hold the flap, and therefore affecting the modal behavior of the flap and not the wing. Therefore, we can approximate that the modal frequencies of the wing will not be affected, in the case that this hypothesis is not taken, it would be very complicated to perform a modal analysis of this structure, as it would require a finite element calculation in the wing, to see this contribution. And in this case, the main idea of the project is to focus on the buffeting risk, and not on the performance of a finite element analysis (FEA).

In the case of the Junkers flap, it is taken that these joints between the wing and the Junkers flap will affect the natural frequencies of the Junkers flap, since due to the presence of these joints, the flap, will not vibrate freely through its entire span dimension. And so, it is assumed that these joints are strong enough so that they do not produce transfer of torsional and bending stress from the wing to the flap. And so, these joints are taken as fixed supports for the modal analysis.

The dimensions of the initial design and geometries to analyze are the following:

	Profile	%Thickness	Chord [m]	Thickness [m]	Span [m]
WING	NACA 4412	12.00%	1	0.1200	6
Junkers Flap (Central)	NACA 2312	12.00%	0.325	0.0390	3
Junkers Flap (Left/Right)	NACA 2312	12.00%	0.325	0.0390	1.5

Table 7. Wing & Junkers Flap Dimensions for Modal Analysis

- ***Initial Design.***

The position of the joints are placed 1.5m from the both tips of the wing, separation between them of 3m.

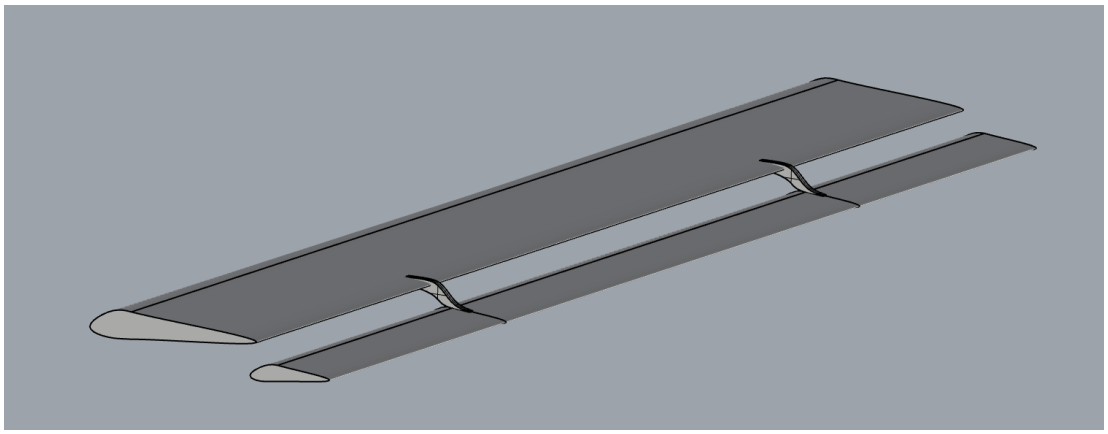

Figure 43. Initial Design Iso Left View

4.7.2 Modal Analysis Results.

- ***Initial Design.***

	WING [Hz]	FLAP (Left Part; 1.5m) [Hz]	FLAP (Central Part) [Hz]	FLAP (Right Part; 1.5m) [Hz]
MODE 1	2.32	11.86	18.84	11.86
MODE 2	14.45	73.91	51.78	73.91
MODE 3	18.16	91.81	101.05	91.81
MODE 4	32.10	129.16	128.84	129.16
MODE 5	40.18	204.90	142.97	204.90
MODE 6	77.95	387.88	166.21	387.88

Table 8. Natural Frequency Modes (Initial Design)

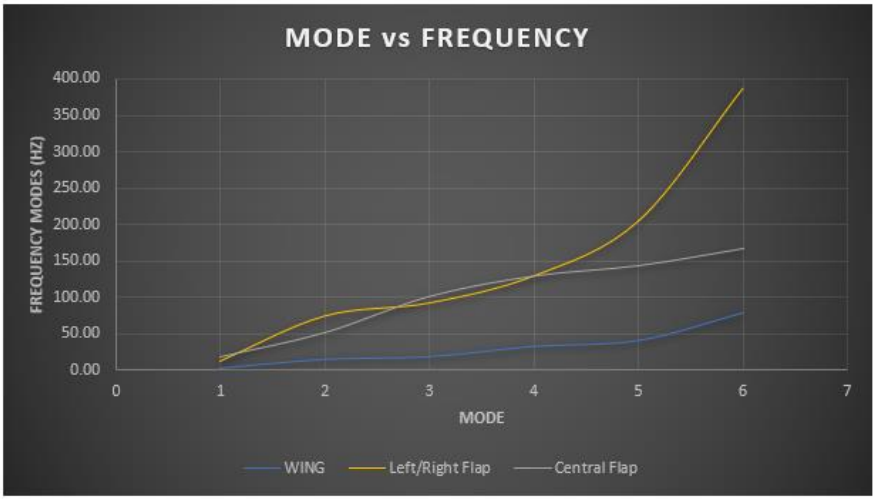

Figure 44. Natural Frequency Graph (Initial Design)

- ***First Redesigning.***
  - Wing chord: 1.4m
  - Junkers Flap chord: 0.325m

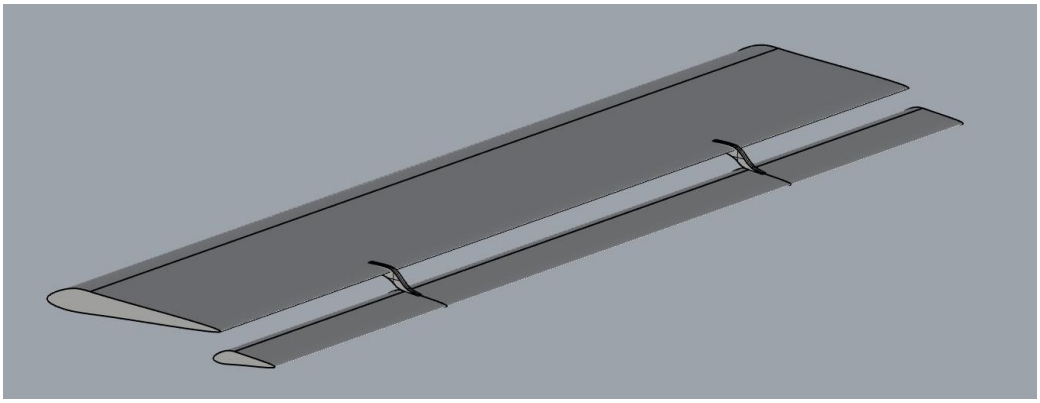

Figure 45. First Redesigning Design Left Iso View

	WING [Hz]	FLAP (Left Part; 1.5m) [Hz]	FLAP (Central Part) [Hz]	FLAP (Right Part; 1.5m) [Hz]
MODE 1	3.37	11.86	18.84	11.86
MODE 2	20.87	73.91	51.78	73.91
MODE 3	25.11	91.81	101.05	91.81
MODE 4	32.46	129.16	128.84	129.16
MODE 5	57.49	204.90	142.97	204.90
MODE 6	97.15	387.88	166.21	387.88

Table 9. Natural Frequency Modes (First Redesigning)

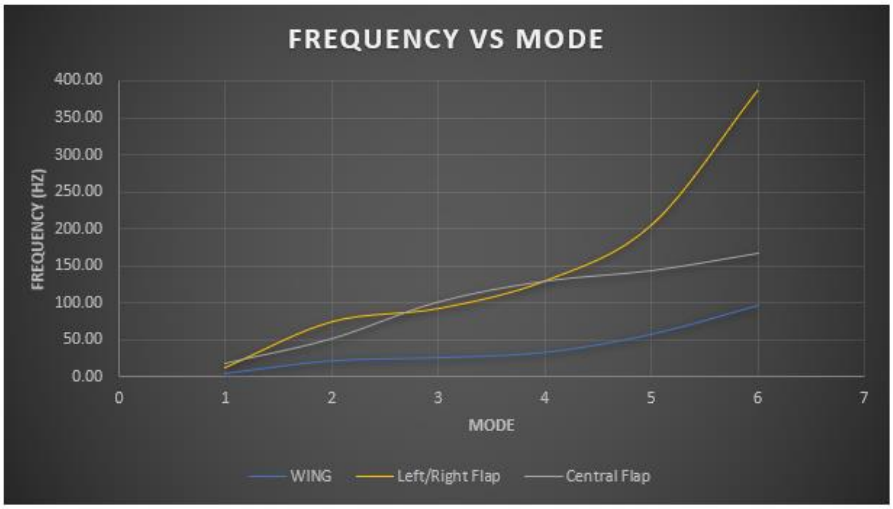

Figure 46. Natural Frequency Modes Graph (First Redesigning)

- ***Second Redesigning.***

    - Addition of joints between wing and Junkers flap at the tips.

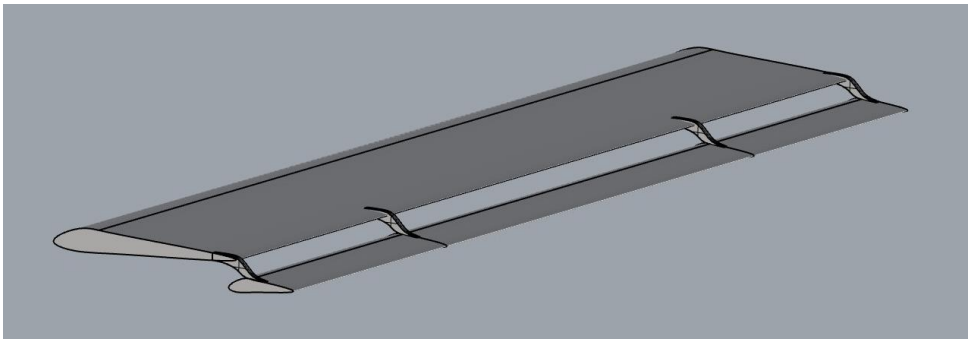

Figure 47. Second Redesigning Design Iso Left View

	WING [Hz]	FLAP (Left Part; 1.5m) [Hz]	FLAP (Central Part) [Hz]	FLAP (Right Part; 1.5m) [Hz]
MODE 1	3.37	76.75	18.84	76.75
MODE 2	20.87	208.49	51.78	208.49
MODE 3	25.11	267.43	101.05	267.43
MODE 4	32.46	400.86	128.84	400.86
MODE 5	57.49	518.60	142.97	518.60
MODE 6	97.15	537.78	166.21	537.78

Table 10. Natural Frequency Modes (Second Redesigning)

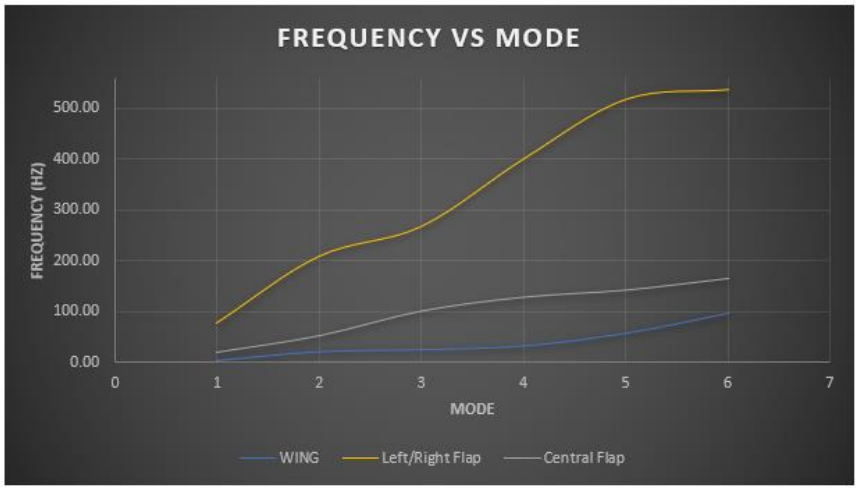

Figure 48. Natural Frequency Modes Graph (Second Redesigning)

4.7.3 Strouhal Number Calculation Results.

Once performed the modal analysis of the structures to analyze. We then must make the calculation of the Strouhal number. For it, we used the software ANSYS Fluent to obtain this value. Even though, the results obtained in ANSYS software weren't coherent at all.

I faced several problems when calculating the Strouhal number through the ANSYS software, as I had to make a transient analysis, and so, the power in terms of computation was very high required, and so I obtained values not coherent at all. And so, to be able to keep with my aeroelastic analysis, I found an analytical graph that related the Reynolds number to the Strouhal number.

This method is not as good in terms of accuracy, however, it can be used, since the Strouhal number as discussed above depends on the characteristic length of the object and the velocity of the fluid, parameters that in this case are collected through the Reynolds number. However, although it is not as accurate as a CFD analysis, this method allows us to see the influence of each parameter (velocity, chord length, fluid density) on the results of the analysis, which in terms of being able to make decisions at the redesign level, allows us a better conclusion on it.

Since the Strouhal number depends on the velocity of the flow and the dimensions of the characteristic length of the geometry, we will have different Strouhal numbers for the different conditions of flow, and changes in the geometry that will be made.

For the sensibility analysis of the risk of buffeting formation, we must take the Strouhal number for the initial geometry at different flight speeds, in order to see which value is the critical velocity (velocity at which buffeting occurs). And also, we must obtain the value of the Strouhal number at a given flight speed (initial speed), in order to see the critical geometries (dimensions at which buffeting is more prone to occur).

For calculating the Reynolds number, we will take the longitudinal characteristic length as the sum of the chords of the wing and the flap, since the Karman Vortex occur due to the influence of both geometries on the flow, and so is the same for both of them.

- Initial Configuration & Conditions:

Velocity [m/s]	Geometry Dimensions	St(Analytical Approx)	St(ANSYS Results)
75	Wing 1m & Flap 0.325m	0.2381	0.6866

Table 11. Strouhal Number Init. Conditions

- Variation of Strouhal Number with Velocity.

Geometry Dimensions	Velocity [m/s]	St (Analytical Approx)	St (ANSYS Results)
Wing 1m & Flap 0.325m	50	0.2223	0.5769
Wing 1m & Flap 0.325m	55	0.2237	0.6255
Wing 1m & Flap 0.325m	60	0.2250	0.6673
Wing 1m & Flap 0.325m	65	0.2264	0.6713
Wing 1m & Flap 0.325m	70	0.2277	0.6826
Wing 1m & Flap 0.325m	75	0.2290	0.6866
Wing 1m & Flap 0.325m	80	0.2304	0.7234
Wing 1m & Flap 0.325m	85	0.2317	0.7304
Wing 1m & Flap 0.325m	90	0.2331	0.7459
Wing 1m & Flap 0.325m	95	0.2344	0.7499

Table 12. Strouhal Number Variation with Velocity

- Variation of Strouhal Number with geometry dimensions, constant velocity:

Velocity	Total Chord	St (Analytical Approx.)	St (ANSYS Results)
75	1.325	0.2290	0.6866
75	1.425	0.2306	0.6911
75	1.525	0.2321	0.6924
75	1.625	0.2336	0.6984
75	1.725	0.2351	0.7231
75	1.825	0.2366	0.7256
75	1.925	0.2381	0.7341
75	2.025	0.2397	0.7425
75	2.125	0.2412	0.7498

Table 13. Strouhal Number Variation with Geometry

4.7.4 Vortex Shedding Frequency Calculation Results.

Once obtained the values of the Strouhal number for different geometry dimensions, we have to calculate the frequency of the vortex shedding or Karman vortex frequency.

For obtaining this frequency we will be using the following equation $fv = \frac{St \cdot U_\infty}{l}$; this equation relates the Strouhal number to the vortex shedding frequencies. In this equation, l stands for the characteristic length of the object that in this case will be the chord. For the value of the chord, we will be assuming that the total chord is the sum of the wing chord plus the flap chord, since the flap is taken to be an extension of the wing, and therefore the total chord will be the sum of the two. When increasing the total chord length, the dimension that is variated is the chord of the wing, while keeping the chord of the flap constant.

- Vortex Shedding Frequency Variation with Velocity.

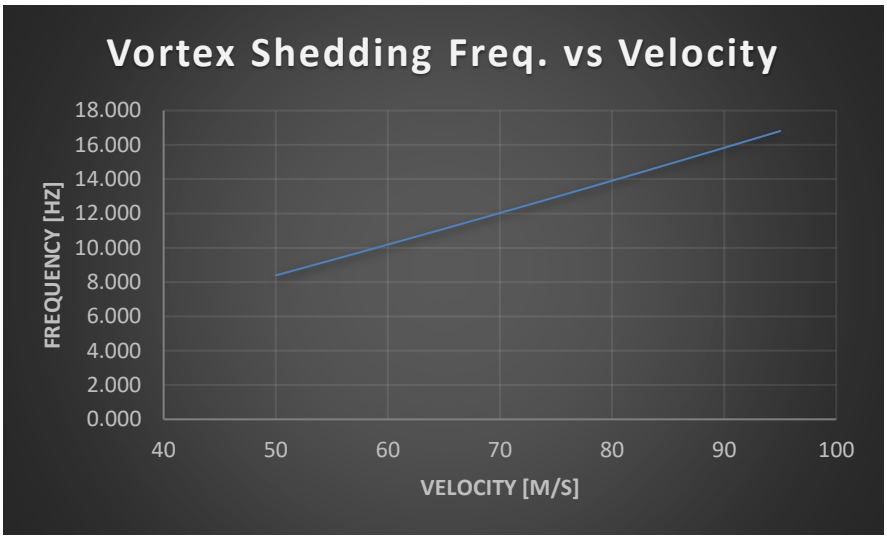

Figure 49. Vortex Shedding Freq. Variation with Velocity

- Vortex Shedding Freq. Variation with Geometry Dimensions.

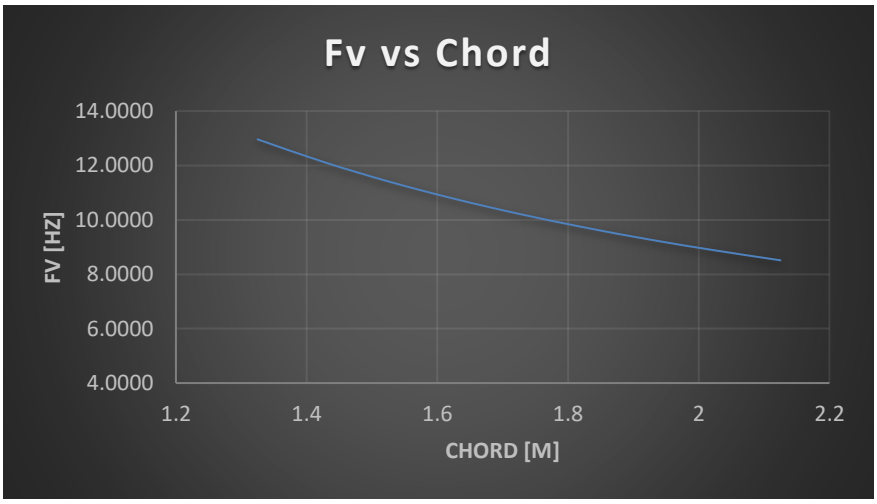

Figure 50. Vortex Shedding Freq. Variation With Geometry

From this graph we can observe how for a constant velocity, if increasing the characteristic length, the vortex shedding frequency is reduced. This is essential for our analysis of risk of VIV formation, since we can make a better decision on the redesigning part, where depending on the position of the buffeting phenomenon's and based on the natural frequencies of the structure, we can decide on whether increasing or decreasing the total characteristic length.

4.7.5 Risk of VIV formation Calculations.

- ***Initial Design.***
  - Wing Chord: 1m
  - Junkers Flap Chord: 0.325m

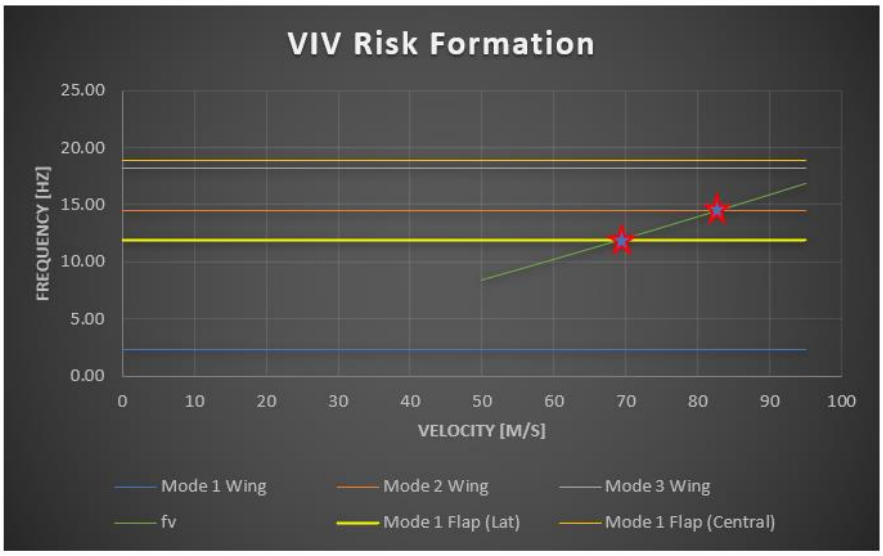

Figure 51. VIV Risk Formation Graph Results Init. Design

We can observe that for the initial geometry dimensions that we chose, VIV (buffeting) occurs at a critical speed of approximately 70 m/s at the Junkers Flap lateral portions, and at the wing, at a critical speed of approximately 85 m/s. Not more natural frequencies are plotted since the vortex shedding frequency oscillates between 5 and 20 Hz; and so, the other natural frequencies are not a problem in terms of buffeting phenomenon.

- ***First Redesigning.***

For avoiding the VIV (buffeting) phenomenon in the wing and in the flap, we will redesign the wing. The decision taken for the redesign is to increase the wing chord, resulting in an increase of the total characteristic length of the geometries. The decision to increase the chord instead of decreasing it is based on the results of the graph obtained on the variation of the vortex shedding (Karman vortex) frequency with the characteristic length. We observe that as the length increases, it decreases, which is convenient for us because we have a range between 5 and 12 Hz where no natural frequency is found, therefore it is convenient for us to decrease the value of the Karman vortex frequency. Also, by increasing the chord of the wing, we increase the natural frequencies of the wing. Thus, eliminating the buffeting phenomenon.

- Wing Chord: 1.4m
- Junkers Flap Chord: 0.325m
- Total Characteristic Length: 1.725m

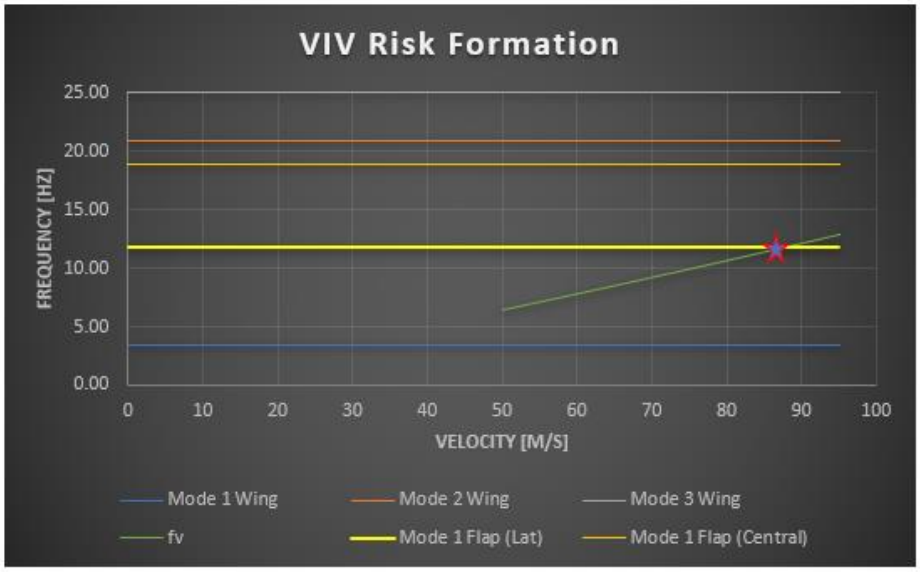

Figure 52. VIV Risk Formation Graph (First Redesigning)

From the graph we can observe that we have eliminated the risk of VIV in the wing, but the risk of VIV at the lateral portions of the Junkers flaps still exist. And so, for eliminating VIV from the flpa, we will make a redesign in term of junctions, since by adding joints at the tips of the wing to the flap,we can obtain higher natural frequencies of the lateral portions of the Junkers flap, which leads to an elimination of risk of VIV formation at the lateral portion of the Junkers flap

- ***Second Redesigning.***
    - Addition of junctions between wing and Junkers flap at the tips.

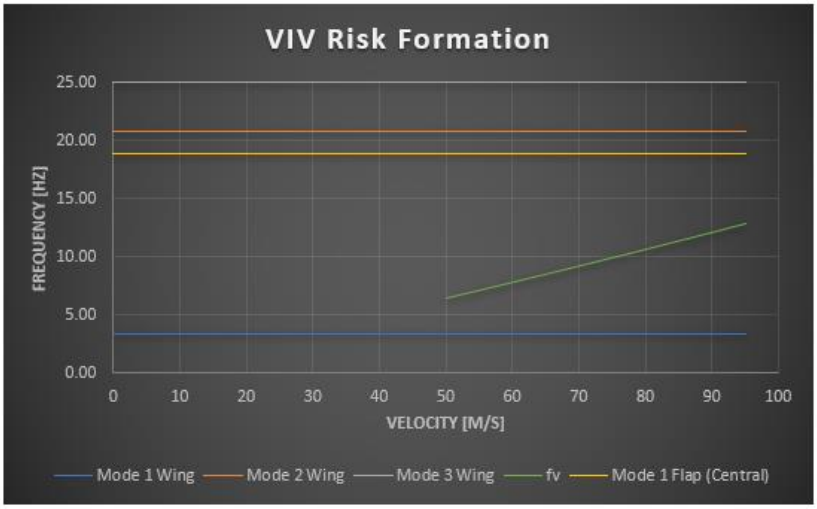

Figure 53. VIV Risk Formation Graph (Second Redesigning).

4.7.6 Aeroelastic Analysis Conclusions.

In conclusion to the aeroelastic analysis, we can say that we have achieved the objective set at the beginning of the analysis, where we wanted to eliminate the risk of buffeting through the redesign of the structures. Through these redesigns we have been able to improve the stability of the aircraft and reduce the risk of Vortex Induced Vibrations (VIV) formation at the wing and at the Junkers flap.

The aeroelastic analysis has shown that the changes made in the redesign have achieved a reduction of unwanted vibrations and oscillations that could lead to buffeting formation, and so, it has contributed to improve the safety and performance of the aircraft.

Therefore, the aeroelastic analysis concludes that the redesign of the structures has been essential to achieve the mitigation of the risk of buffeting in the wing and Junker's flap.

Chapter 5. CONCLUSIONS AND FUTURE WORKS

As a general conclusion of the project, where the influence of adding a Junkers flap to the wing of an aircraft has been studied, analyzing its advantages and disadvantages. An aeroelastic analysis was also carried out to evaluate the risk of buffeting in the Junkers flap and the wing, using a redesign approach to mitigate this phenomenon.

We can say that CFD is an essential tool to obtain values that will allow us to make decisions on the implementation of new aerodynamic devices. As it allows you to obtain very accurate values of the fluid behavior without the need for a wind tunnel.

The analysis showed that the implementation of the Junkers flap was successful, as significant improvements in the overall performance of the wing have been observed. The implementation of the Junkers flap helped to increase lift and improve efficiency, resulting in better aircraft performance.

Also, in terms of the aeroelastic analysis, we have seen that the redesigning of the structures where crucial for eliminating VIV risk formation on the structures.

Even though, we have to highlight that due to the fact that the computational power of the computer used wasn't powerful enough, not very precise results of the Strouhal number could be achieved. This was due to the need to make a transient analysis, which demanded too much computational power. For future studies it is recommended to use more powerful computational resources for obtaining more precise results of the aeroelastic analysis.

Also, the use of a student license software limited the number of modes in the meshing, which also affected the precision of the results obtained from the performance analysis. For future studies it is recommended to use commercial licenses to obtain a more exhaustive analysis and more precise results.

As ideas for future works, it could be interesting to make an aeroelastic analysis of the wing and the flap, but in this case instead of using the redesigning as tool for eliminating the buffeting phenomenon. To use implementation of internal structure of the wing (spars, ribs and stringers).

Also, a study based on different material used could be interesting as well, in order to see the influence of the material chosen.

In summary, this work highlights the importance of CFD analysis in the evaluation of aerodynamic devices configurations, such as the Junker flap. The proposed redesign improved wing aeroelastic performances, and even though there were computational limitations, the aeroelastic analysis provided a solid base for future improvements and optimizations in buffeting mitigation.

Chapter 6. APPENDICES

Appendix 1. NACA 4412 Airfoil Points

#Group	#Points	#X_coord	#Y_coord	#Z_coord
1	1	1000	0	0
1	2	999.622	0.107	0
1	3	998.488	0.427	0
1	4	996.6	0.959	0
1	5	993.961	1.7	0
1	6	990.573	2.647	0
1	7	986.442	3.794	0
1	8	981.573	5.137	0
1	9	975.972	6.669	0
1	10	969.648	8.383	0
1	11	962.609	10.271	0
1	12	954.864	12.323	0
1	13	946.424	14.531	0
1	14	937.301	16.885	0
1	15	927.507	19.373	0
1	16	917.057	21.985	0
1	17	905.965	24.709	0
1	18	894.246	27.533	0
1	19	881.917	30.445	0
1	20	868.997	33.433	0
1	21	855.503	36.484	0
1	22	841.455	39.585	0
1	23	826.873	42.724	0
1	24	811.779	45.889	0
1	25	796.195	49.065	0
1	26	780.144	52.241	0
1	27	763.65	55.404	0
1	28	746.737	58.542	0
1	29	729.431	61.641	0
1	30	711.758	64.691	0
1	31	693.744	67.68	0
1	32	675.418	70.594	0
1	33	656.806	73.424	0
1	34	637.938	76.158	0
1	35	618.842	78.785	0
1	36	599.548	81.294	0
1	37	580.087	83.676	0
1	38	560.488	85.92	0

1	39	540.782	88.018	0
1	40	521	89.96	0
1	41	501.174	91.737	0
1	42	481.336	93.343	0
1	43	461.516	94.768	0
1	44	441.746	96.008	0
1	45	422.059	97.055	0
1	46	402.486	97.904	0
1	47	382.788	98.51	0
1	48	363.224	98.806	0
1	49	343.869	98.792	0
1	50	324.757	98.469	0
1	51	305.921	97.84	0
1	52	287.396	96.911	0
1	53	269.213	95.689	0
1	54	251.404	94.181	0
1	55	234.002	92.396	0
1	56	217.037	90.347	0
1	57	200.539	88.044	0
1	58	184.536	85.502	0
1	59	169.056	82.734	0
1	60	154.126	79.758	0
1	61	139.77	76.589	0
1	62	126.014	73.244	0
1	63	112.88	69.743	0
1	64	100.389	66.103	0
1	65	88.56	62.343	0
1	66	77.413	58.482	0
1	67	66.964	54.54	0
1	68	57.229	50.535	0
1	69	48.221	46.485	0
1	70	39.953	42.41	0
1	71	32.437	38.325	0
1	72	25.681	34.248	0
1	73	19.693	30.193	0
1	74	14.482	26.176	0
1	75	10.051	22.209	0
1	76	6.405	18.304	0
1	77	3.547	14.471	0
1	78	1.478	10.718	0
1	79	0.198	7.052	0
1	80	-0.294	3.478	0
1	81	0	0	0
1	82	1.065	-3.324	0
1	83	2.885	-6.437	0

1	84	5.454	-9.337	0
1	85	8.765	-12.027	0
1	86	12.81	-14.507	0
1	87	17.579	-16.779	0
1	88	23.063	-18.843	0
1	89	29.25	-20.704	0
1	90	36.128	-22.363	0
1	91	43.684	-23.825	0
1	92	51.904	-25.093	0
1	93	60.773	-26.172	0
1	94	70.275	-27.066	0
1	95	80.396	-27.782	0
1	96	91.117	-28.326	0
1	97	102.423	-28.706	0
1	98	114.294	-28.927	0
1	99	126.714	-29	0
1	100	139.663	-28.932	0
1	101	153.123	-28.733	0
1	102	167.074	-28.414	0
1	103	181.496	-27.985	0
1	104	196.371	-27.457	0
1	105	211.676	-26.841	0
1	106	227.393	-26.15	0
1	107	243.499	-25.397	0
1	108	259.974	-24.594	0
1	109	276.797	-23.753	0
1	110	293.945	-22.888	0
1	111	311.395	-22.012	0
1	112	329.126	-21.137	0
1	113	347.114	-20.277	0
1	114	365.336	-19.444	0
1	115	383.767	-18.65	0
1	116	402.423	-17.905	0
1	117	421.506	-17.16	0
1	118	440.716	-16.386	0
1	119	460.025	-15.589	0
1	120	479.405	-14.778	0
1	121	498.826	-13.96	0
1	122	518.259	-13.14	0
1	123	537.677	-12.326	0
1	124	557.05	-11.522	0
1	125	576.348	-10.734	0
1	126	595.542	-9.966	0
1	127	614.603	-9.222	0
1	128	633.503	-8.505	0

1	129	652.211	-7.818	0
1	130	670.699	-7.163	0
1	131	688.939	-6.542	0
1	132	706.902	-5.955	0
1	133	724.559	-5.403	0
1	134	741.884	-4.886	0
1	135	758.849	-4.404	0
1	136	775.426	-3.957	0
1	137	791.59	-3.543	0
1	138	807.315	-3.162	0
1	139	822.575	-2.811	0
1	140	837.346	-2.49	0
1	141	851.604	-2.197	0
1	142	865.326	-1.93	0
1	143	878.488	-1.688	0
1	144	891.071	-1.469	0
1	145	903.052	-1.271	0
1	146	914.412	-1.092	0
1	147	925.133	-0.931	0
1	148	935.195	-0.787	0
1	149	944.583	-0.659	0
1	150	953.279	-0.545	0
1	151	961.271	-0.443	0
1	152	968.543	-0.354	0
1	153	975.084	-0.277	0
1	154	980.882	-0.21	0
1	155	985.928	-0.153	0
1	156	990.212	-0.105	0
1	157	993.728	-0.067	0
1	158	996.468	-0.037	0
1	159	998.429	-0.017	0
1	160	999.607	-0.004	0
1	0			

Appendix 2. NACA 2412 Airfoil Points.

#Group	#Points	#X_coord	#Y_coord	#Z_coord
1	1	325	0	0
1	2	324.87585	0.02665	0
1	3	324.50405	0.10595	0
1	4	323.884275	0.2379	0
1	5	323.018475	0.42185	0
1	6	321.906975	0.6565	0
1	7	320.55205	0.9412	0
1	8	318.955325	1.27465	0
1	9	317.1194	1.6549	0
1	10	315.04655	2.08065	0
1	11	312.7397	2.549625	0
1	12	310.20275	3.059875	0
1	13	307.43895	3.609125	0
1	14	304.452525	4.194775	0
1	15	301.248025	4.81455	0
1	16	297.829675	5.46585	0
1	17	294.203	6.14575	0
1	18	290.3732	6.85165	0
1	19	286.3458	7.5803	0
1	20	282.126975	8.3291	0
1	21	277.7229	9.095125	0
1	22	273.140075	9.87545	0
1	23	268.38565	10.66715	0
1	24	263.46645	11.466975	0
1	25	258.390275	12.272	0
1	26	253.1646	13.0793	0
1	27	247.7969	13.88595	0
1	28	242.296275	14.689025	0
1	29	236.6702	15.4856	0
1	30	230.92745	16.27275	0
1	31	225.077125	17.047225	0
1	32	219.128	17.80675	0
1	33	213.089175	18.548075	0
1	34	206.96975	19.2686	0
1	35	200.779475	19.9654	0
1	36	194.527775	20.635875	0
1	37	188.224725	21.2771	0
1	38	181.879425	21.8868	0
1	39	175.50195	22.461725	0
1	40	169.102375	22.999925	0
1	41	162.690775	23.498475	0
1	42	156.277225	23.9551	0

1	43	149.871475	24.367525	0
1	44	143.483925	24.7338	0
1	45	137.124325	25.05165	0
1	46	130.803075	25.3188	0
1	47	124.4854	25.527775	0
1	48	118.2194	25.666225	0
1	49	112.021	25.7335	0
1	50	105.900925	25.72895	0
1	51	99.868925	25.65225	0
1	52	93.935075	25.503725	0
1	53	88.10945	25.283375	0
1	54	82.401475	24.9925	0
1	55	76.820575	24.63175	0
1	56	71.37585	24.20275	0
1	57	66.076725	23.707125	0
1	58	60.93165	23.14715	0
1	59	55.949075	22.5251	0
1	60	51.137125	21.843575	0
1	61	46.503925	21.1055	0
1	62	42.0563	20.31445	0
1	63	37.801725	19.473025	0
1	64	33.747025	18.585775	0
1	65	29.8987	17.655625	0
1	66	26.262275	16.687125	0
1	67	22.843925	15.683525	0
1	68	19.6482	14.64905	0
1	69	16.6803	13.5876	0
1	70	13.94445	12.5034	0
1	71	11.44455	11.3997	0
1	72	9.1845	10.280725	0
1	73	7.166575	9.1494	0
1	74	5.39435	8.009625	0
1	75	3.869775	6.864	0
1	76	2.5948	5.715125	0
1	77	1.570725	4.565925	0
1	78	0.798525	3.41835	0
1	79	0.2795	2.274025	0
1	80	0.013325	1.13425	0
1	81	0	0	0
1	82	0.23725	-1.109225	0
1	83	0.722475	-2.173925	0
1	84	1.45405	-3.1941	0
1	85	2.430675	-4.1691	0
1	86	3.650075	-5.098275	0
1	87	5.109975	-5.9813	0

1	88	6.80745	-6.81785	0
1	89	8.7399	-7.6076	0
1	90	10.903425	-8.349575	0
1	91	13.29445	-9.04345	0
1	92	15.909075	-9.689225	0
1	93	18.742425	-10.286575	0
1	94	21.7906	-10.8355	0
1	95	25.048075	-11.33535	0
1	96	28.509975	-11.786775	0
1	97	32.170775	-12.189775	0
1	98	36.02495	-12.544675	0
1	99	40.066325	-12.85245	0
1	100	44.28905	-13.113425	0
1	101	48.686625	-13.3289	0
1	102	53.25255	-13.500175	0
1	103	57.980325	-13.628225	0
1	104	62.8628	-13.714675	0
1	105	67.89315	-13.761475	0
1	106	73.063575	-13.7709	0
1	107	78.367575	-13.74425	0
1	108	83.7967	-13.68445	0
1	109	89.3438	-13.593775	0
1	110	95.000425	-13.474825	0
1	111	100.7591	-13.3302	0
1	112	106.61105	-13.1625	0
1	113	112.548475	-12.974975	0
1	114	118.5626	-12.7699	0
1	115	124.64465	-12.550525	0
1	116	130.792675	-12.319125	0
1	117	137.034625	-12.06855	0
1	118	143.31655	-11.795225	0
1	119	149.62935	-11.5011	0
1	120	155.963275	-11.18845	0
1	121	162.309225	-10.85955	0
1	122	168.657125	-10.516675	0
1	123	174.997225	-10.161775	0
1	124	181.320425	-9.7968	0
1	125	187.61665	-9.424025	0
1	126	193.876475	-9.045075	0
1	127	200.09015	-8.661575	0
1	128	206.24825	-8.27515	0
1	129	212.34135	-7.887425	0
1	130	218.360025	-7.499375	0
1	131	224.295175	-7.1123	0
1	132	230.13705	-6.727825	0

1	133	235.876875	-6.346925	0
1	134	241.505875	-5.969925	0
1	135	247.01495	-5.59845	0
1	136	252.395975	-5.23315	0
1	137	257.63985	-4.874675	0
1	138	262.738775	-4.523675	0
1	139	267.68495	-4.181125	0
1	140	272.47025	-3.847675	0
1	141	277.086875	-3.52365	0
1	142	281.528	-3.210025	0
1	143	285.78615	-2.90745	0
1	144	289.854825	-2.61625	0
1	145	293.727525	-2.337075	0
1	146	297.39775	-2.0709	0
1	147	300.859975	-1.81805	0
1	148	304.108675	-1.579175	0
1	149	307.138	-1.354925	0
1	150	309.943725	-1.14595	0
1	151	312.520975	-0.952575	0
1	152	314.86585	-0.7761	0
1	153	316.974125	-0.6162	0
1	154	318.84255	-0.47385	0
1	155	320.4682	-0.3497	0
1	156	321.84815	-0.243425	0
1	157	322.980125	-0.156325	0
1	158	323.862825	-0.088075	0
1	159	324.4943	-0.039325	0
1	160	324.873575	-0.00975	0
1	0			

Appendix 3. CFD ANSYS Setup Steps.

The steps are the same for the analysis of only wing and the analysis of wing+junkers flap. The only thing that changes is the geometry importation where we have to add the airfoil points (3D curve) of the Junkers flap.

- ***Import Geometry.***

We import the geometry airfoils using the airfoil points from airfoiltools. We import them as 3D curves. And then we create the surface body, which we will make a boolean of the airfoil geometries.

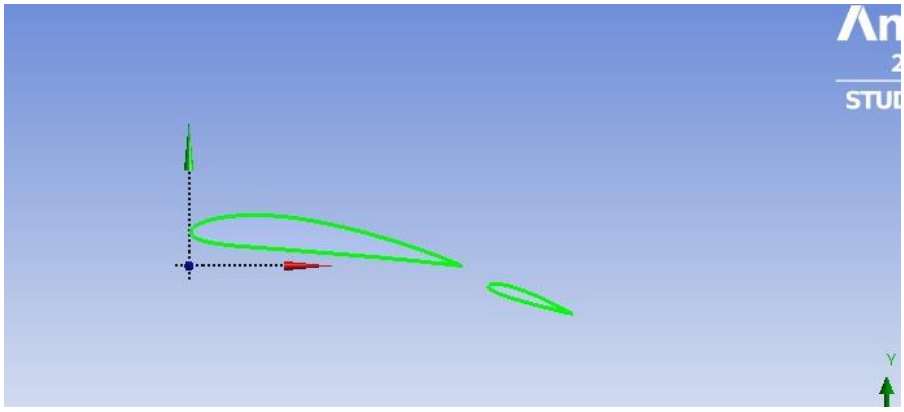

Figure 54. Geometry Importation CFD Analysis

- ***Geometry Meshing.***

For performing the meshing of the geometries I focus mainly on concentrating as much nodes as possible on the area of the boundary layer, for obtaining accurate results, and so getting more accurate separation points of fluid at high angles of attack, for performing this accuracy in the boundary layers of the profiles I have chosen to implement an all-triangles method sufficiently accurate enough for the surface body (air) around the profiles. Then an edge sizing and an inflation was implemented on the surface of the profile. The implementation of the inflation and edge sizing at the wing and Junkers flap was essential for obtaining accurate results at the boundary layer, since the inflation adds additional layers of meshing near the walls of the profile, which is an essential zone for obtaining accurate results of performance of the airfoil, such as separation of the boundary layer. Since velocity and pressure data from the particles that flow around the airfoil are needed to obtain accurate performance information.

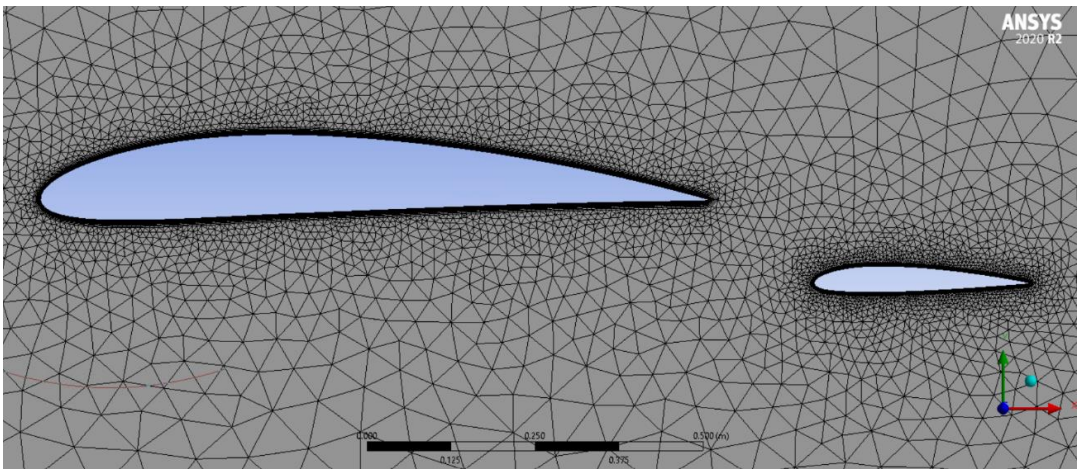

Figure 55. Wing+Flap Meshing Geometries

- ***Turbulence Model Steup.***

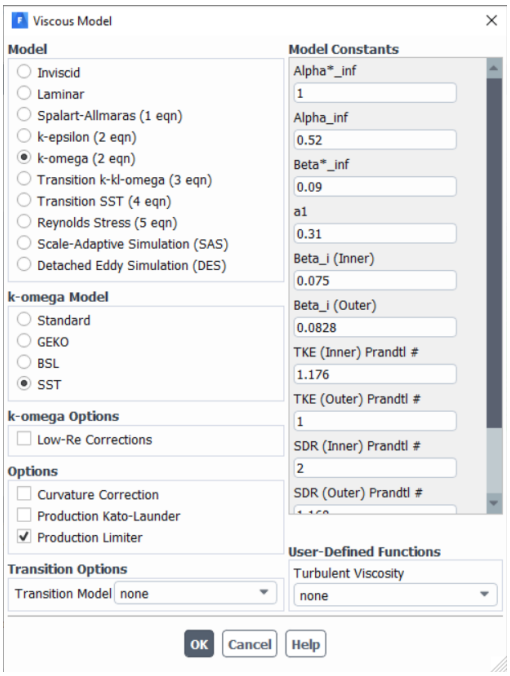

Figure 56. ANSYS Turbulence Model Selection

- ***Boundary Conditions Setup.***

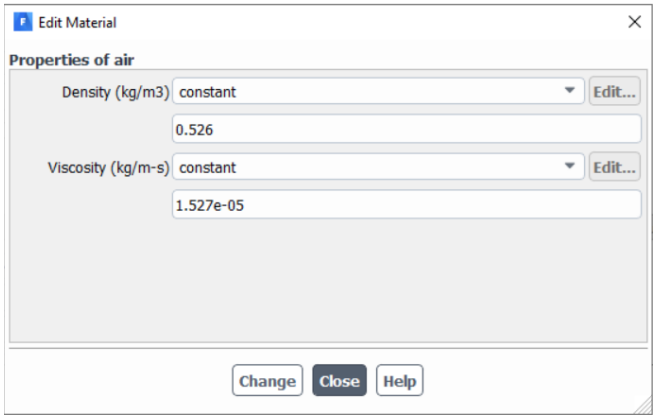

Figure 57. Air Properties ANSYS Analysis

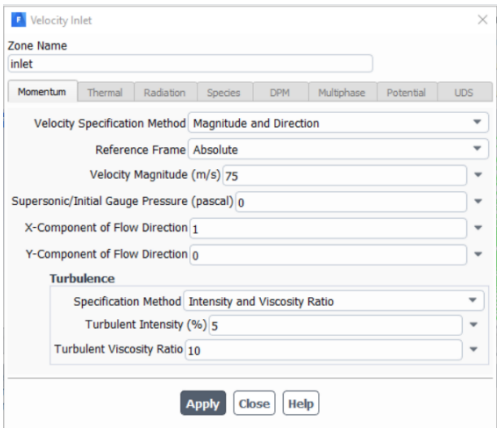

Figure 58. Inlet Boundary Conditions

- ***Report Definitions Setup.***

For obtaining the desired results, we have to add to the report definitions calculations, the calculation of Lift Coefficient (CL) and Drag Coefficient (CD). And, for obtaining the results for each angle of attack of the wing or the flap, we had to project the CL and CD in two different components, X and Y. Where, we have to insert the values of the cosine angle or sine angle of each geometry in the corresponding box, for obtaining a good projection of the results. And so, obtaining accurate values.

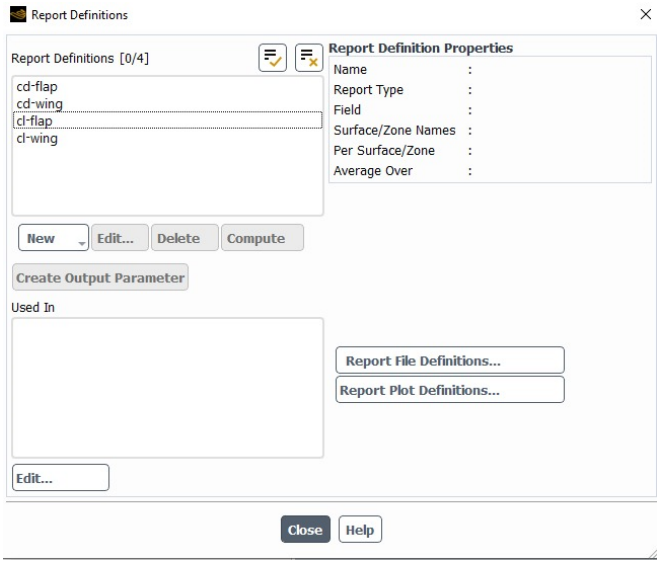

Figure 59. Report Definition CFD Analysis.

Appendix 4. CFD 2D Wing Contour Results

- ***0º Analysis***.

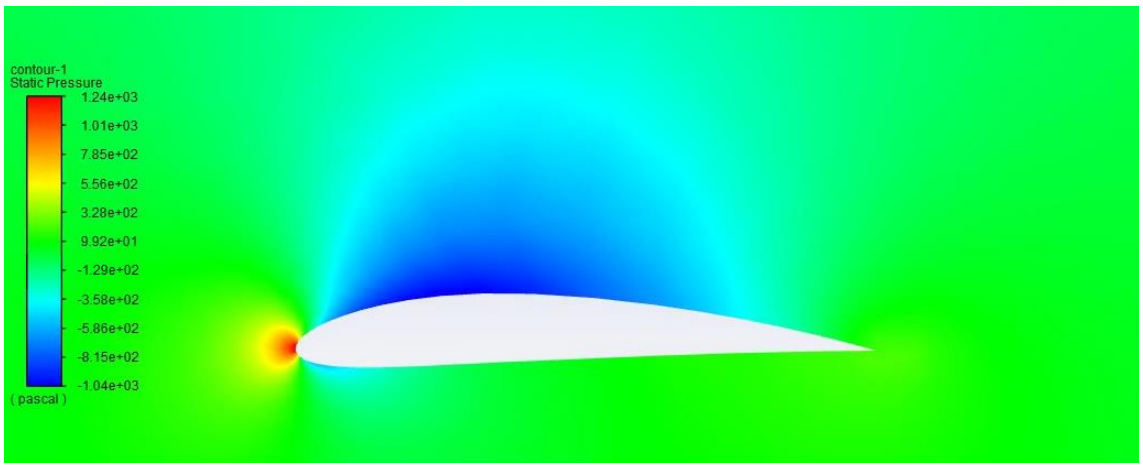

Figure 61. Static Pressure Contour 0º

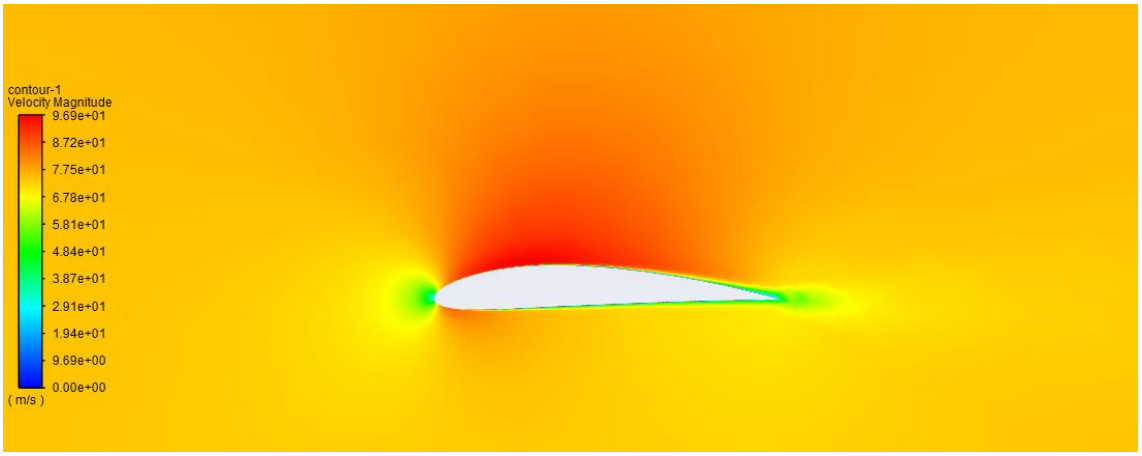

Figure 60.Velocity Contour 0º

- ***5º Analysis***

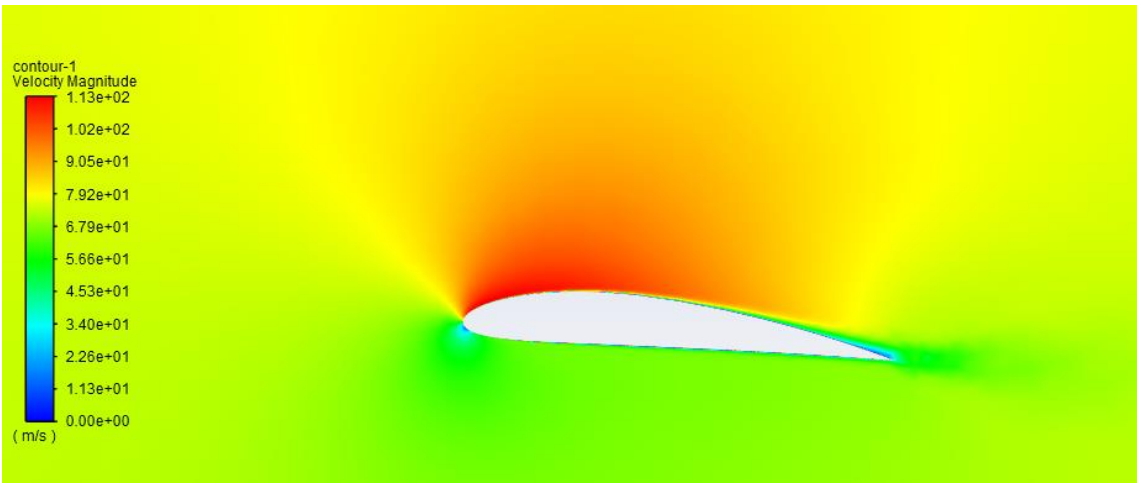

Figure 63. Velocity Contour 5º

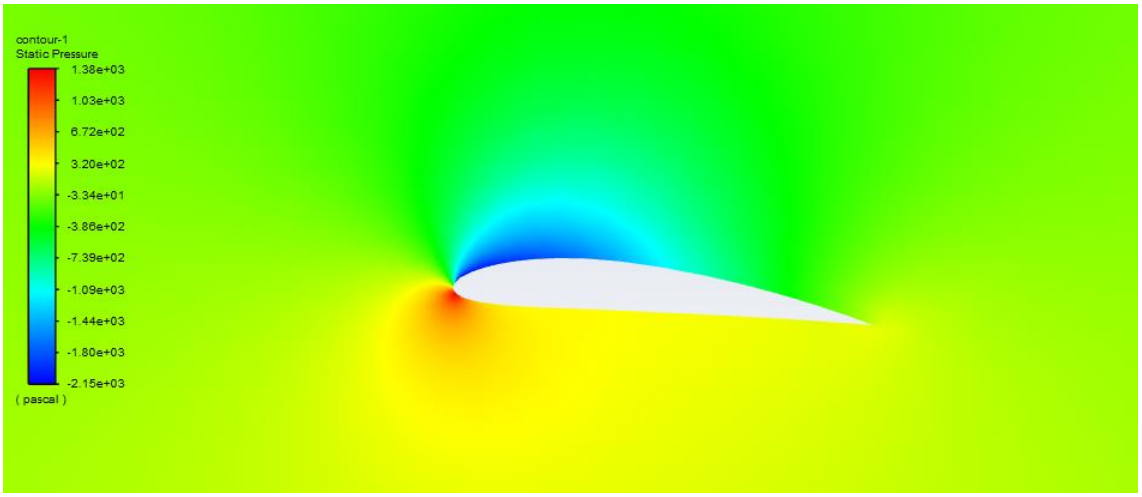

Figure 62. Static Pressure Contour 5º

- ***7º Analysis***.

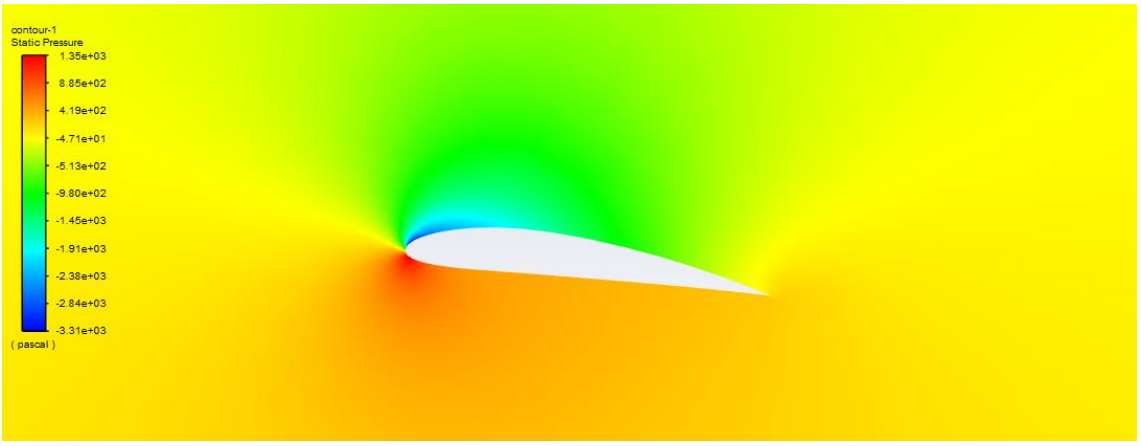

Figure 64. Static Pressure Contour 7º

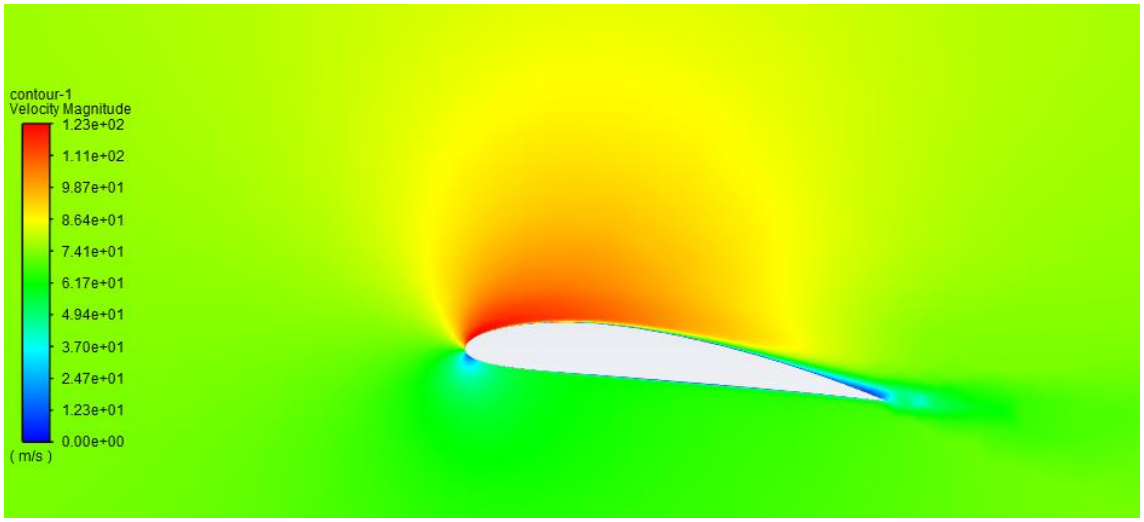

Figure 65. Velocity Contour 7º

- ***10º Analysis.***

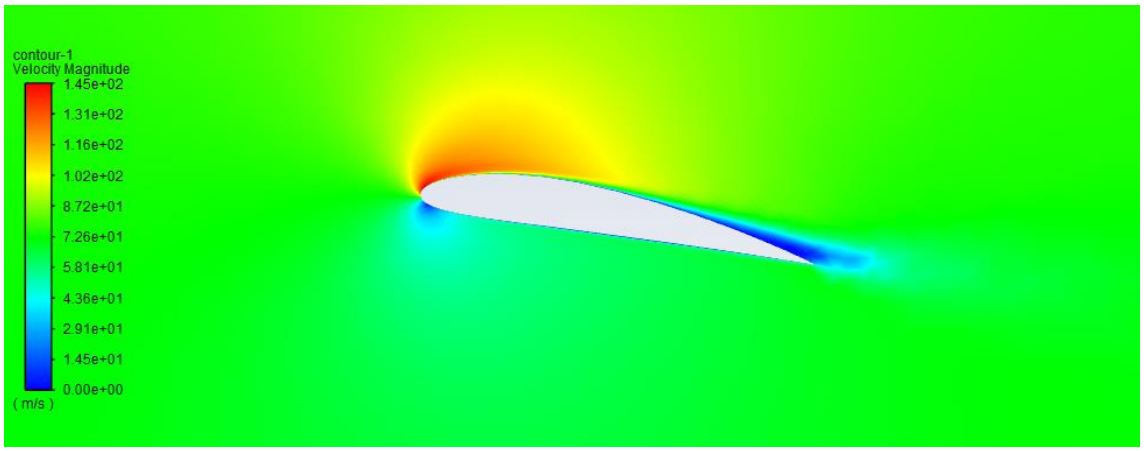

Figure 66. Velocity Contour 10º

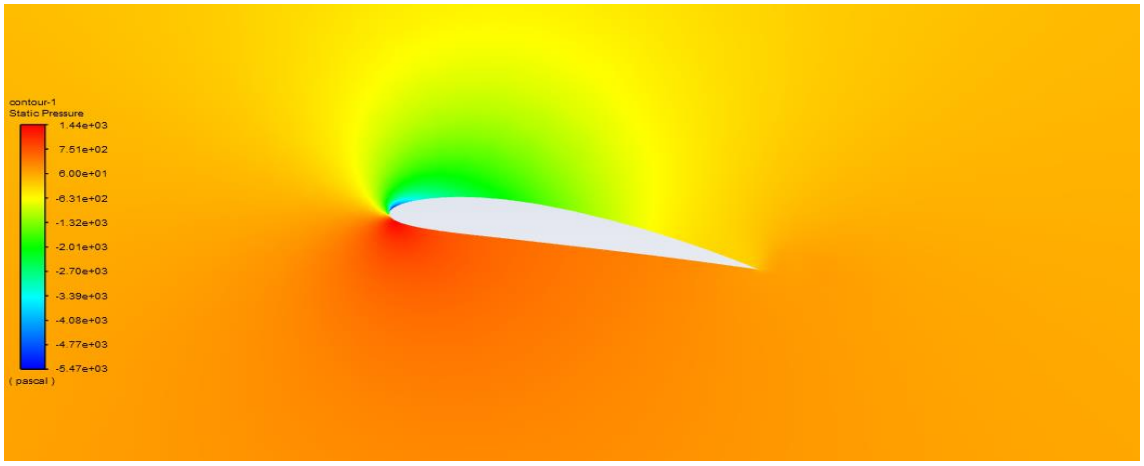

Figure 67. Pressure Contour 10º

- ***12º Analysis.***

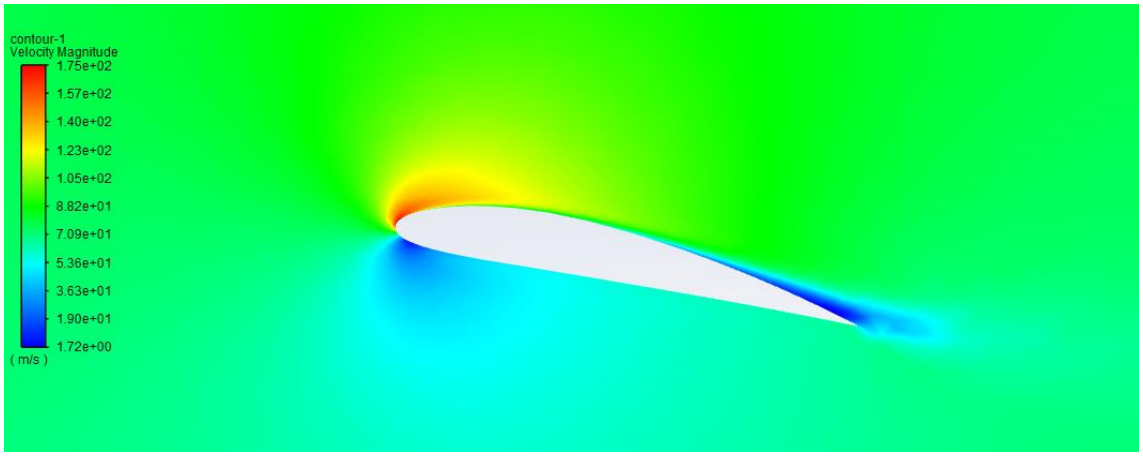

Figure 69. Velocity Contour 12º

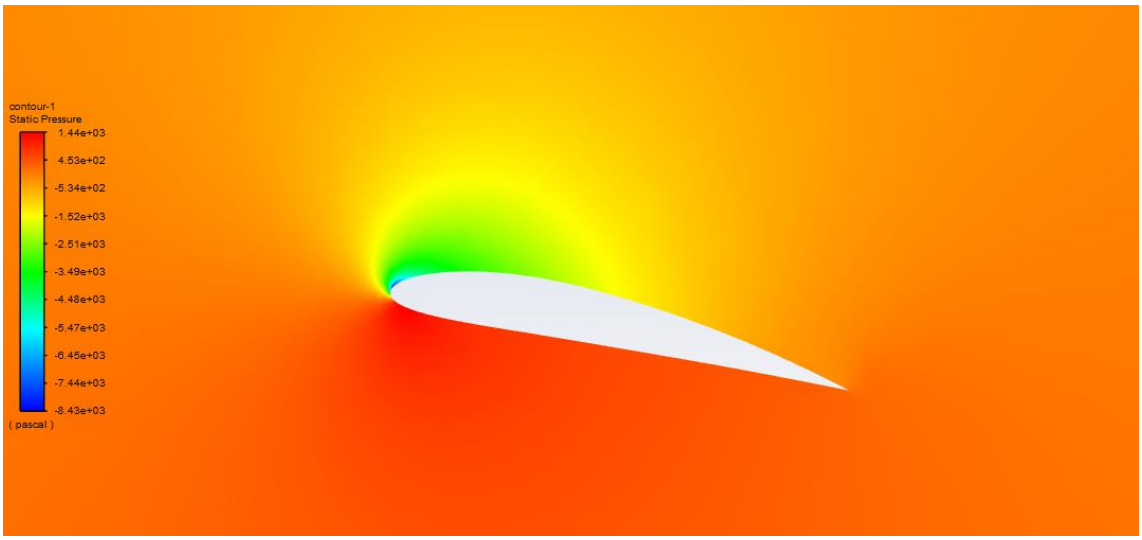

Figure 68. Static Pressure Contour 12º

- ***15º Analysis.***

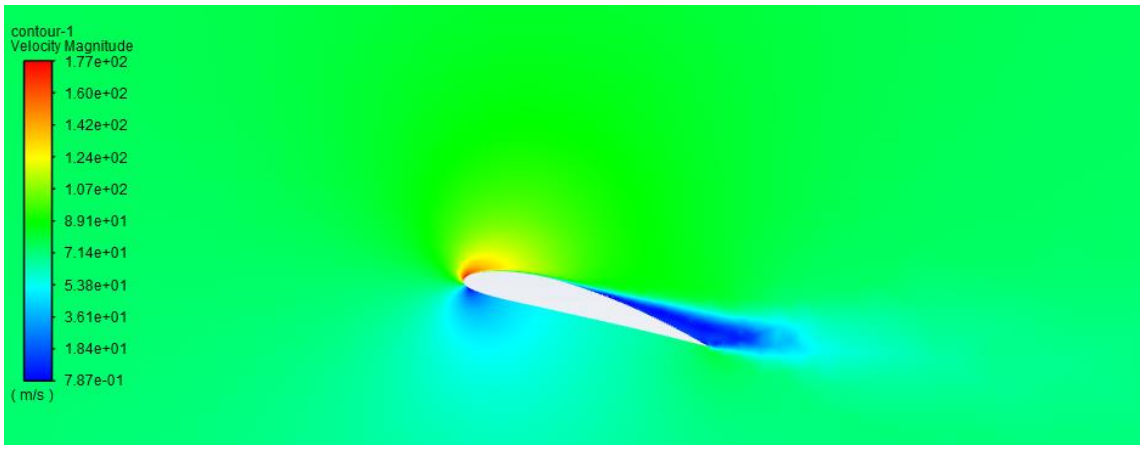

Figure 70. Velocity Contour 15º

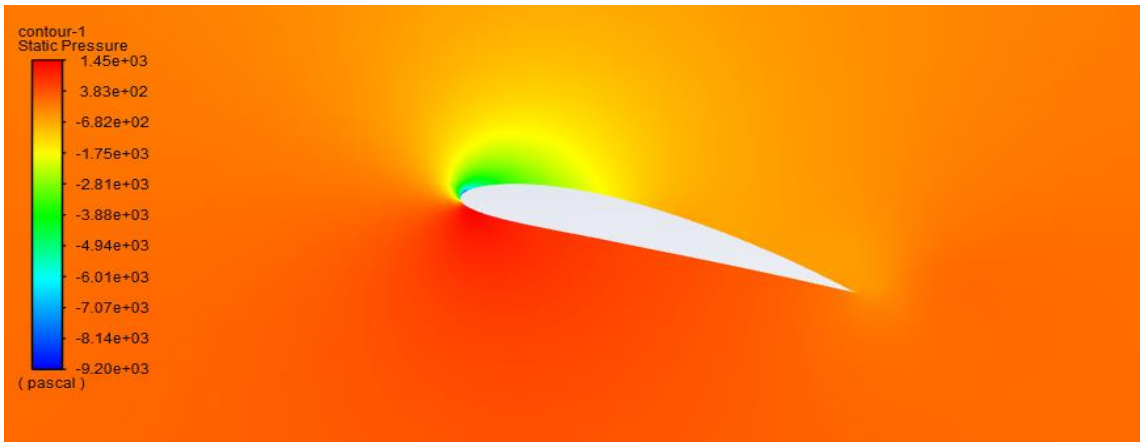

Figure 71. Pressure Contour 15º

- ***17º Analysis.***

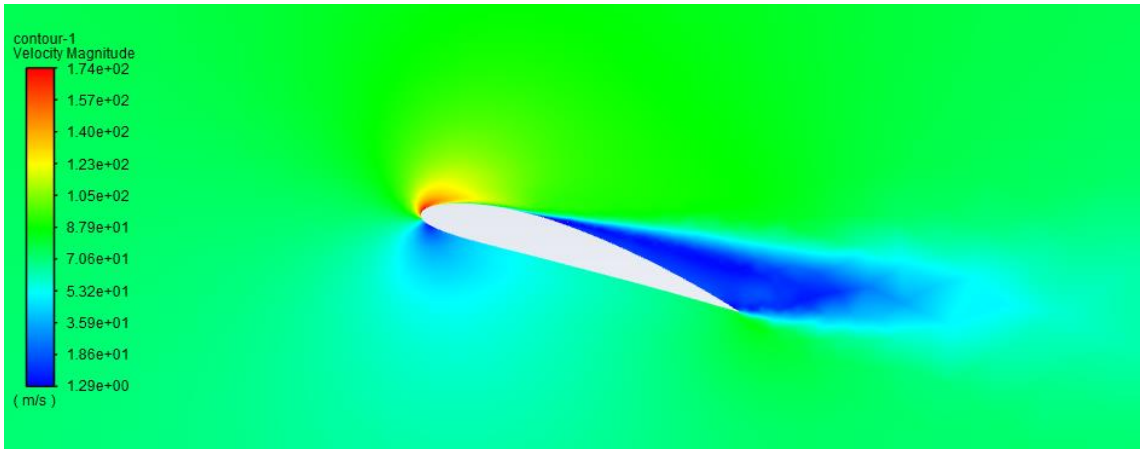

Figure 72. Velocity Contour 17º

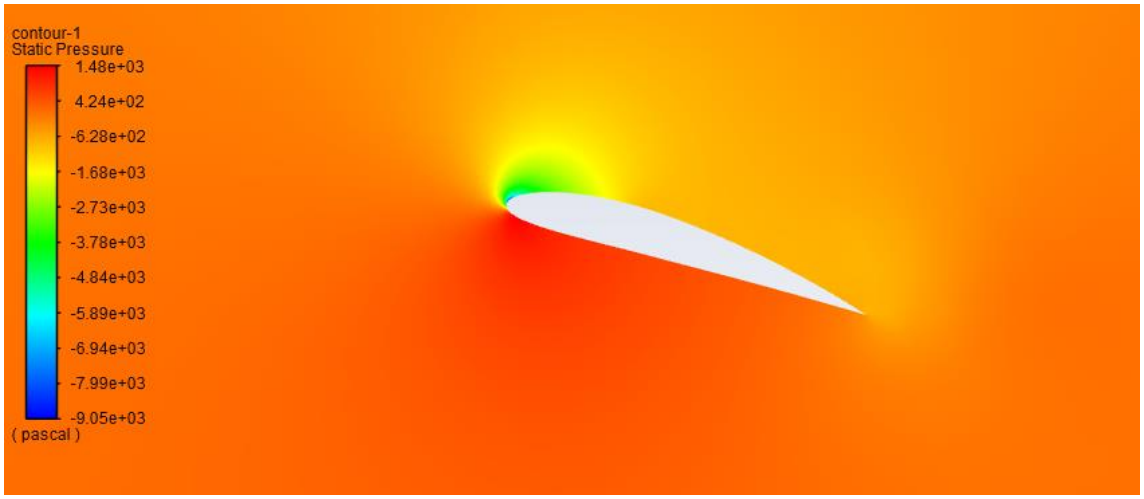

Figure 73. Pressure Contour 17º

- ***20º Analysis.***

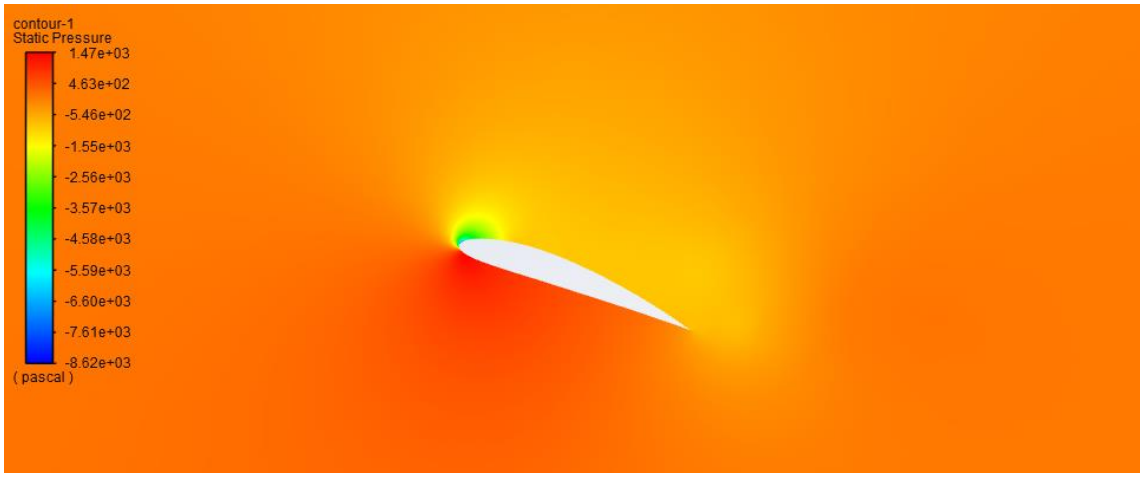

Figure 74. Pressure Contour 20º

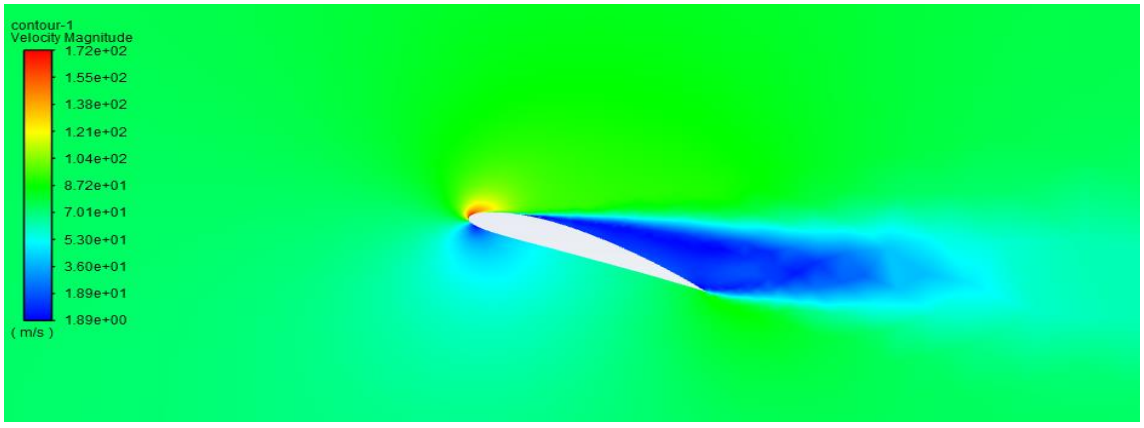

Figure 75. Velocity Contour 20º

Appendix 5. CFD 2D Wing & Flap Contour Results.

- ***Wing 0º. Velocity Contours***.

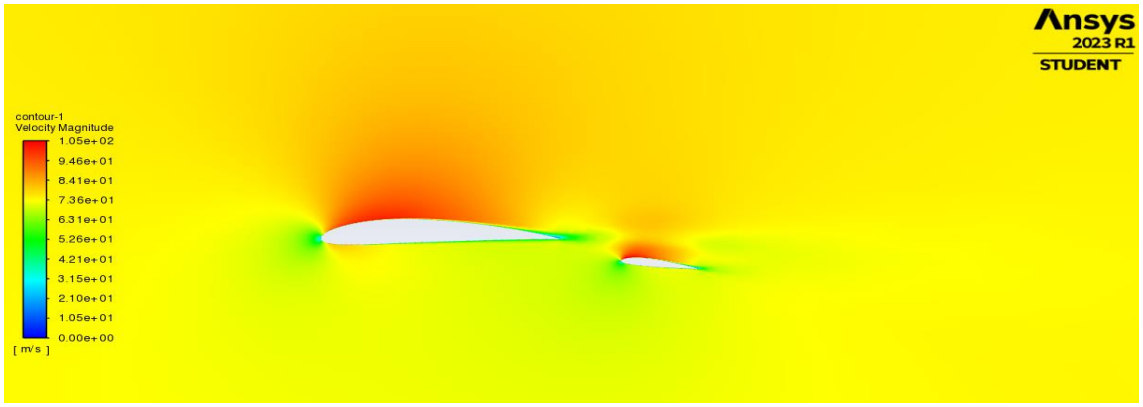

Figure 78. Velocity Contour Wing 0º Flap 7º.

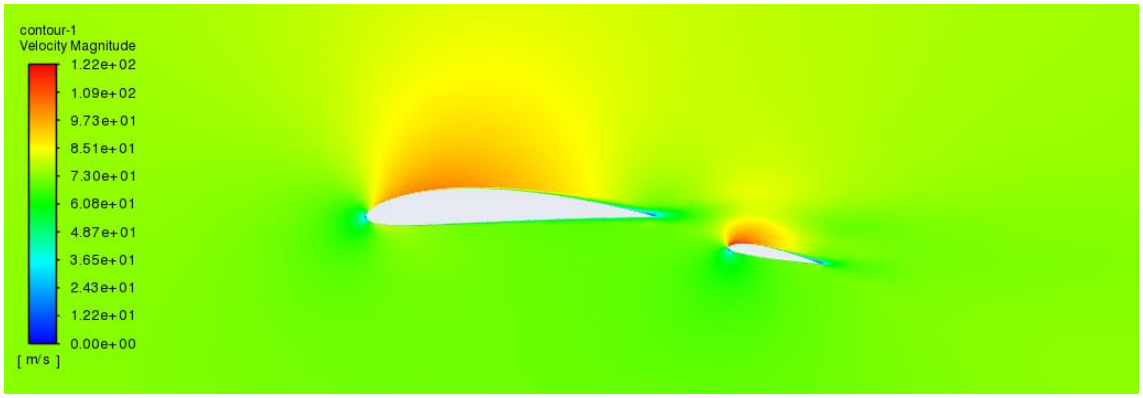

Figure 77. Velocity Contour Wing 0º Flap 10º.

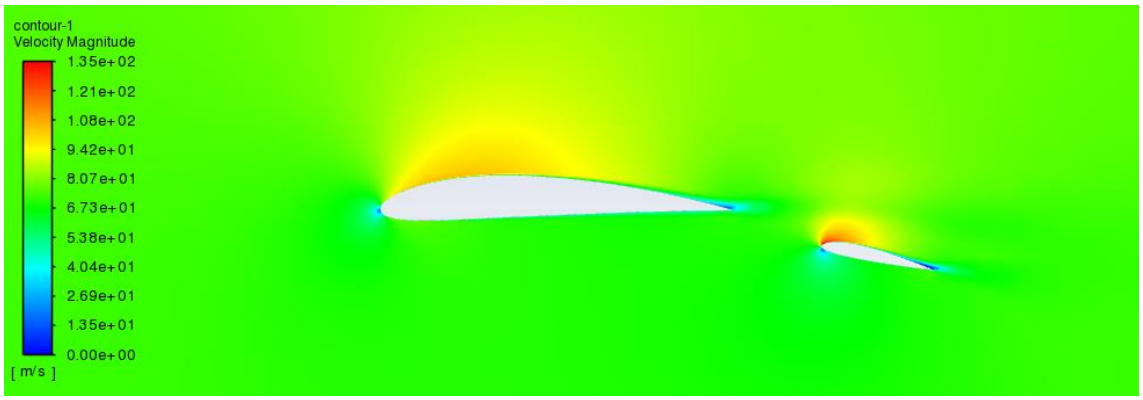

Figure 76. Velocity Contour Wing 0º Flap 15º.

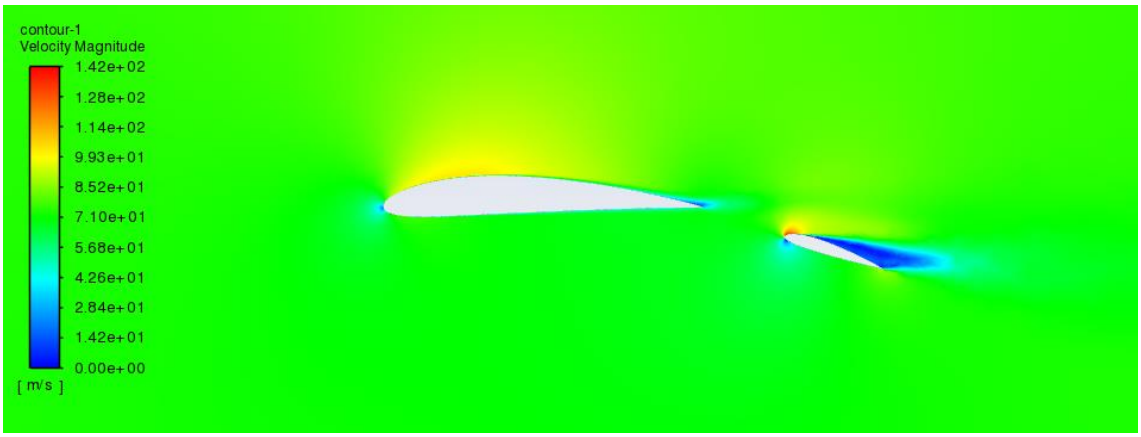

Figure 79. Velocity Contour Wing 0º Flap 18º.

- ***Wing 0º. Pressure Contours***.

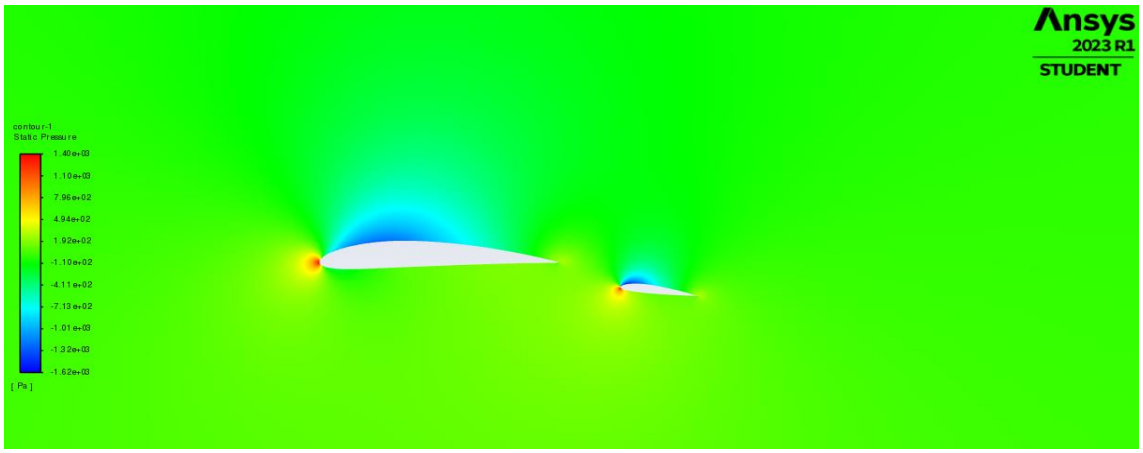

Figure 80. Pressure Contour Wing 0º Flap 7º.

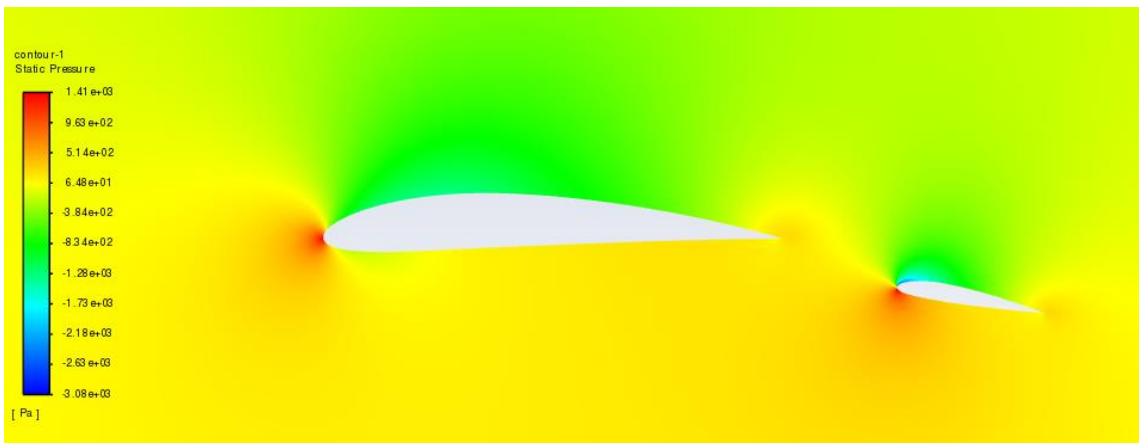

Figure 81. Pressure Contour Wing 0º Flap 10º.

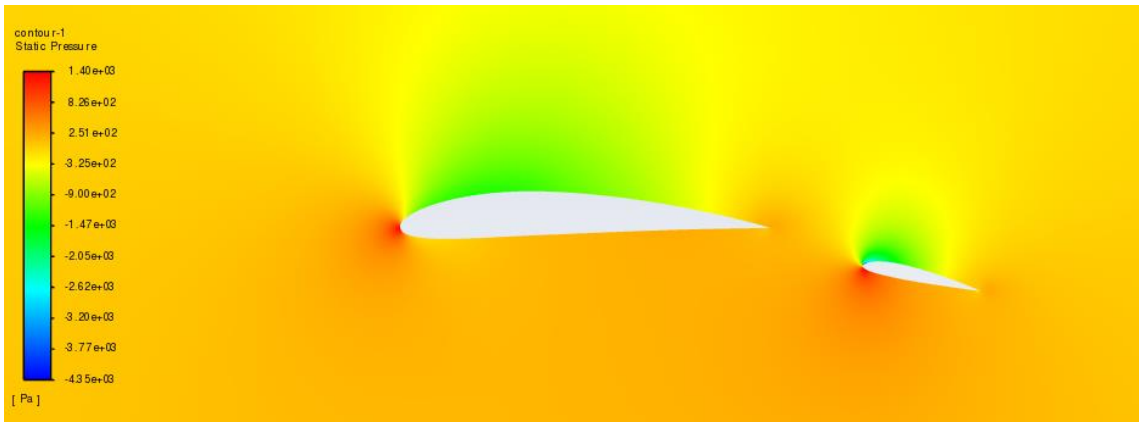

Figure 83. Pressure Contour Wing 0º Flap 12º.

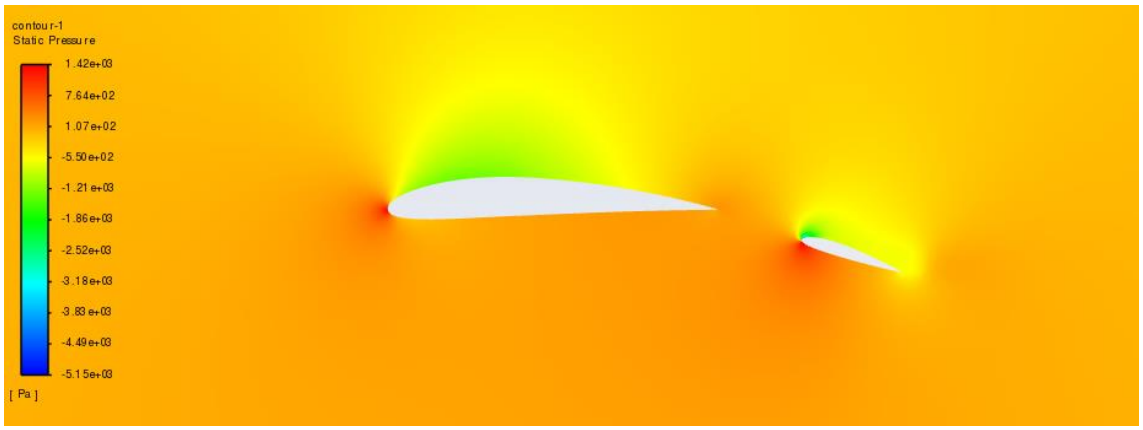

Figure 82. Pressure Contour Wing 0º Flap 18º.

- ***Wing 5º. Velocity Contours***.

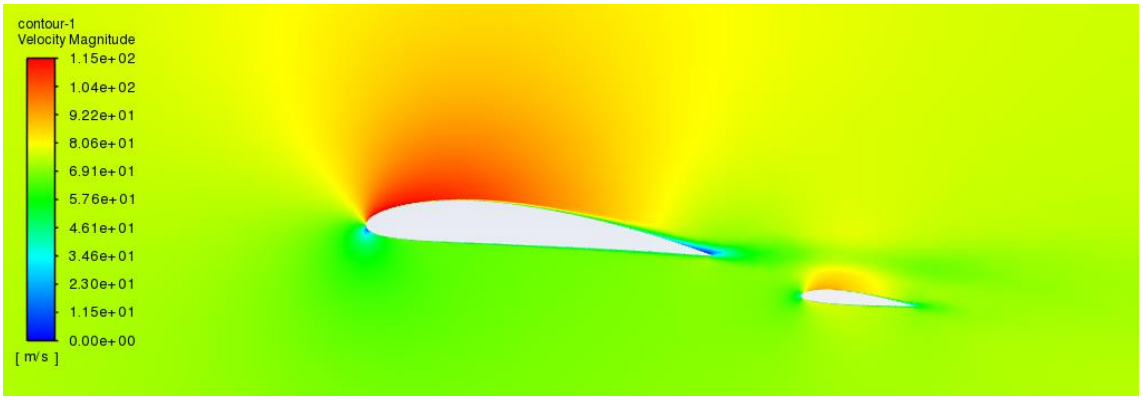

Figure 84. Velocity Contour Wing 5º Flap 5º.

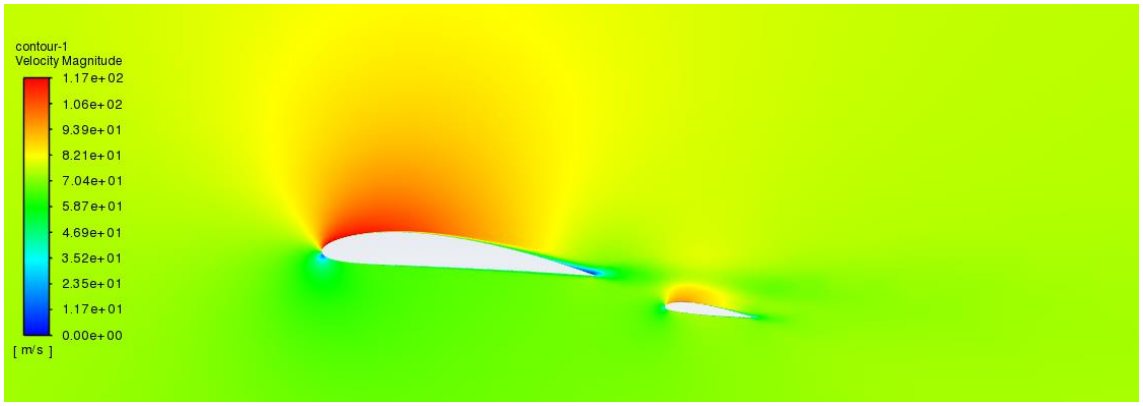

Figure 87. Velocity Contour Wing 5º Flap 7º.

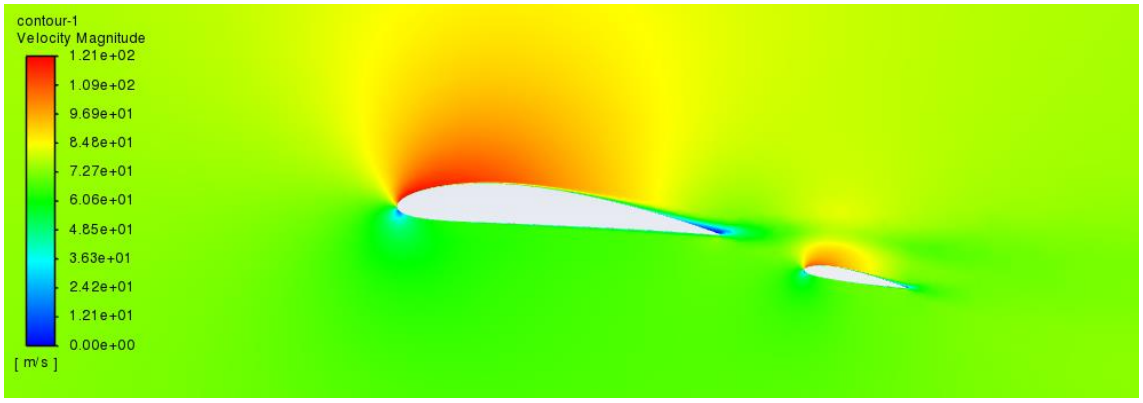

Figure 86. Velocity Contour Wing 5º Flap 10º.

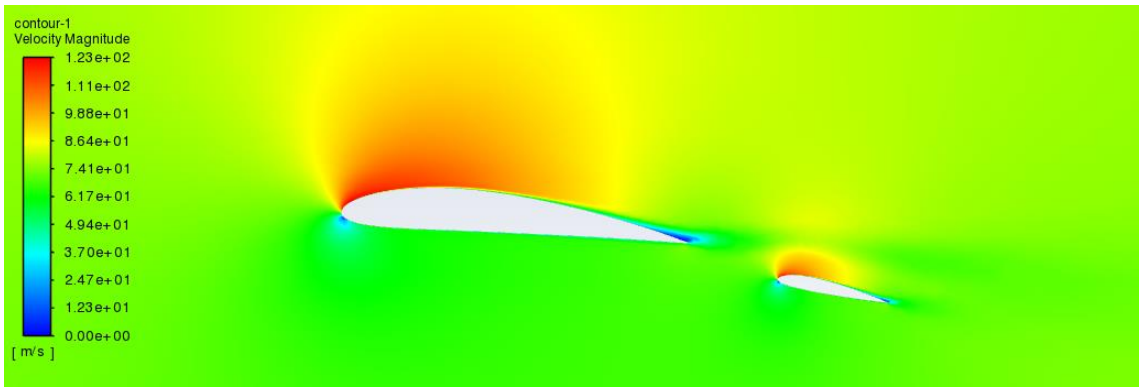

Figure 85. Velocity Contour Wing 5º Flap 12º.

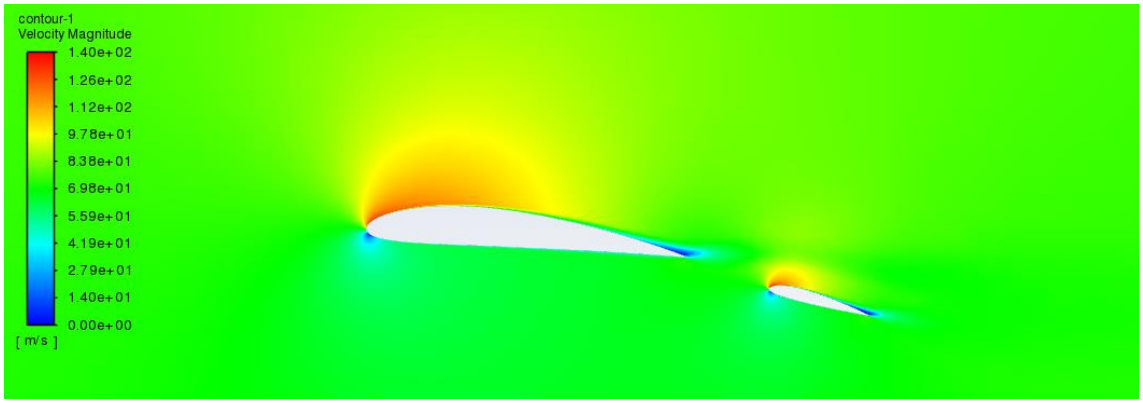

Figure 89. Velocity Contour Wing 5º Flap 15º.

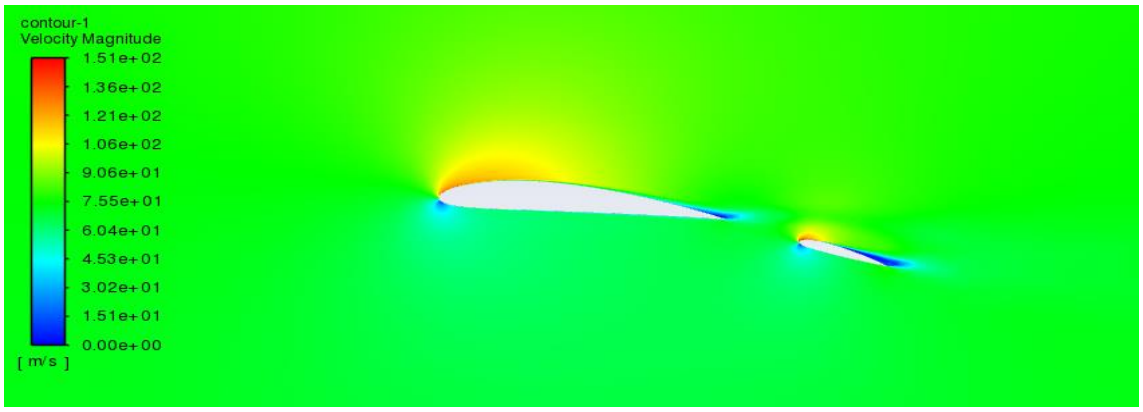

Figure 88. Velocity Contour Wing 5º Flap 18º.

- ***Wing 5º. Pressure Contours***.

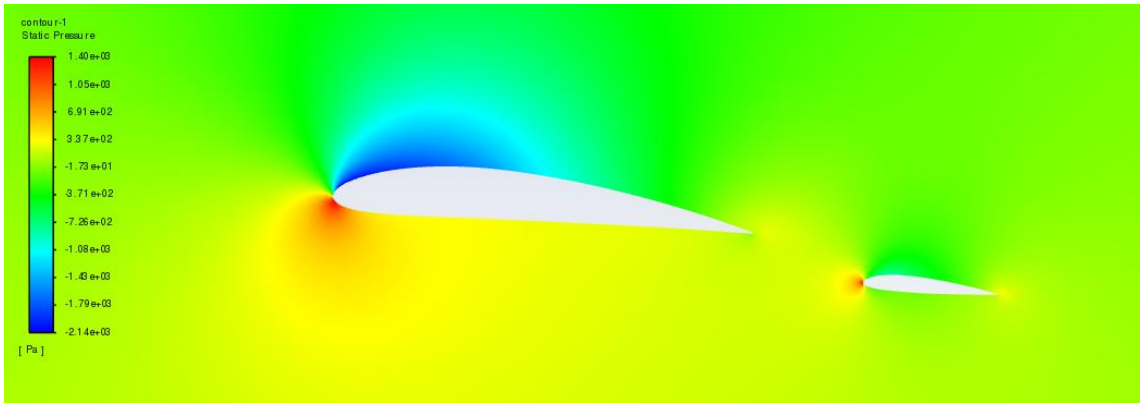

Figure 90. Pressure Contour Wing 5º Flap 5º.

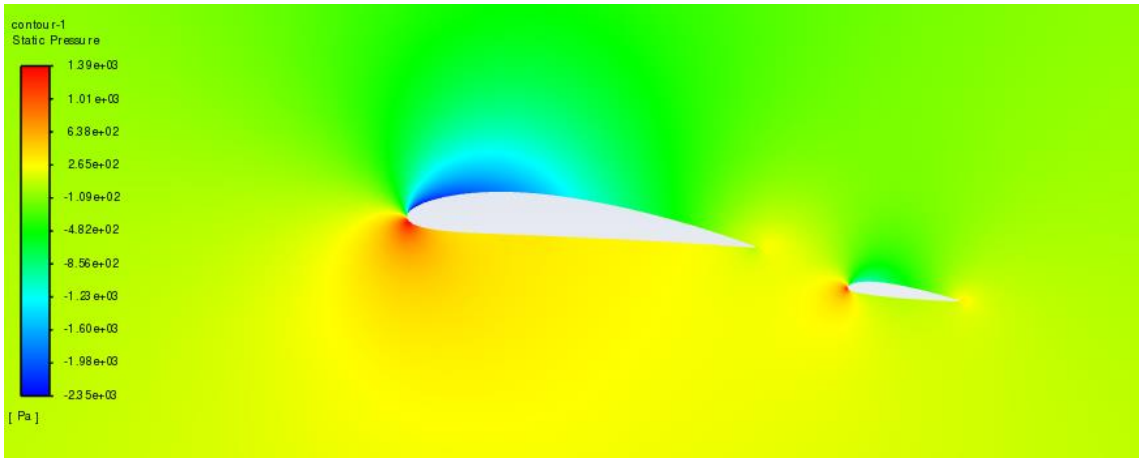

Figure 93.Pressure Contour Wing 5º Flap 7º.

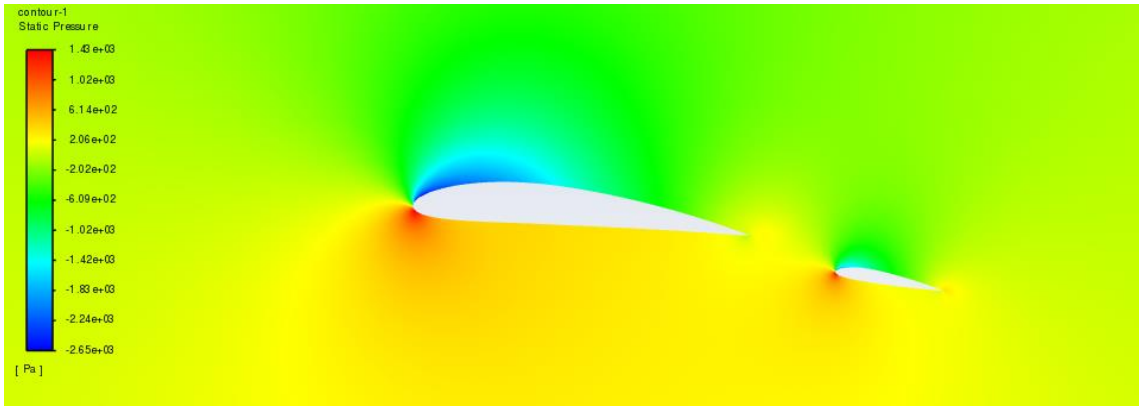

Figure 92. Pressure Contour Wing 5º Flap 10º.

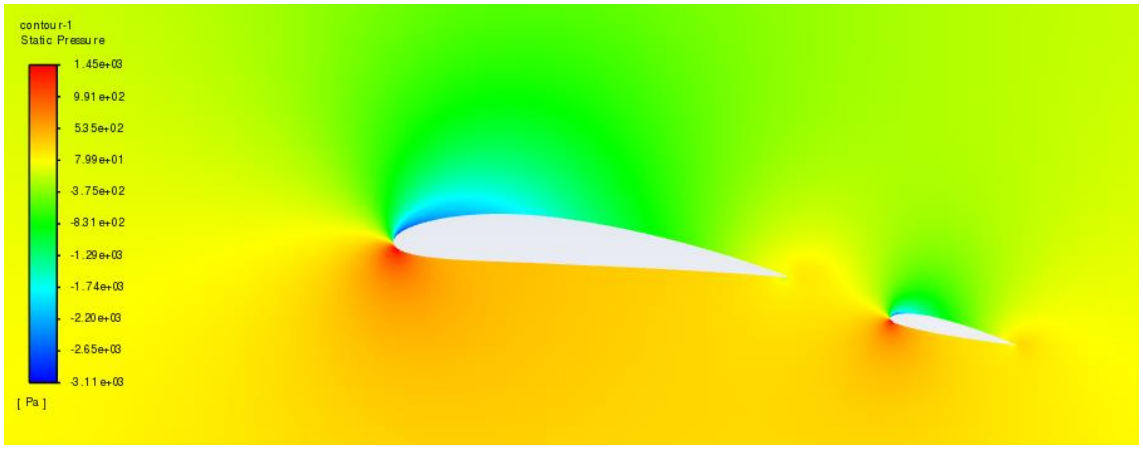

Figure 91. Pressure Contour Wing 5º Flap 12º.

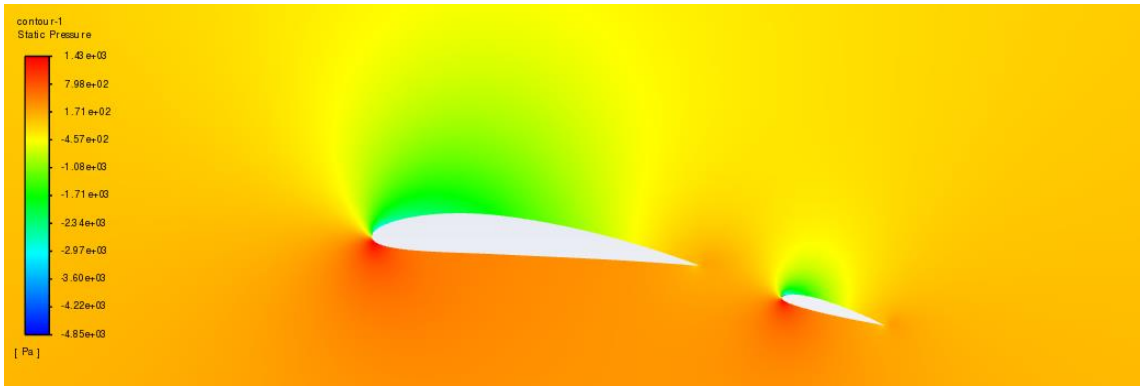

Figure 94. Pressure Contour Wing 5º Flap 15º.

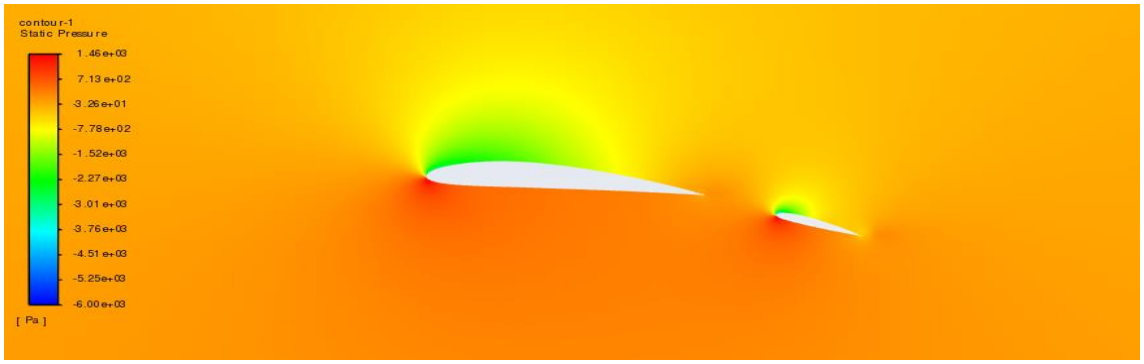

Figure 95. Pressure Contour Wing 5º Flap 18º.

- ***Wing 7º. Velocity Contour***

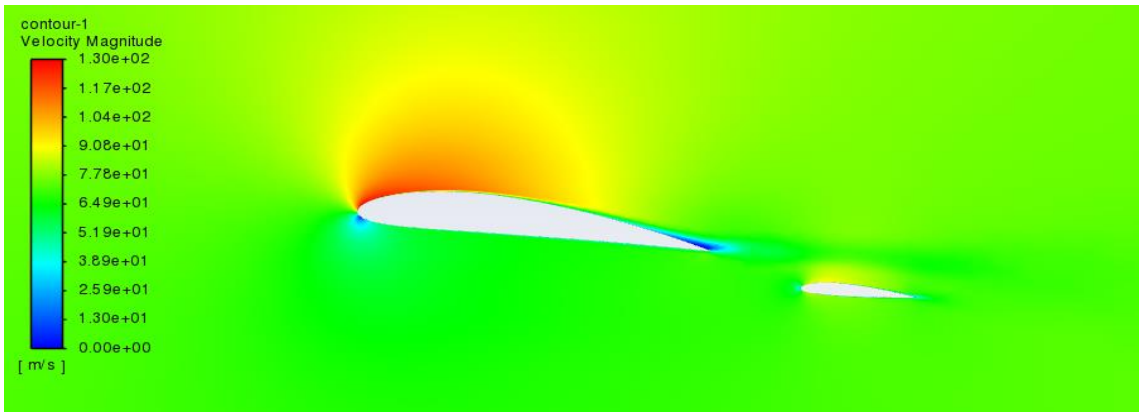

Figure 96. Velocity Contour Wing 7º Flap 5º.

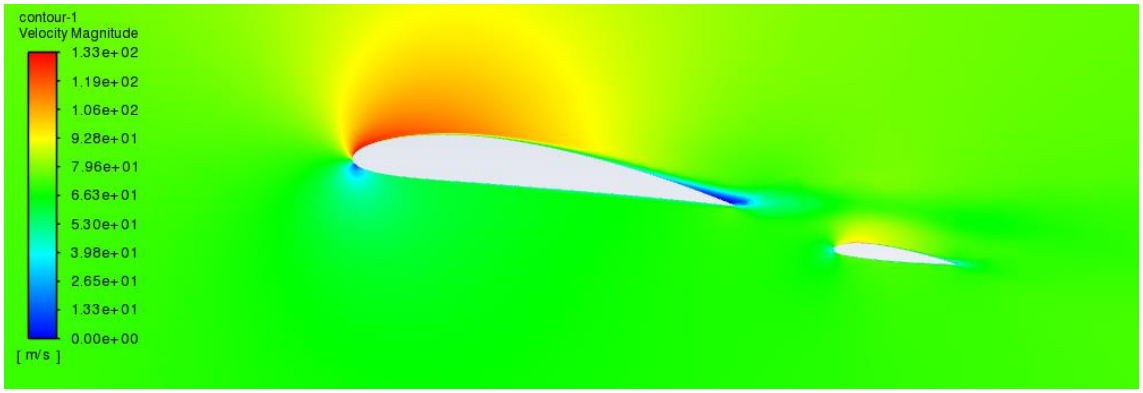

Figure 99. Velocity Contour Wing 7º Flap 7º.

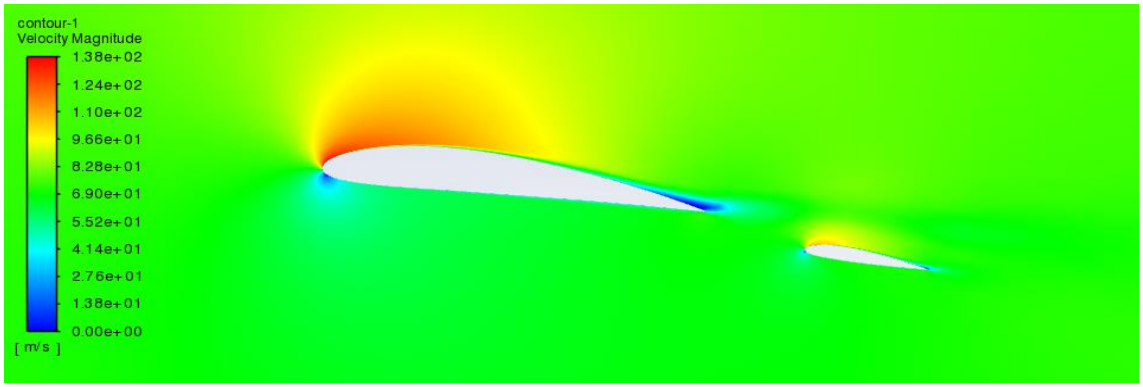

Figure 97. Velocity Contour Wing 7º Flap 10º.

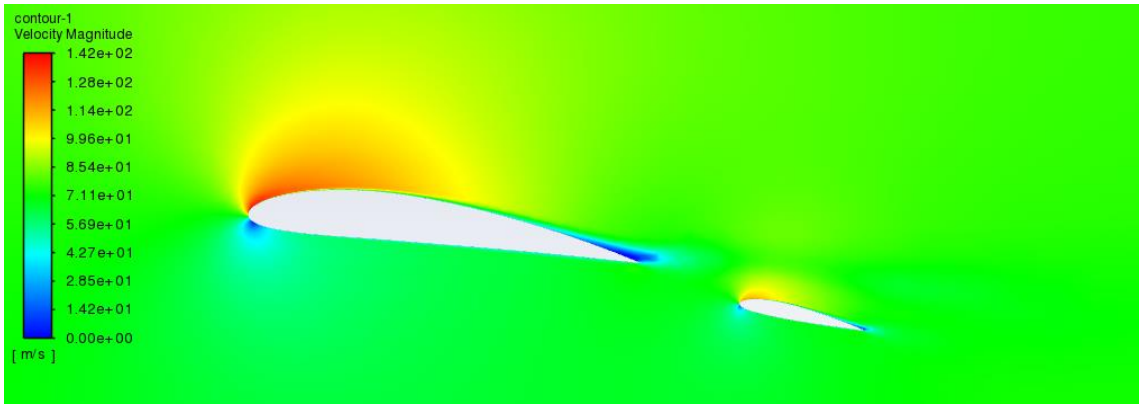

Figure 98. Velocity Contour Wing 7º Flap 12º.

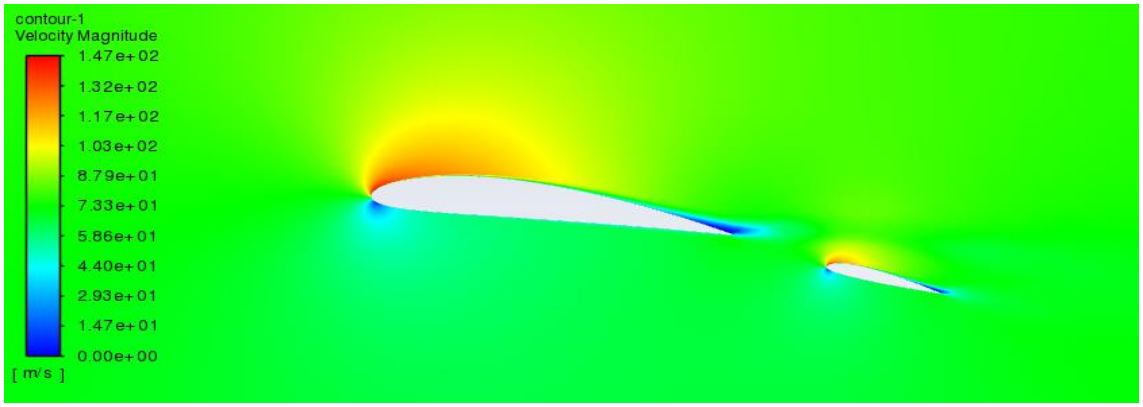

Figure 101. Velocity Contour Wing 7º Flap 15º.

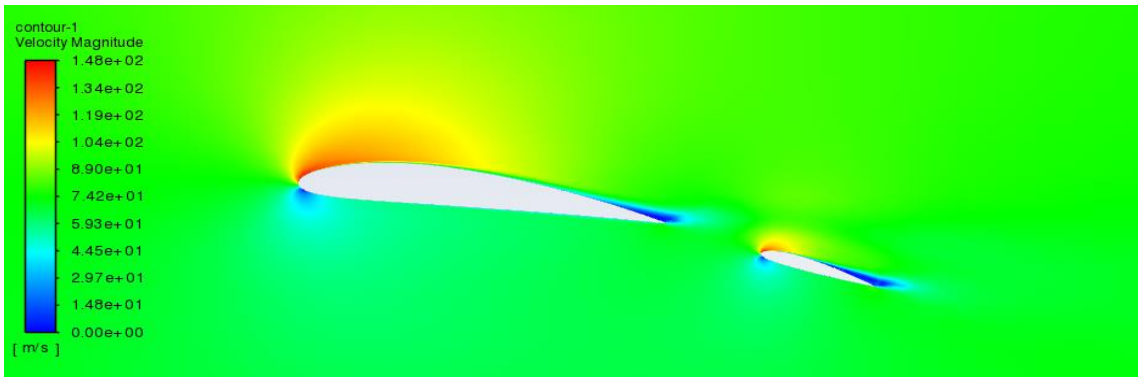

Figure 100. Velocity Contour Wing 7º Flap 18º.

- ***Wing 7º. Pressure Contours.***

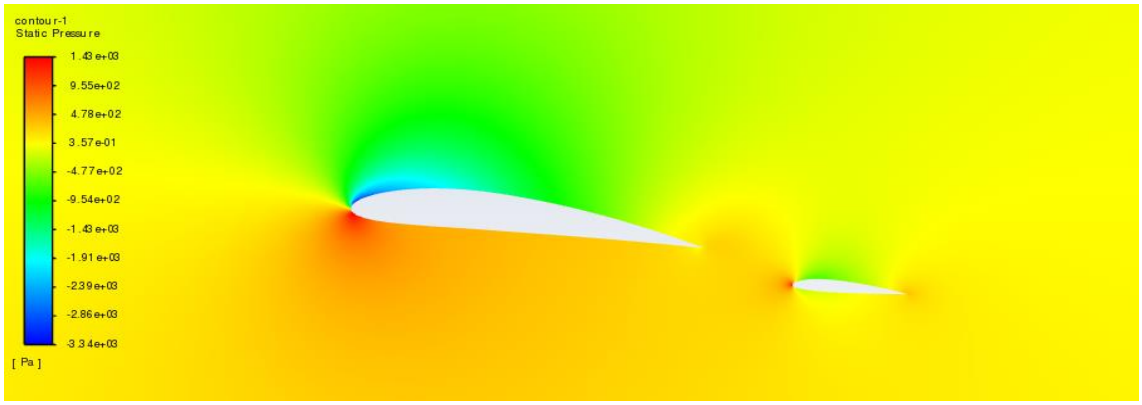

Figure 102. Pressure Contour Wing 7º Flap 5º.

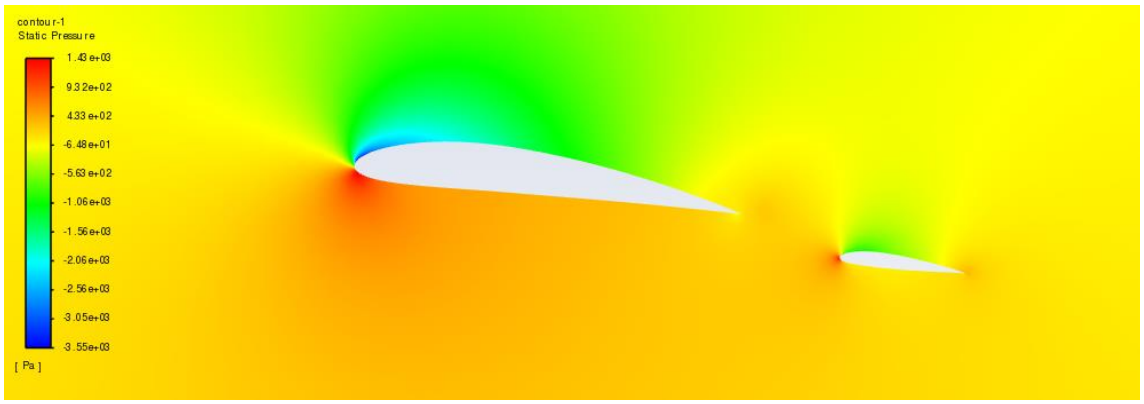

Figure 103. Pressure Contour Wing 7º Flap 7º.

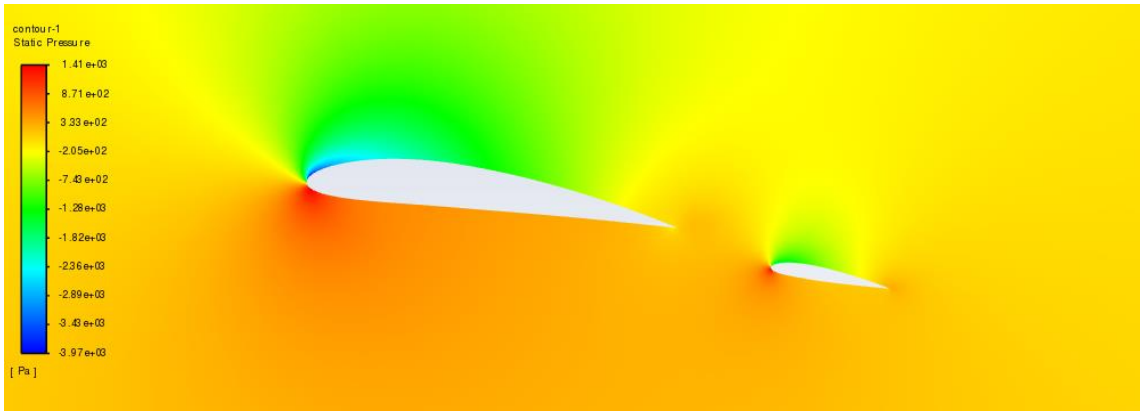

Figure 104. Pressure Contour Wing 7º Flap 10º.

Figure 105. Pressure Contour Wing 7º Flap 12º.

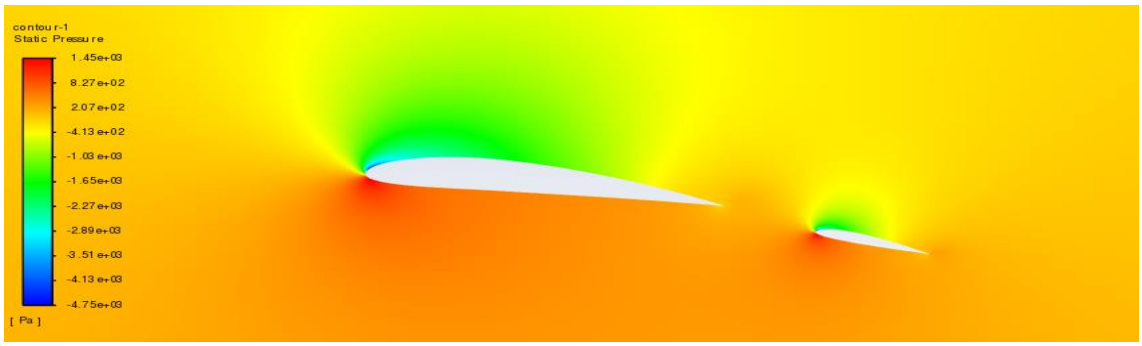

Figure 106. Pressure Contour Wing 7º Flap 15º.

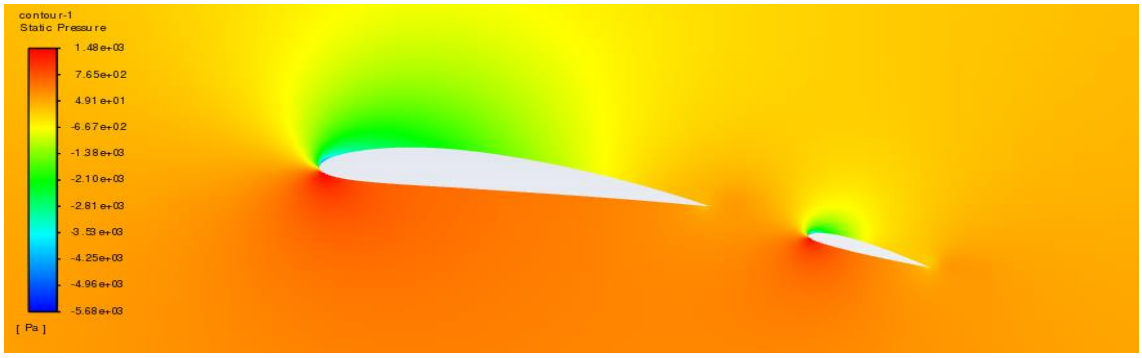

Figure 107. Pressure Contour Wing 7º Flap 18º.

- ***Wing 10º. Velocity Contour***.

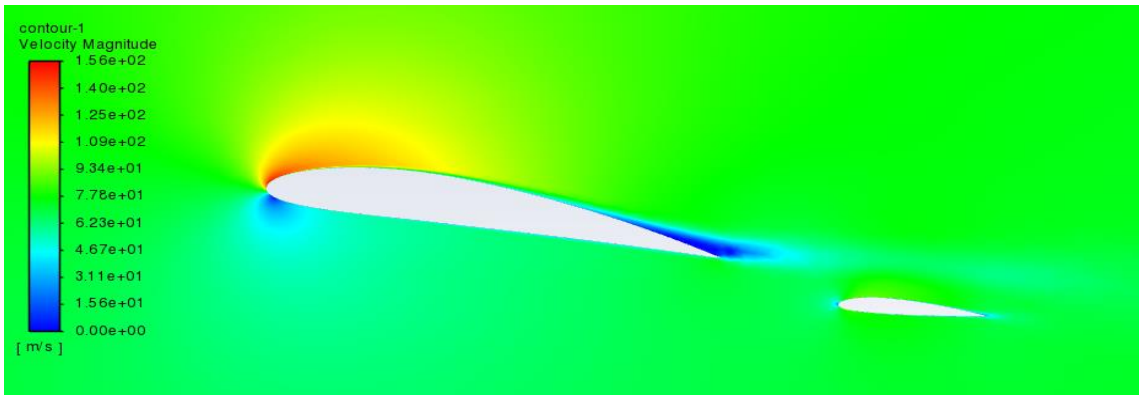

Figure 108. Velocity Contour Wing 10º Flap 5º.

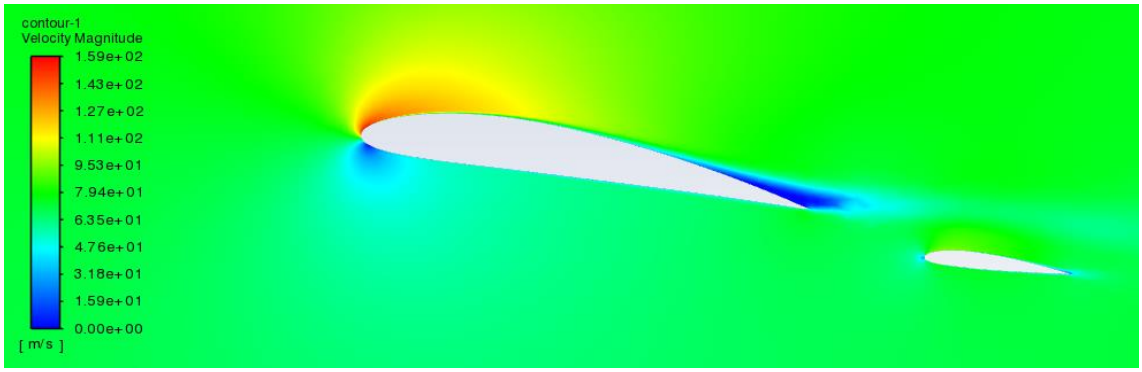

Figure 109. Velocity Contour Wing 10º Flap 7º.

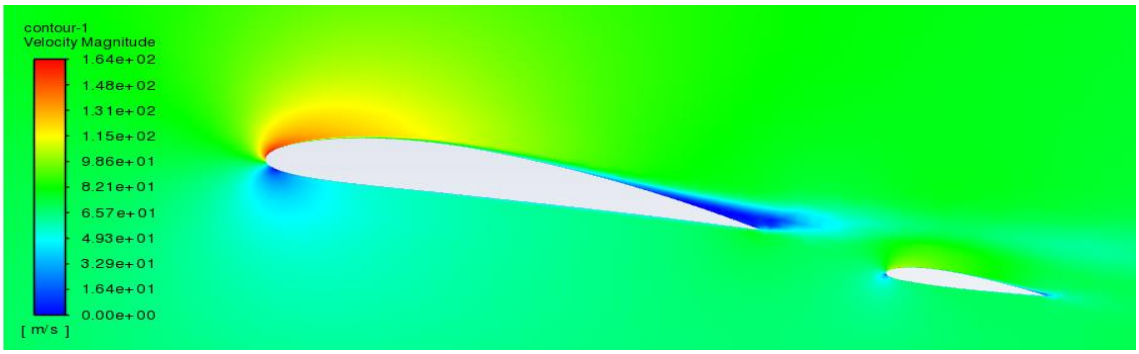

Figure 110. Velocity Contour Wing 10º Flap 10º.

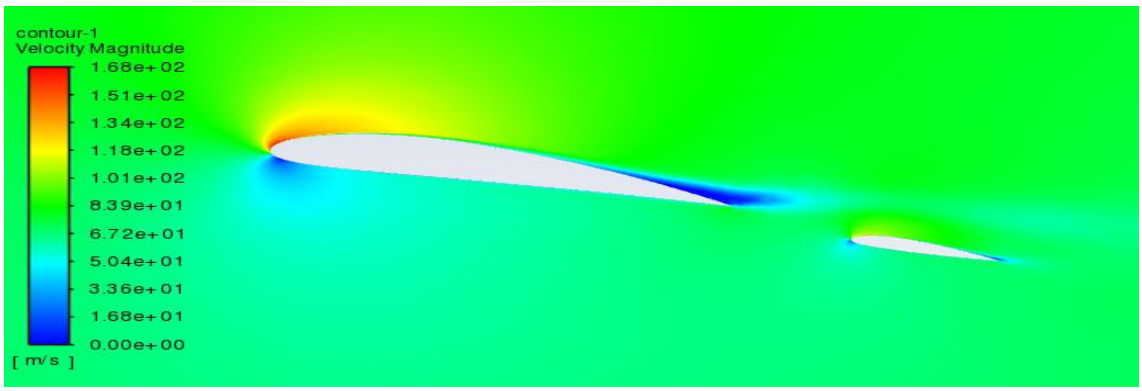

Figure 111. Velocity Contour Wing 10º Flap 12º.

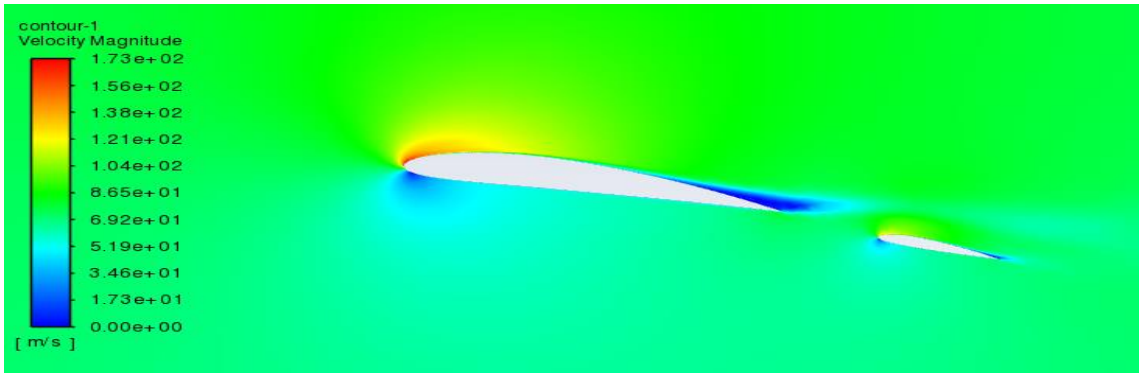

Figure 112. Velocity Contour Wing 10º Flap 15º.

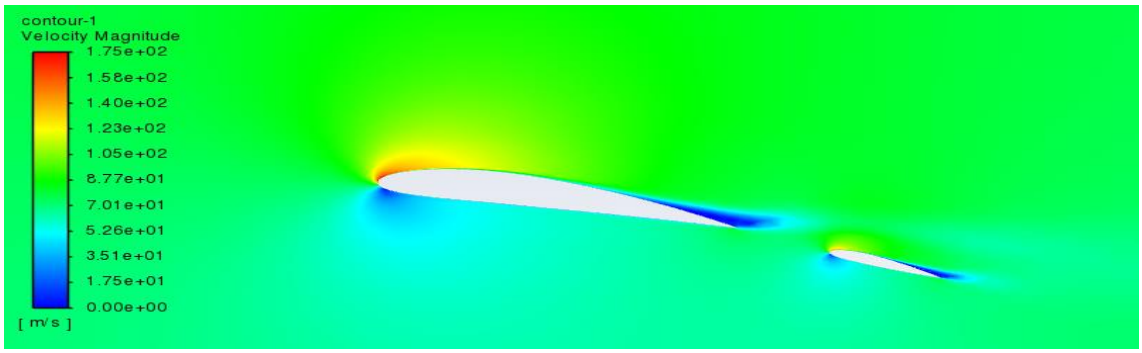

Figure 113. Velocity Contour Wing 10º Flap 18º.

- ***Wing 10º. Pressure Contour***.

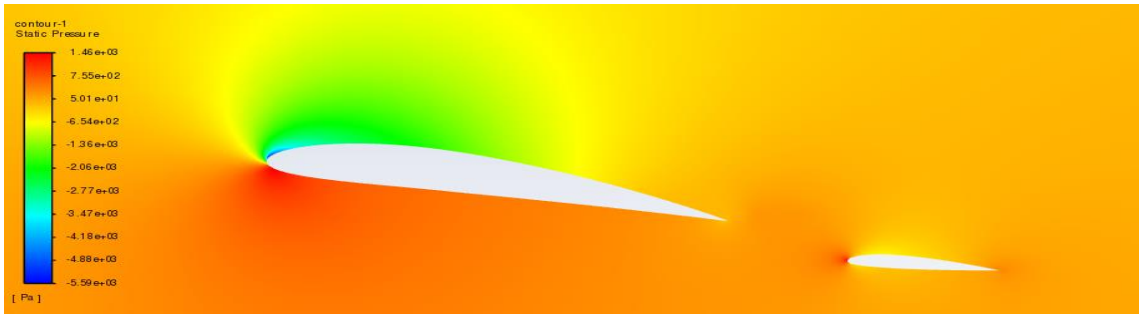

Figure 114. Pressure Contour Wing 10º Flap 5º.

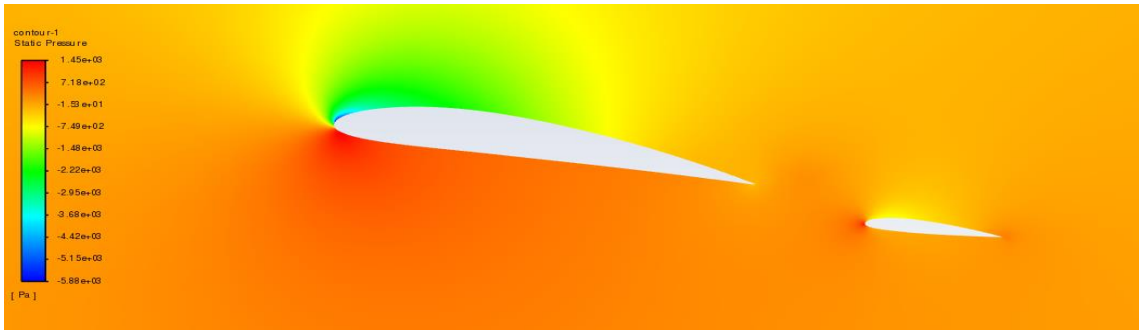

Figure 115. Pressure Contour Wing 10º Flap 7º.

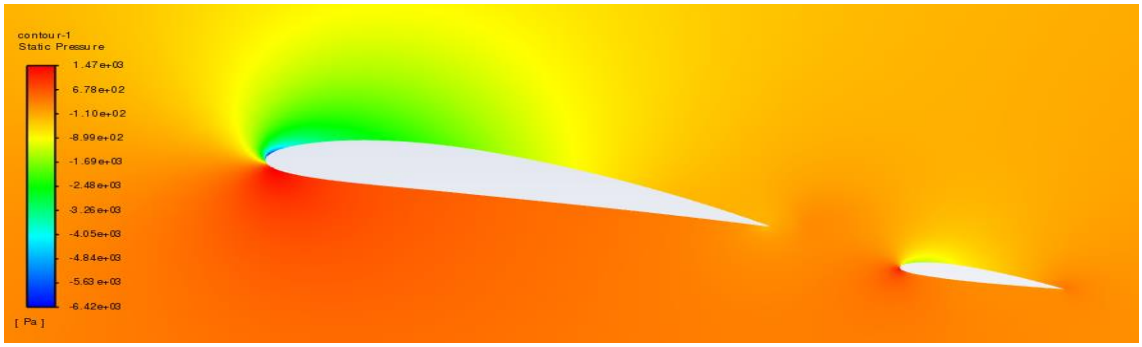

Figure 116. Pressure Contour Wing 10º Flap 10º.

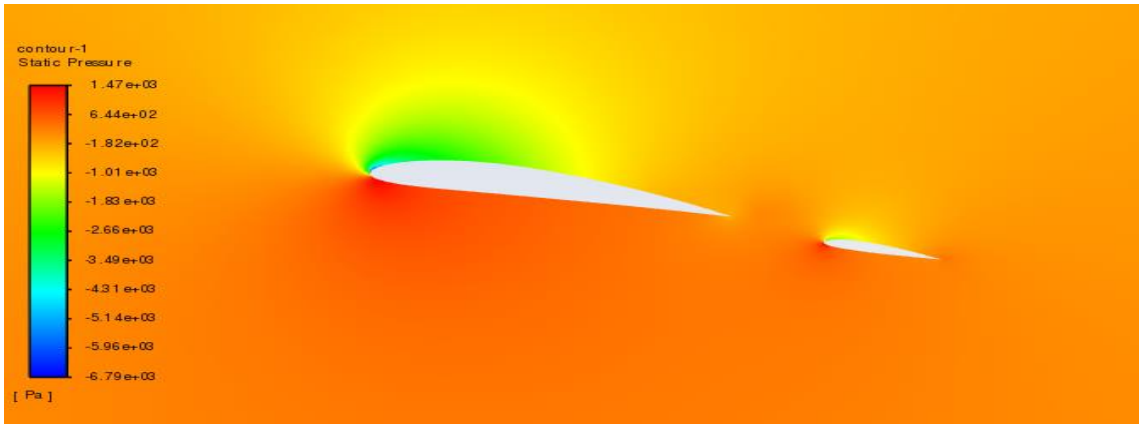

Figure 117. Pressure Contour Wing 10º Flap 12º.

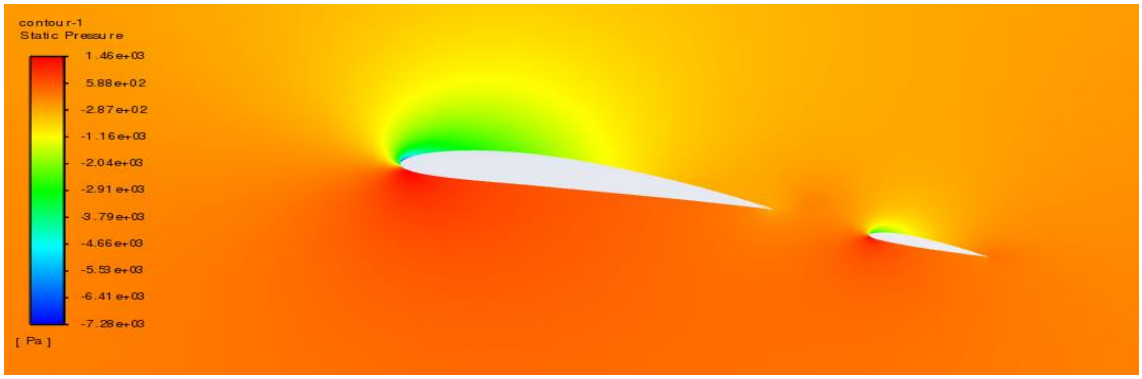

Figure 118. Pressure Contour Wing 10º Flap 15º.

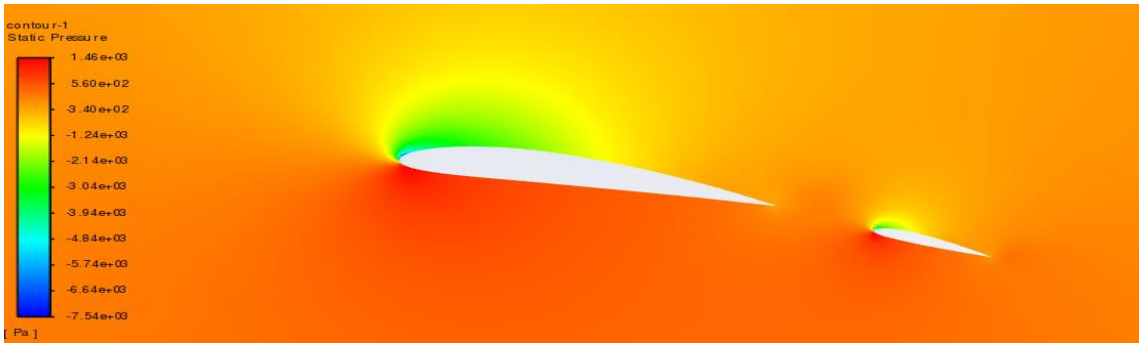

Figure 119. Pressure Contour Wing 10º Flap 18º.

- ***Wing 12º. Velocity Contour***.

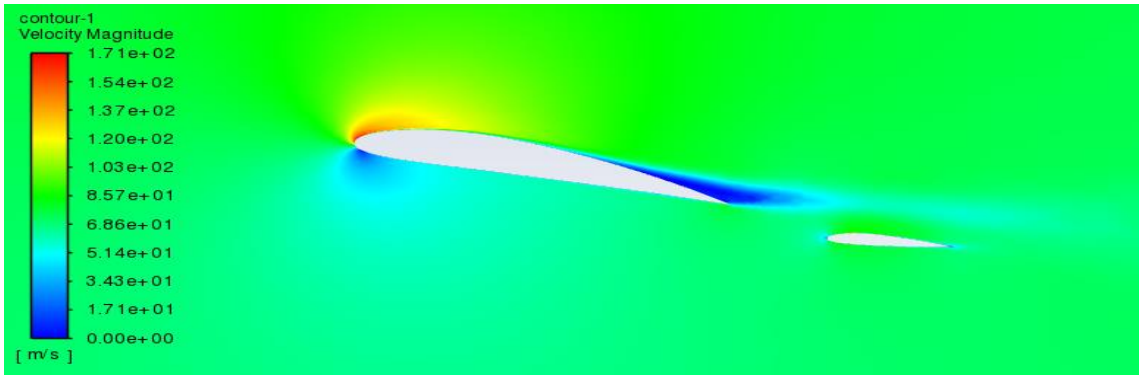

Figure 120. Velocity Contour Wing 12º Flap 5º.

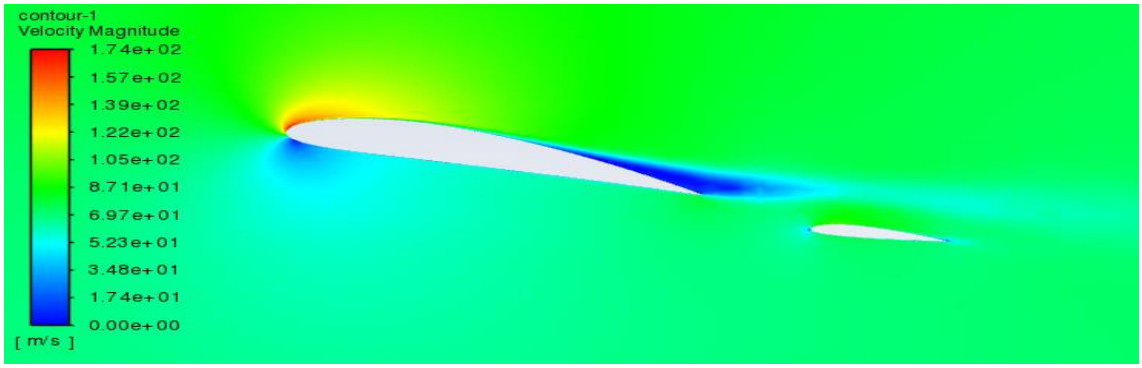

Figure 121. Velocity Contour Wing 12º Flap 7º.

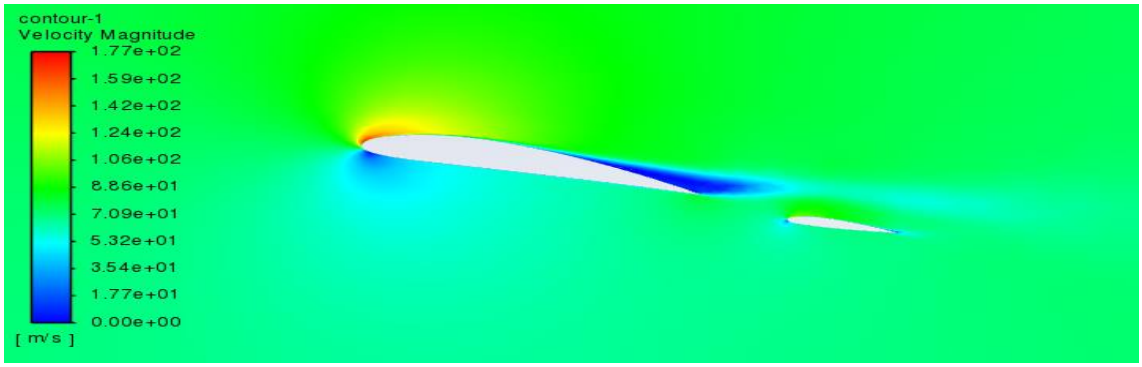

Figure 122. Velocity Contour Wing 12º Flap 10º.

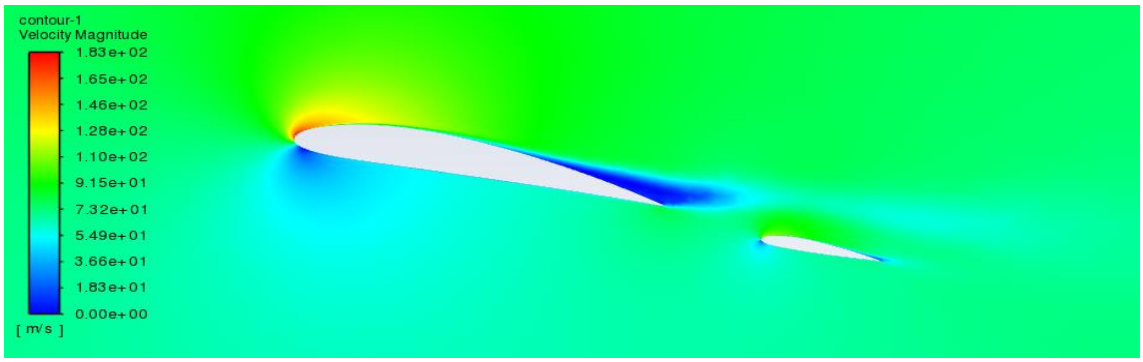

Figure 123. Velocity Contour Wing 12º Flap 12º.

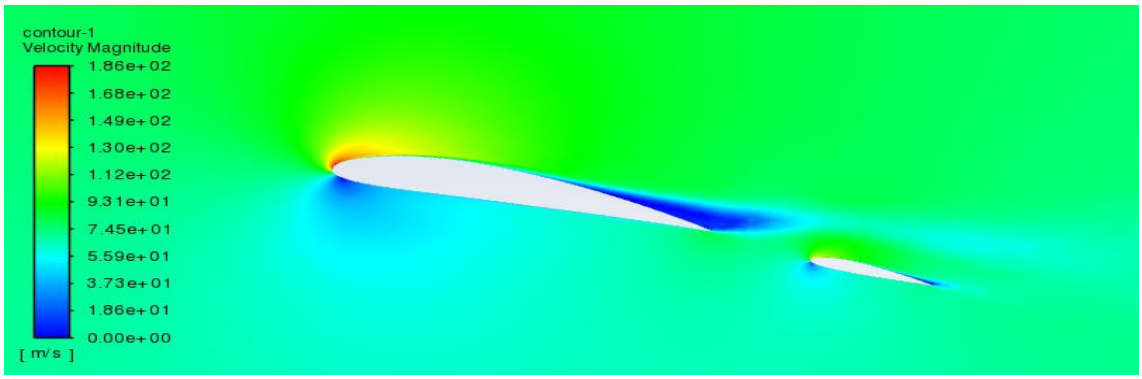

Figure 124. Velocity Contour Wing 12º Flap 15º.

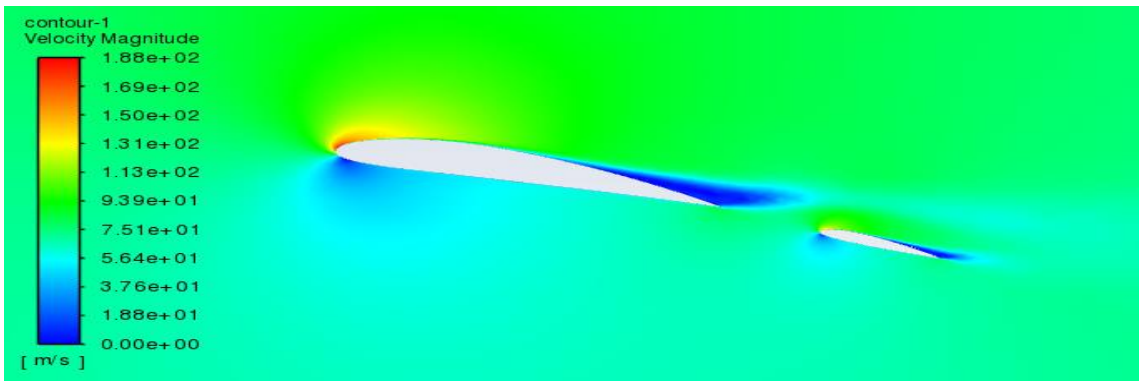

Figure 125. Velocity Contour Wing 12º Flap 18º.

- ***Wing 12º. Pressure Contour***.

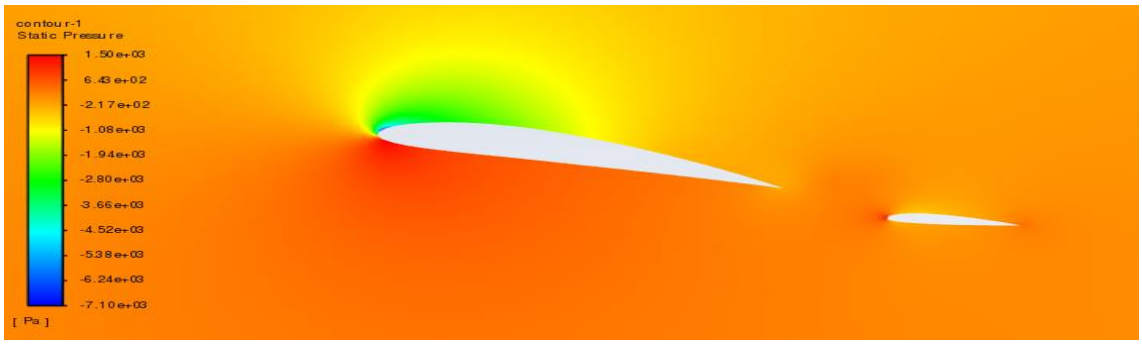

Figure 126. Pressure Contour Wing 12º Flap 5º.

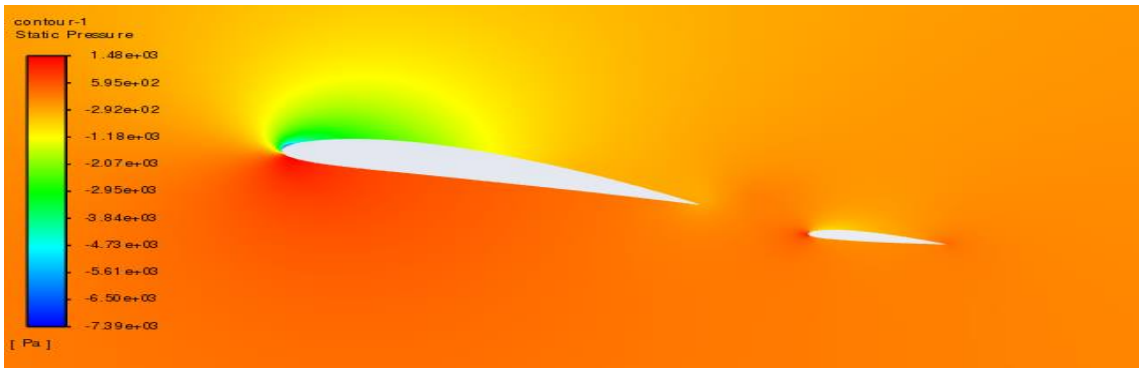

Figure 127. Pressure Contour Wing 12º Flap 7º.

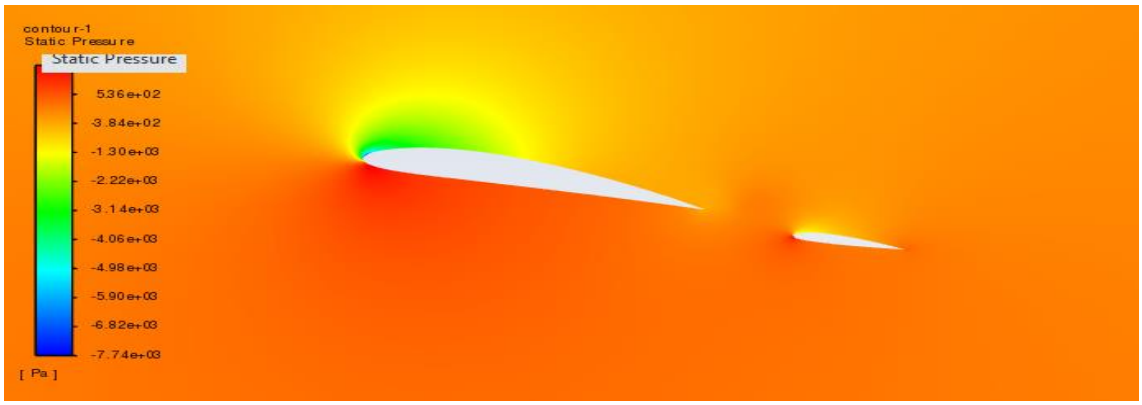

Figure 128. Pressure Contour Wing 12º Flap 10º.

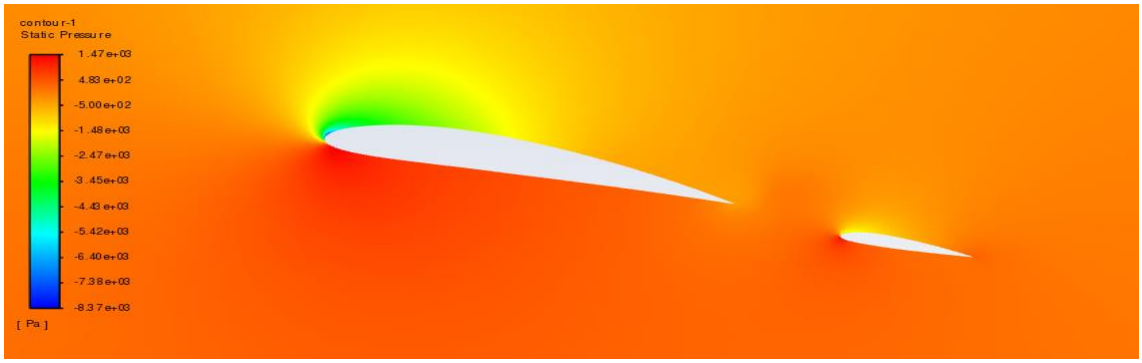

Figure 129. Pressure Contour Wing 12º Flap 12º.

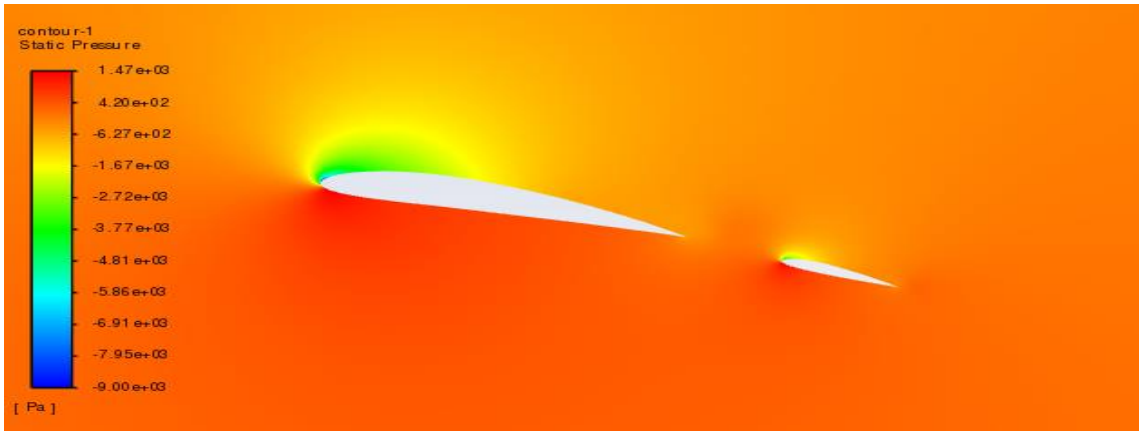

Figure 130. Pressure Contour Wing 12º Flap 18º.

Appendix 6. Modal Analysis Setup Steps.

- ***Step 1: Geometry Creation***.

The first step for performing a modal analysis consists of creating the desirable geometry that we need to analyze. In this case, we will be analyzing a wing geometry and a flap geometry. For creating these geometries, we need to extract the geometry points of our chosen profiles from airfoiltools database, once we extract these points, and create a .txt archive, we can import them into ANSYS Geometry as a 3D curve.

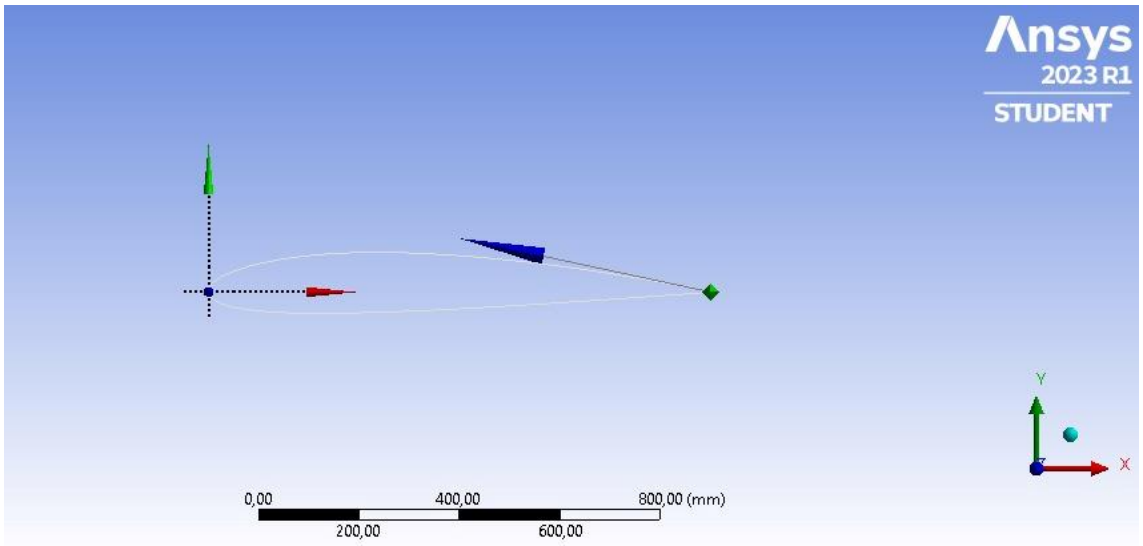

Figure 131. 3D Curve Profile Geometry (Wing)

Once the 3D curve is imported, then we need to create a surface from edges of the 3D curve, to add solid inside the wing geometry.

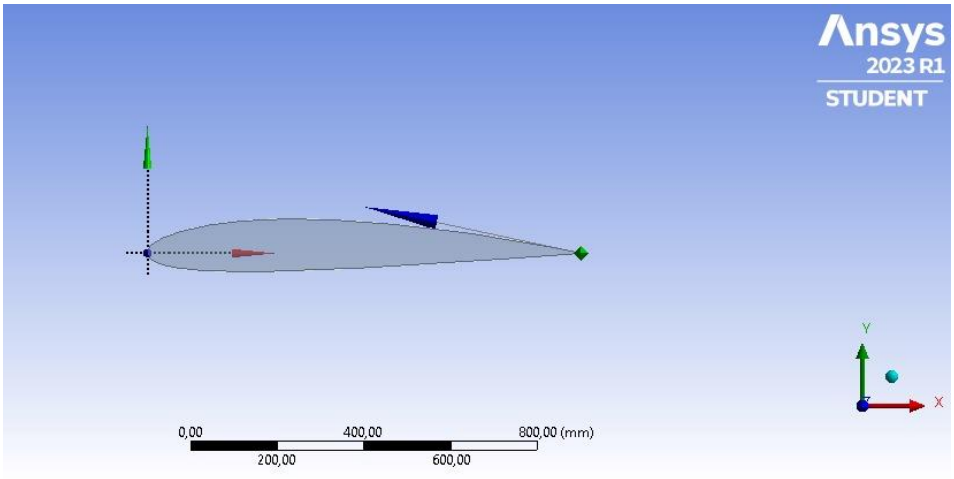

Figure 132. Surface from Edges Geometry (Wing)

Once the surface from edges is created, we have to create an extrude of these surfaces, in order to get the final geometry of the wing, in this case we will make a extrude depth of 5.5 m.

- ***Step 2: Geometry Meshing***.

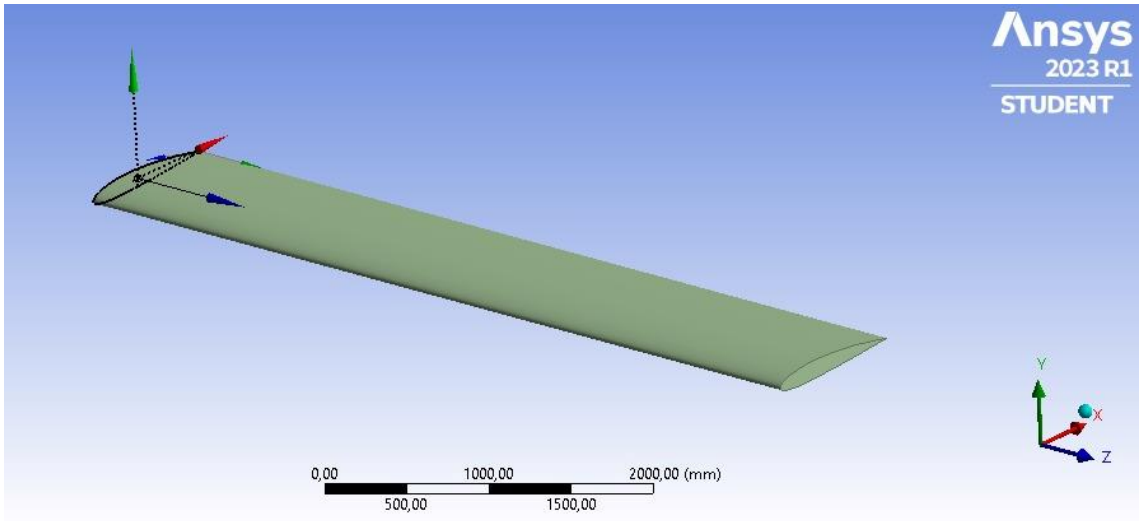

Figure 133. Wing Geometry

Once the wing geometry has been created, we need to mesh the geometry to obtain accurate results in the analysis, for meshing the geometry we will be using ANSYS Meshing, where we will be inserting an edge sizing in the root and tip of the geometry. This step is crucial since if the meshing is not done accurate, then, the results won't be accurate as well.

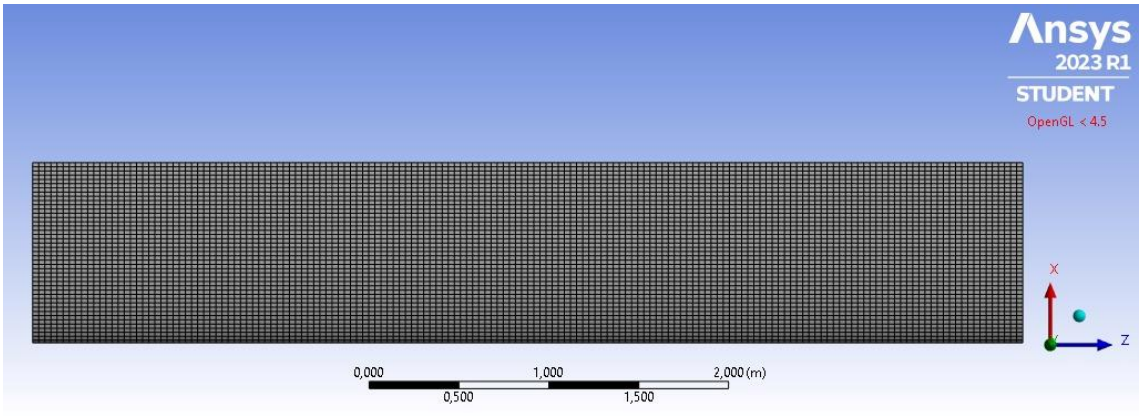

Figure 134. Meshing Geometry (Wing)

- ***Step 3: Analysis Setting Setup***.

Once we have meshed the geometry, we need to setup the analysis settings of the modal analysis, for it, we have to insert a fixed support on the root of the geometry, since this will simulate as if the wing is embedded to the fuselage. After inserting the fixed support, we have to setup the number of vibrational modes that we want ANSYS to analyze, in our case we setup to finding 12 vibrational modes.

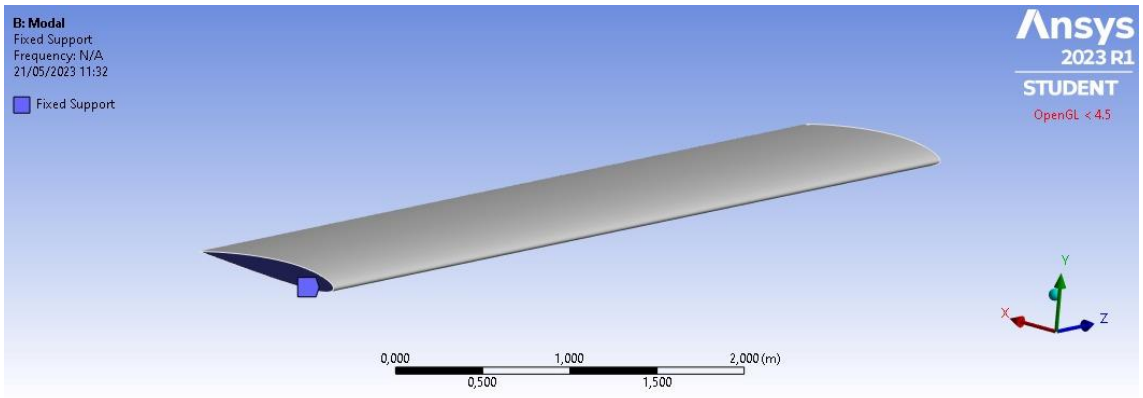

Figure 135. Fixed Support Wing Geometry

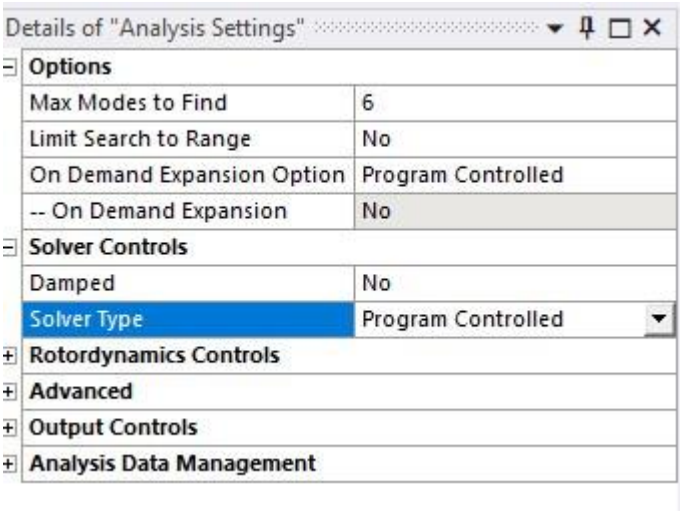

Figure 136. Analysis Setting Modal Analysis

All these steps shown are for creating the modal analysis of the wing, but for creating the modal analysis of the flap, it would be the same, but instead, in the step 1, we will be implementing the profile points of the flap, instead of the wing points profile. And, we will be adding fixed supports at the position of the junctions. Dividing the flap in sections parts at these positions of the junctions.

Appendix 7. Modal Analysis Mode Shapes Results.

Wing Mode Shapes.

- ***Vibrational Mode 1***

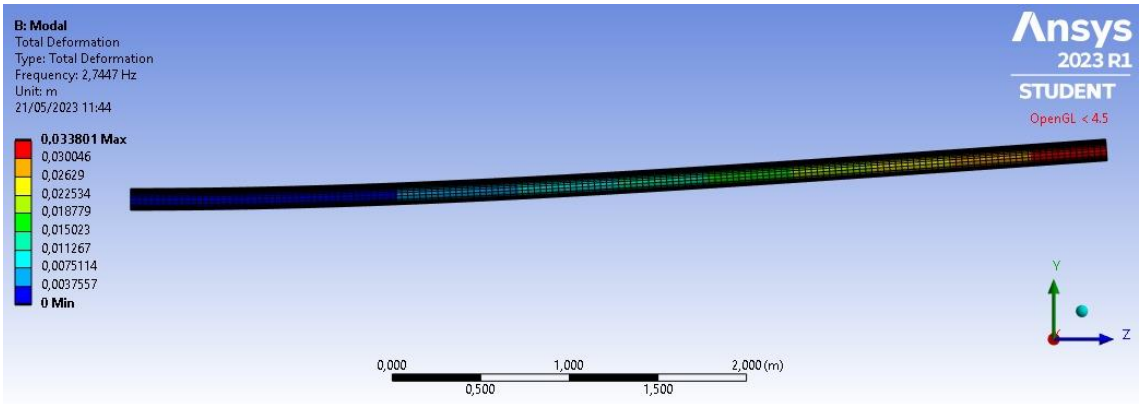

Figure 137. Wing Vibrational Mode 1

- ***Vibrational Mode 2.***

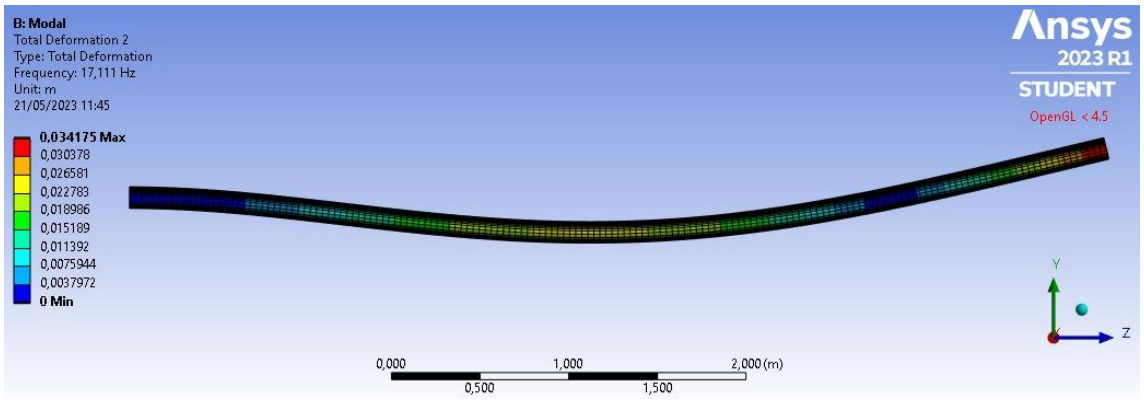

Figure 138. Wing Vibrational Mode 2

- ***Vibrational Mode 3.***

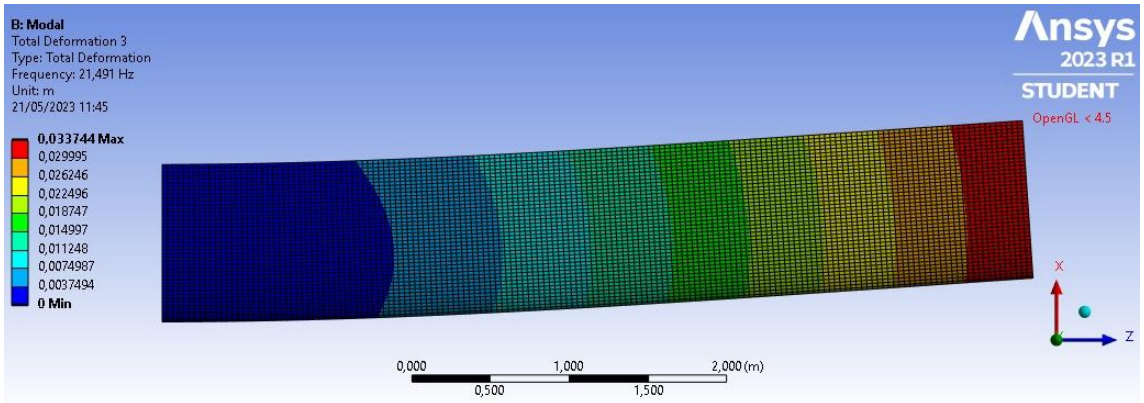

Figure 139. Wing Vibrational Mode 3

- ***Vibrational Mode 4.***

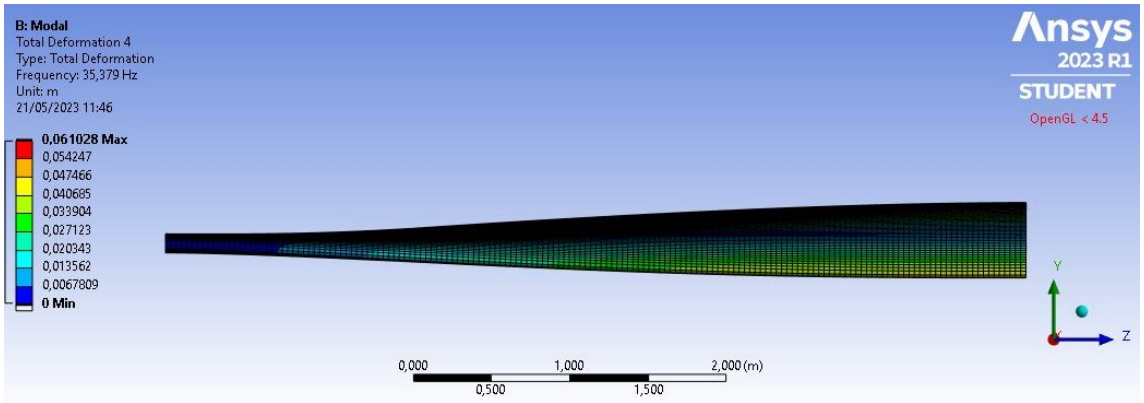

Figure 140. Wing Vibrational Mode 4

- ***Vibrational Mode 5.***

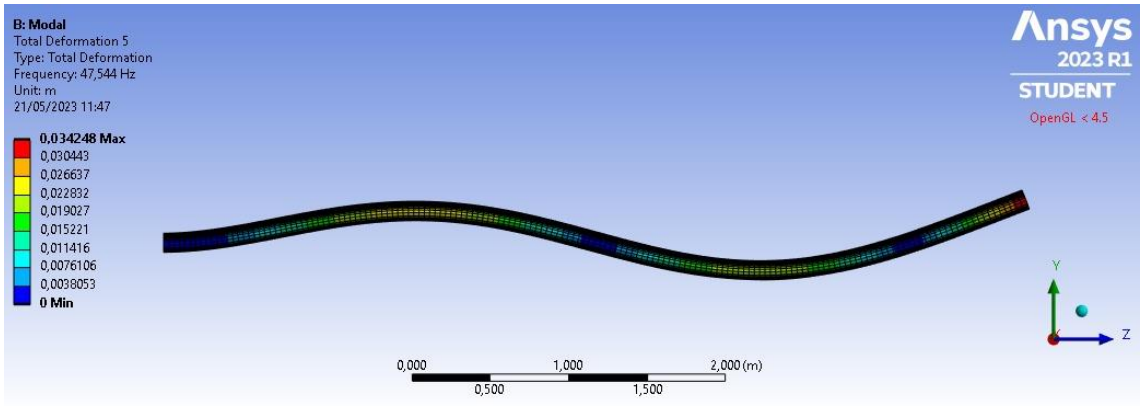

Figure 141. Wing Vibrational Mode 5

- ***Vibrational Mode 6.***

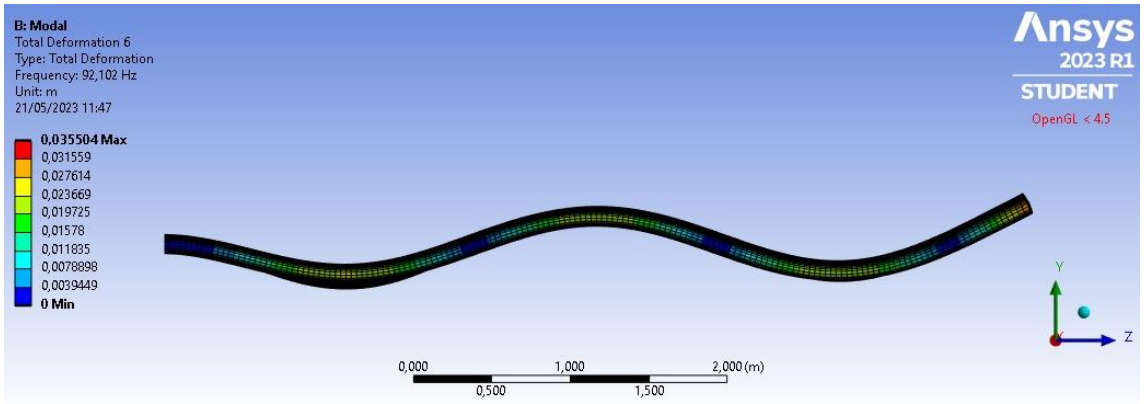

Figure 142. Wing Vibrational Mode 6

Junkers Flap Central Mode Shapes Results.

- ***Vibrational Mode 1.***

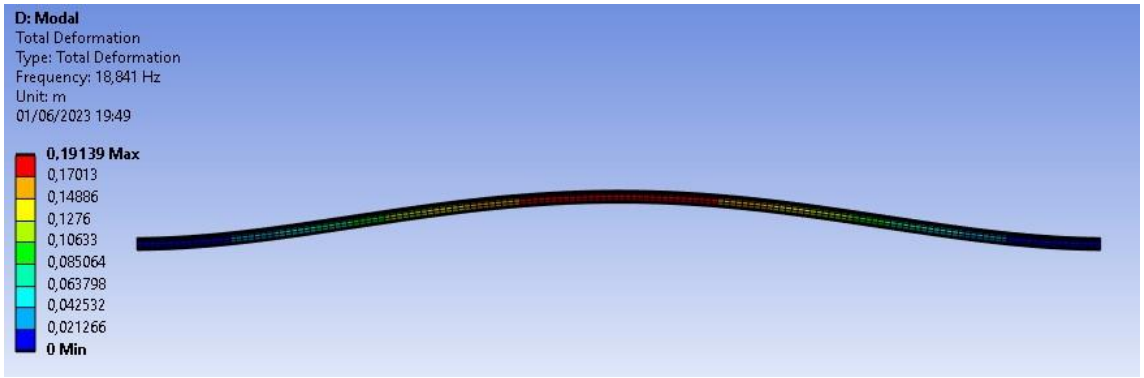

Figure 143. Vibrational Mode 1 Junkers Flap Central

- ***Vibrational Mode 2.***

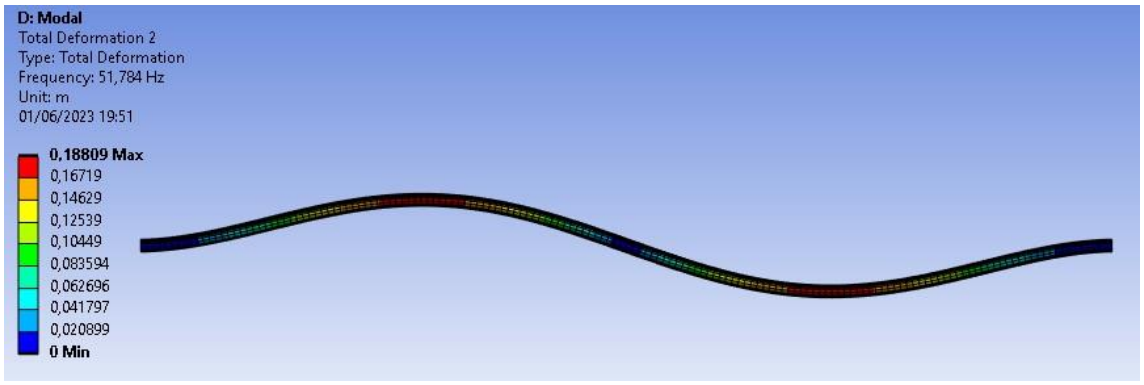

Figure 144. Vibrational Mode 2 Junkers Flap Central

- ***Vibrational Mode 3.***

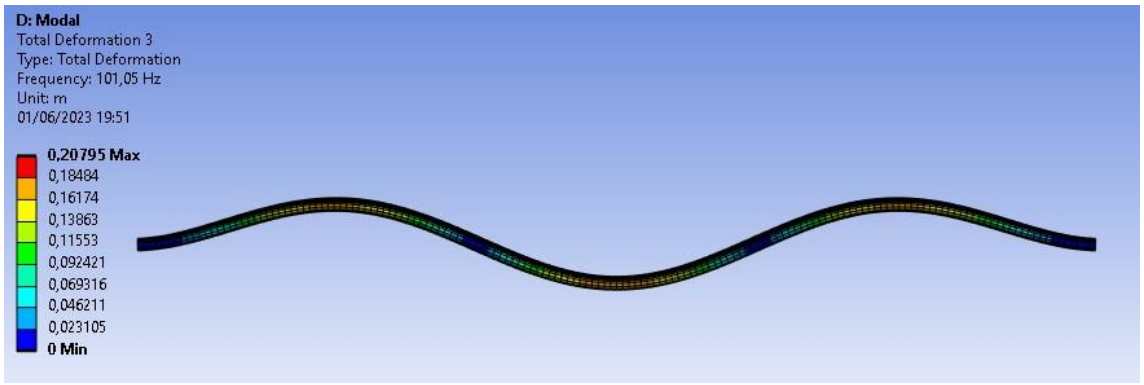

Figure 145. Vibrational Mode 3 Junkers Flap Central

- ***Vibrational Mode 4.***

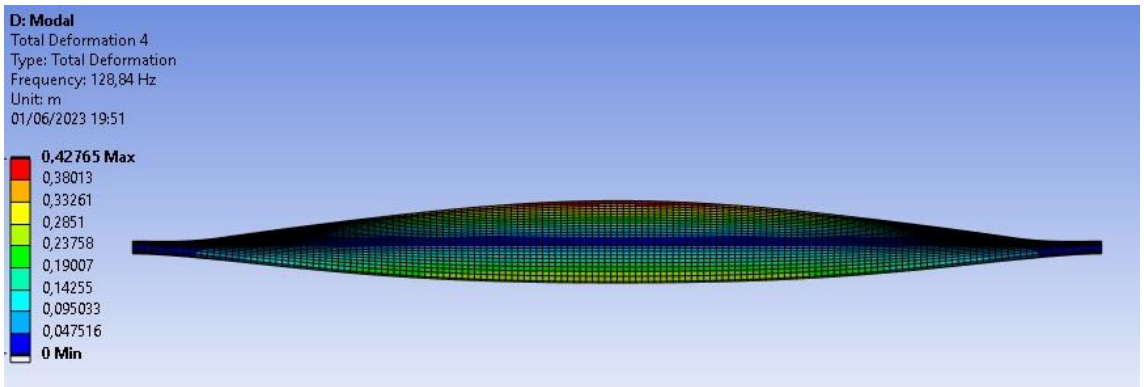

Figure 146. Vibrational Mode 4 Junker Flap Central

- ***Vibrational Mode 5.***

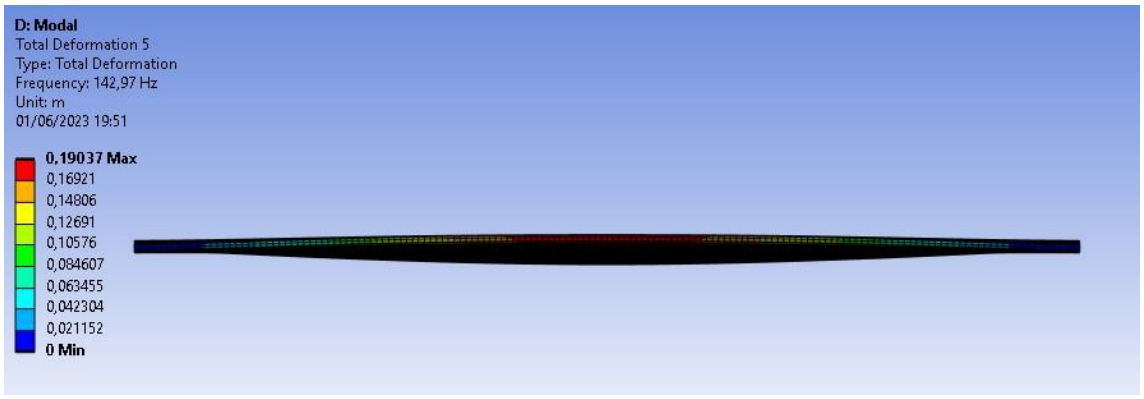

Figure 147. Vibrational Mode 5 Junkers Flap Central

- ***Vibrational Mode 6.***

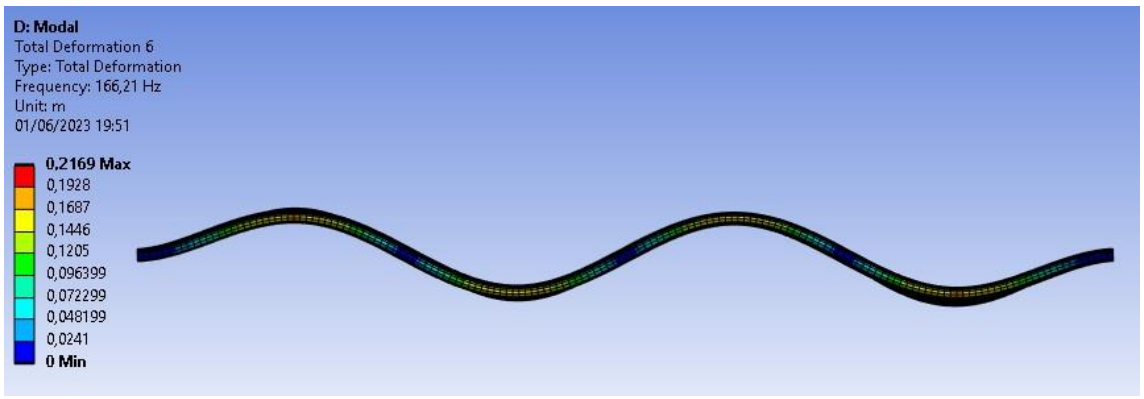

Figure 148. Vibrational Mode 6 Junkers Flap Central

Junkers Flap Lateral (without tip joints) Mode Shapes Results.

They are the same for the left and right Junkers flap.

- ***Vibrational Mode 1.***

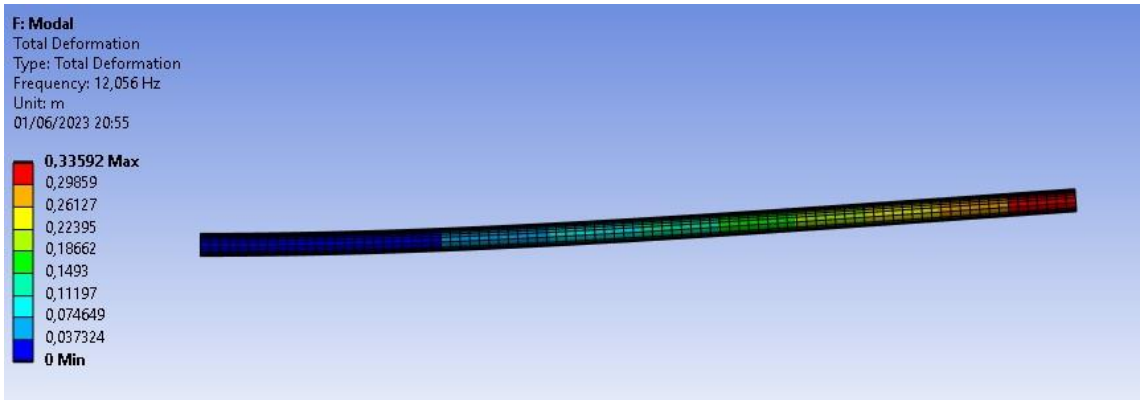

Figure 149. Vibrational Mode 1 Junkers Flap Lat. (W/o tip joints)

- ***Vibrational Mode 2.***

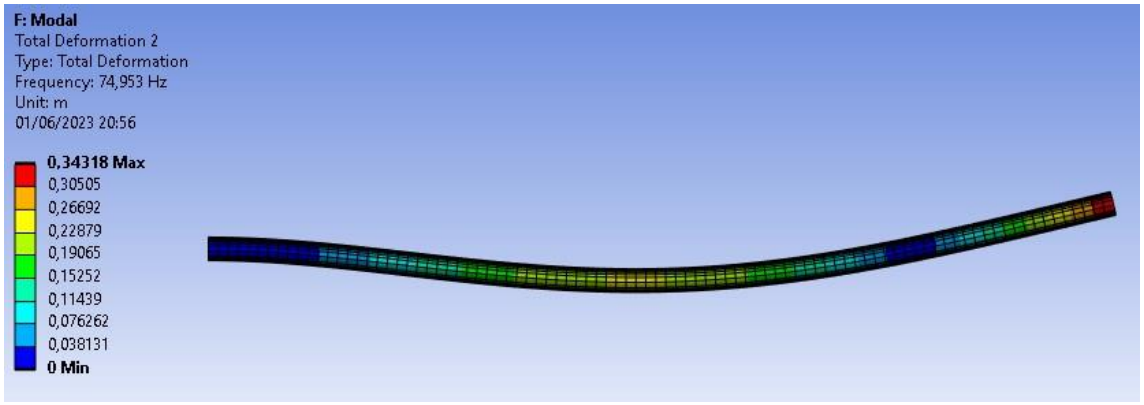

Figure 150. Vibrational Mode 2 Junker Flap Lat(W/o tip Joints)

- ***Vibrational Mode 3.***

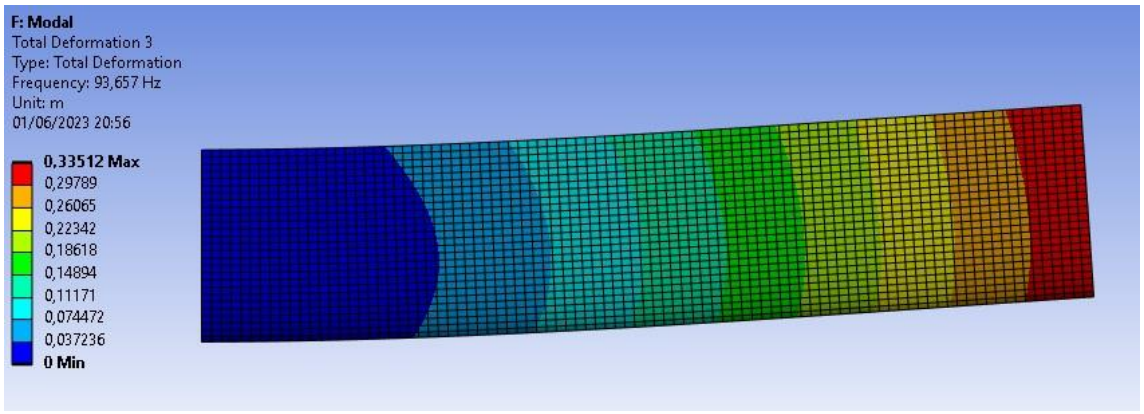

Figure 151. Vibrational Mode 3 Junkers Flap Lat. (W/o Tip Joints)

- ***Vibrational Mode 4.***

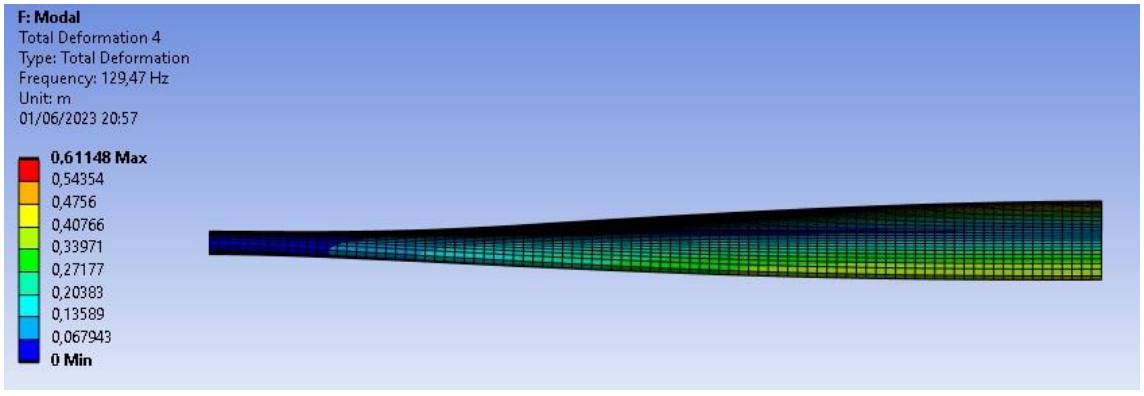

Figure 152. Vibrational Mode 4 Junkers Flap Lat (W/o Tip Joints)

- ***Vibrational Mode 5.***

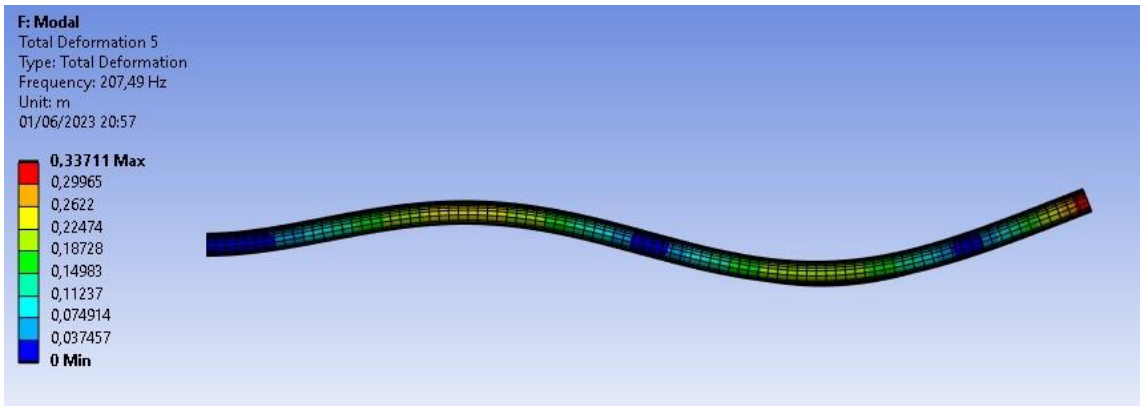

Figure 153. Vibrational Mode 5 Junkers Flap Lat (W/o Tip Joints)

- ***Vibrational Mode 6.***

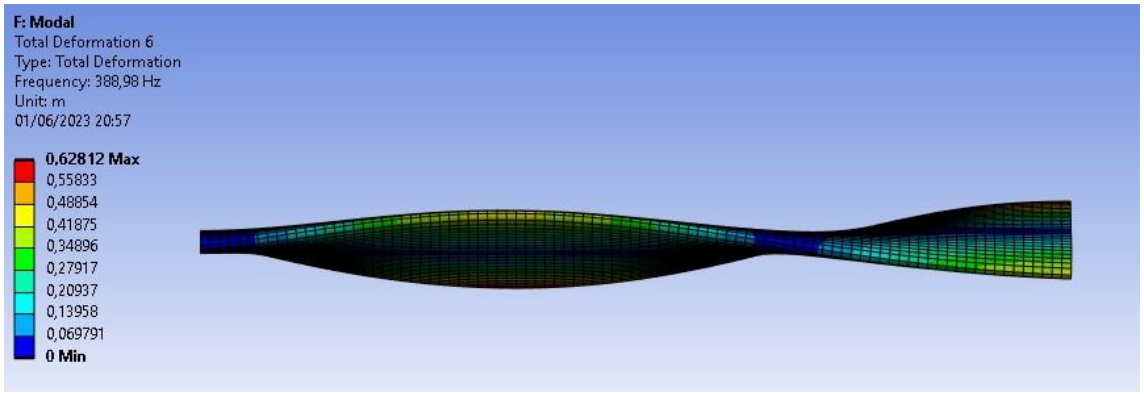

Figure 154. Vibrational Mode 6 Junkers Flap Lat. (W/o Tip Joints)

Junkers Flap Lateral (with tip joints) Mode Shapes Results.

They are the same for left and right Junkers flap.

- ***Vibrational Mode 1.***

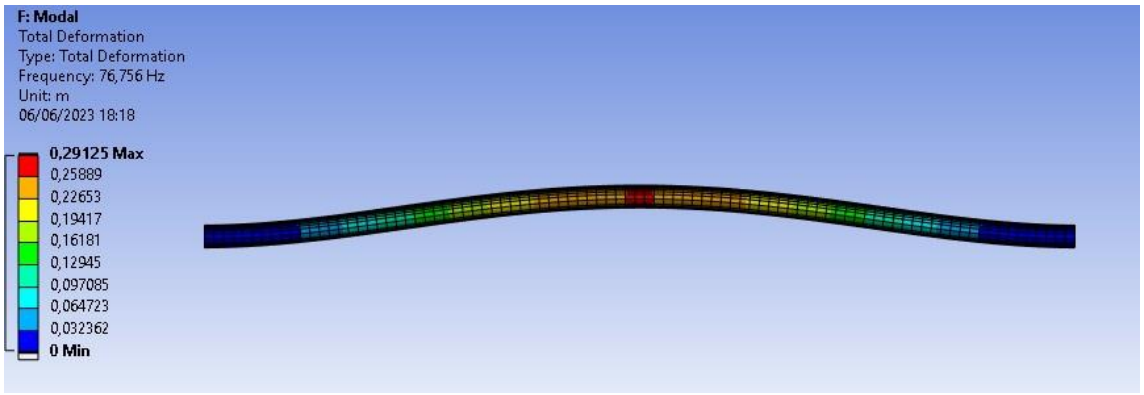

Figure 155. Vibrational Mode 1 Junkers Flap Lat (W/ Tip joints)

- ***Vibrational Mode 2.***

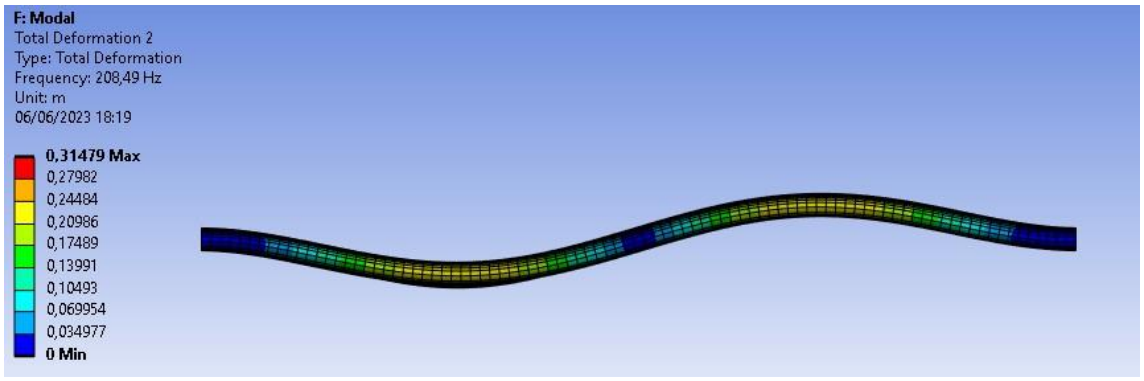

Figure 156. Vibrational Mode 2 Junkers Flap Lat (W/ Tip Joints)

- ***Vibrational Mode 3.***

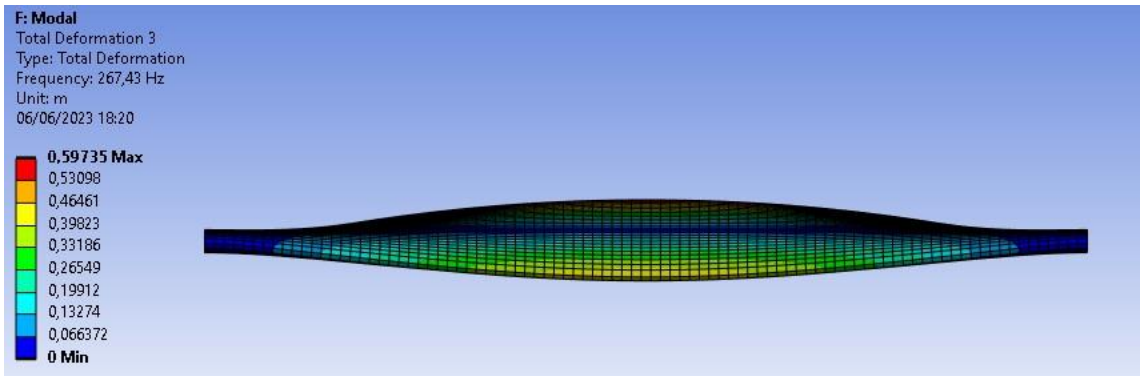

Figure 157. Vibrational Mode 3 Junker Flap Lat. (W/ Tip Joints)

- ***Vibrational Mode 4.***

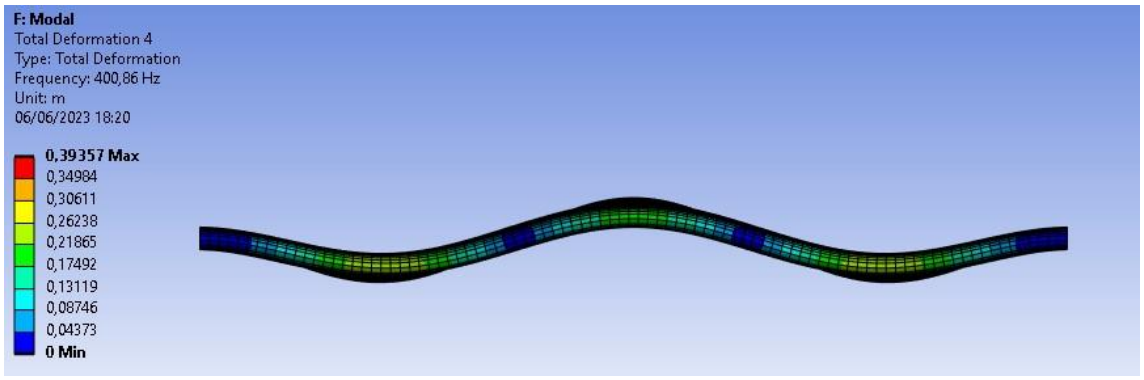

Figure 158. Vibrational Mode 4 Junkers Flap Lat. (W/ Tip Joints)

- ***Vibrational Mode 5.***

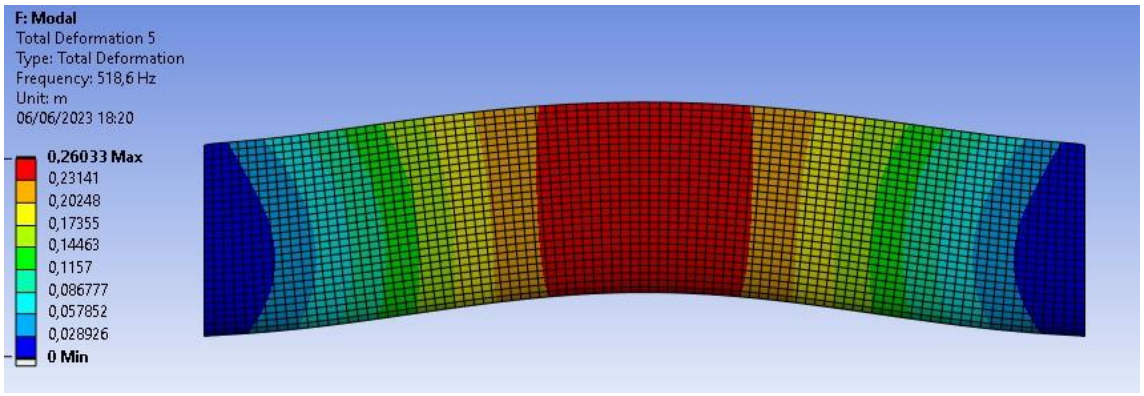

Figure 159. Vibrational Mode 5 Junkers Flap Lat (W/Tip Joints)

- ***Vibrational Mode 6.***

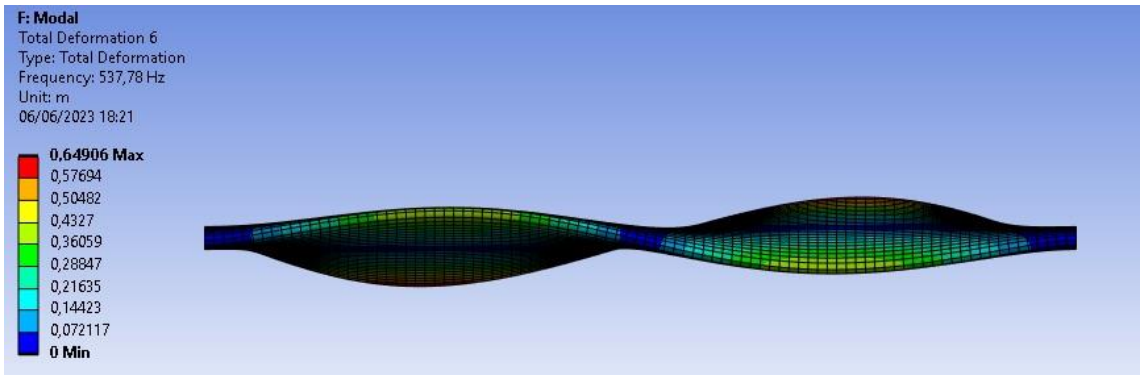

Figure 160. Vibrational Mode 6 Junkers Flap Lat (W/Tip Joints)

Appendix 8. Strouhal Number ANSYS Setup Steps.

- ***Step 1: Airfoils Importation Geometry.***

We import the wing and the flap Junkers airfoils, by using the airfoil points shown before.

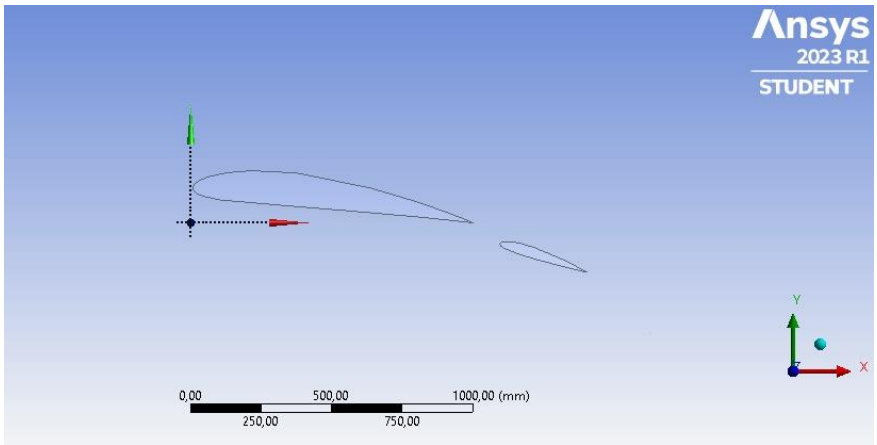

Figure 161. St Analysis Airfoil Importation

- ***Step 2: Surface Boundary Creation.***

For the surface boundary creation, we had to make a more large surface in order to let the vortex to form, and so to visualize them. Also, we include lines between the surface, which we will make a projection in order to better concentrate the mesh behind the geometries which is the place at which vortex will be more prone to occur.

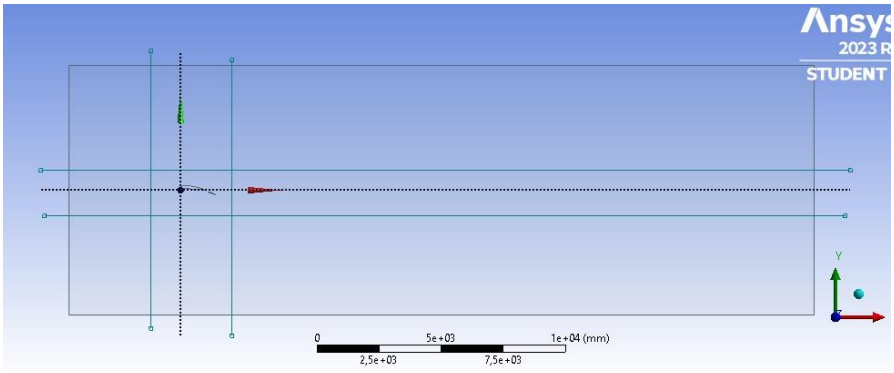

Figure 162. Surface Boundary St Analysi

- ***Meshing:***

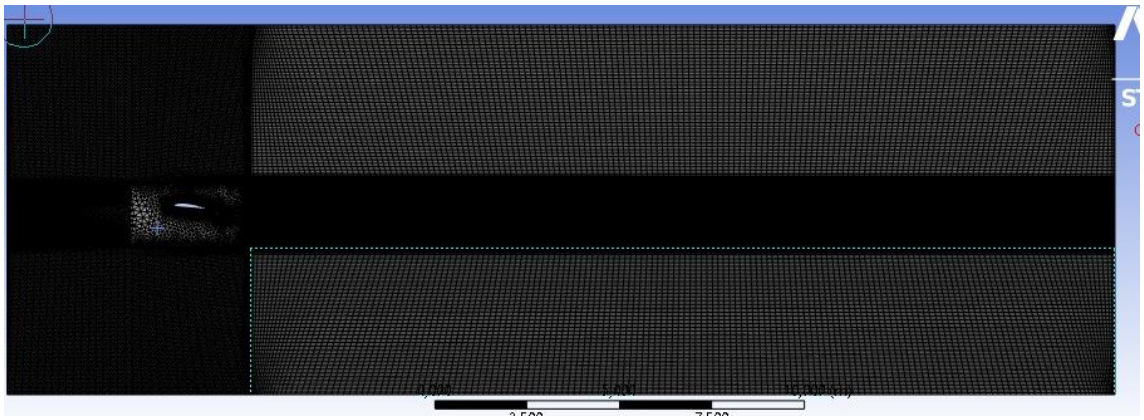

Figure 163. Geometry Meshing St Analysis.

- ***Analysis Settings Setup.***

Regarding the turbulence model used, I opted for the SST-SAS model, this decision was made based on previous analysis done in other projects. And a transient flow for the analysis [31]

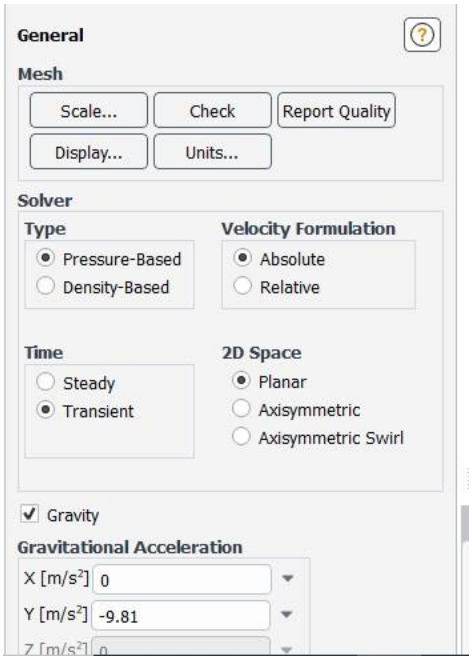

Figure 164. Settings Setup St Analysis

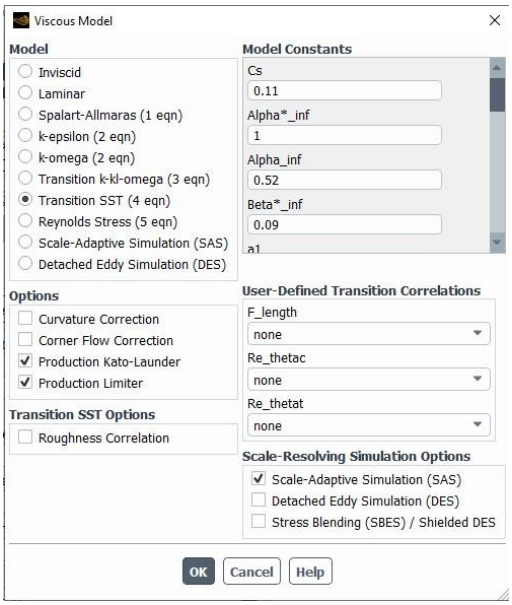

Figure 165. Viscous Model St Analysis

- ***Run Calculation Setup.***

For the calculation steps I decided to use a time step solver, in order to obtain data at short period of times. We used the following equations to approximate the time steps. $Time\ Step\ Size = \frac{T}{20}$ and $Number\ of\ Time\ Steps = \frac{Total\ Analysis\ Time}{Time\ Step\ Size}$ The setup decided is the following.

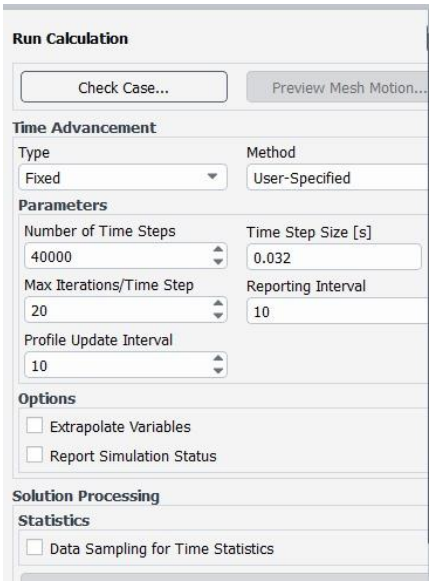

Figure 166. Calculation Setup St Analysis

- ***Strouhal Number Calculation.***

For obtaining the Strouhal number value, we make use of the Fast Fourier Transformation (FFT) that Ansys provides us. For obtaining it we have to insert the velocity values obtained from the probe location, from an external file into the FFT. But values and contours obtained were not coherent at all.

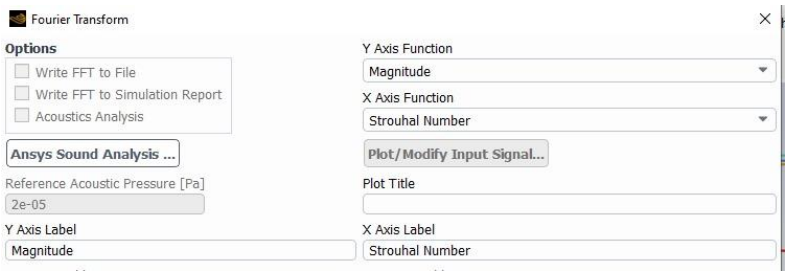

Figure 167. Strouhal Number Calculation

Appendix 9. Strouhal Number vs Reynolds Number.

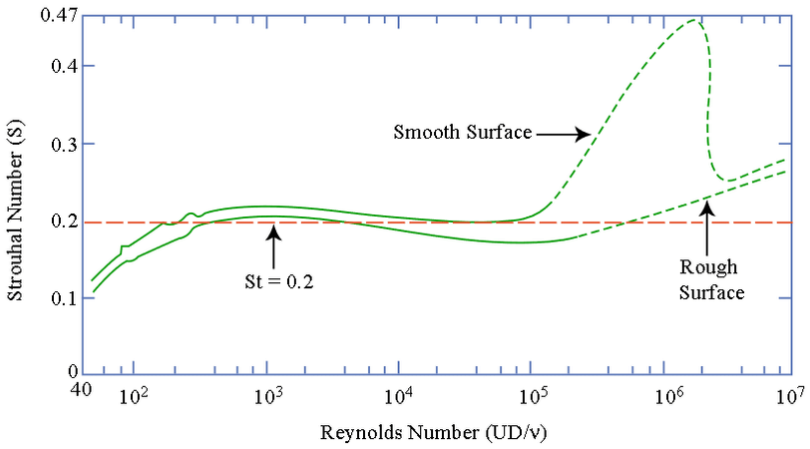

Figure 168. Strouhal Number vs Reynolds Number

Appendix 10. Material Properties.

The material used for the analysis was aluminum alloy with the following properties.

Properties of Outline Row 3: Aluminum Alloy

	A	B	C	D	E
1	Property	Value	Unit		
2	Material Field Variables	Table			
3	Density	2770	kg m^-3		
4	Isotropic Secant Coefficient of Thermal Expansion				
6	Isotropic Elasticity				
12	S-N Curve	Tabular			
16	Tensile Yield Strength	2,8E+08	Pa		
17	Compressive Yield Strength	2,8E+08	Pa		
18	Tensile Ultimate Strength	3,1E+08	Pa		
19	Compressive Ultimate Strength	0	Pa		
20	Isotropic Thermal Conductivity	Tabular			
23	Specific Heat Constant Pressure, C_p	875	J kg^-1 C^-1		
24	Isotropic Relative Permeability	1			
25	Isotropic Resistivity	Tabular			

Figure 169. Aluminum Alloy, Material Properties.

REFERENCES

[1] A: Properties of standard atmosphere. (2007). In *Aircraft Performance* (pp. 258–259). John Wiley & Sons, Inc. Retrieved June 5, 2023, from http://www.braeunig.us/space/atmos.htm

[2] ANSYS FLUENT 12.0 Theory Guide - 4.10 Detached Eddy Simulation (DES). (n.d.). Retrieved June 5, 2023, from Enea.It. https://www.afs.enea.it/project/neptunius/docs/fluent/html/th/node88.htm

[3] Chai, Y., Gao, W., Ankay, B., Li, F., & Zhang, C. (2021). Aeroelastic analysis and flutter control of wings and panels: A review. *International Journal of Mechanical System Dynamics*, *1*(1), 5–34. Retrieved June 5, 2023, from https://doi.org/10.1002/msd2.12015

[4] Cooper, J. E. (2001). AEROELASTIC RESPONSE. In *Encyclopedia of Vibration* (pp. 87–97). Elsevier. Retrieved June 5, 2023, from https://www.sciencedirect.com/topics/physics-and-astronomy/karman-vortex-street

[5] El-Reedy, M. A. (2012). Offshore Structure Platform Design. In *Offshore Structures* (pp. 93–211). Elsevier Retrieved June 5, 2023, from https://www.sciencedirect.com/topics/engineering/strouhal-number

[6] Harish, A. (2016, December 14). *What is modal analysis and why is it necessary?* Retrieved June 5, 2023, from SimScale. https://www.simscale.com/blog/what-is-modal-analysis/

[7] Here's how leading edge slats get you off the ground. (n.d.). Retrieved June 5, 2023, from Boldmethod.com. https://www.boldmethod.com/learn-to-fly/aircraft-systems/here-is-how-leading-edge-slats-work-to-get-you-off-the-ground/

[8] High lift devices. (n.d.). Retrieved June 5, 2023, from Skybrary.Aero. https://www.skybrary.aero/articles/high-lift-devices

[9] How the 4 types of aircraft flaps work. (n.d.). Retrieved June 5, 2023, from Boldmethod.com https://www.boldmethod.com/learn-to-fly/aircraft-systems/how-the-4-types-of-aircraft-flaps-work/

[10] Johnston, M. (2019, August 16). *Wing flaps: How do they function and what is their purpose?* CAU; CAU California Aeronautical University. Retrieved June 5, 2023, from https://calaero.edu/wing-flaps-function-and-purpose/

[11] NACA 4 digit airfoil generator (NACA 2312 AIRFOIL). (n.d.). Retrieved June 5, 2023, from Airfoiltools.com http://airfoiltools.com/airfoil/naca4digit?MNaca4DigitForm%5Bcamber%5D=2&MNaca4DigitForm%5Bposition%5D=30&MNaca4DigitForm%5Bthick%5D=12&MNaca4DigitForm%5BnumPoints%5D=81&MNaca4DigitForm%5BcosSpace%5D=0&MNaca4DigitForm%5BcosSpace%5D=1&MNaca4DigitForm%5BcloseTe%5D=0

[12] NACA 4 digit airfoil generator (NACA 4412 AIRFOIL). (n.d.). Retrieved June 5, 2023, from Airfoiltools.com http://airfoiltools.com/airfoil/naca4digit?MNaca4DigitForm%5Bcamber%5D=4&MNaca4D

[13] Navier-Stokes equation for 3D compressible and incompressible flows. (n.d.). Retrieved June 7, 2023, from Blogspot.com http://petersengineering.blogspot.com/2015/06/navier-stokes-equation-for-3d.html

[14] No title. (n.d.). Retrieved June 5, 2023, from Baesystems.com https://www.baesystems.com/en/heritage/vickers-viscount

[15] (N.d.). Retrieved June 5, 2023, from Researchgate.net https://www.researchgate.net/publication/236678225_A_Retrospective_of_High-Lift_Device_Technology

[16] (N.d.). Retrieved June 5, 2023, from Researchgate.net https://www.researchgate.net/publication/336769980_Non-synchronous_vibration_in_axial_compressors_Lock-in_mechanism_and_semi-analytical_model

[17] (N.d.-b). Retrieved June 5, 2023, from Researchgate.net https://www.researchgate.net/publication/344016445_Heritability_of_haemodynamics_in_the_ascending_aorta

[18] (N.d.-c). Retrieved June 5, 2023, from Researchgate.net https://www.researchgate.net/publication/361581023_Evaluation_of_CFD_URANS_Turbulence_Models_for_the_Building_under_Environmental_Wind_Flow_with_Experimental_Validation

[19]Researchgate.net. Retrieved June 5, 2023, from https://www.researchgate.net/publication/322836602_Investigation_of_vortex_shedding_from_an_airfoil_by_CFD_simulation_and_computer-aided_flow_visualization

[20] Sirohi, J. (2021). Wind energy harvesting using piezoelectric materials. In *Ferroelectric Materials for Energy Harvesting and Storage* (pp. 187–207). Elsevier. Retrieved June 5, 2023, from https://www.sciencedirect.com/topics/materials-science/vortex-induced-vibration

[21] The Junkers flap: Lesser known flap designs. (n.d.). Retrieved June 5, 2023, from Boldmethod.com https://www.boldmethod.com/learn-to-fly/aircraft-systems/junkers-flap/

[22] Travelaviation [@travelaviation494]. (2022, October 7). *Karman Vortex street behind an airfoil (NACA 4412)*. Retrieved June 5, 2023, from Youtube. https://www.youtube.com/watch?v=axYlsPxkMrw

[23] Turbulence models in CFD. (2019, August 30). Retrieved June 5, 2023, from IdealSimulations. https://www.idealsimulations.com/resources/turbulence-models-in-cfd/

[24] Vortex-Induced Vibration (VIV). (2022). In *Encyclopedia of Ocean Engineering* (pp. 2111–2111). Springer Nature Singapore. Retrieved June 5, 2023, from https://uwaterloo.ca/computational-fluid-dynamics-turbulence-modeling-laboratory/research/vortex-induced-vibration-viv

[25] Wang, W., Mao, Z., Tian, W., & Zhang, T. (2019). Numerical investigation on vortex-induced vibration suppression of a circular cylinder with axial-slats. *Journal of Marine Science and Engineering*, *7*(12), 454. Retrieved June 5, 2023, from https://doi.org/10.3390/jmse7120454

[26] Wikipedia contributors. (2022, September 13). *Blown flap*. Retrieved June 5, 2023, from Wikipedia, The Free Encyclopedia. https://en.wikipedia.org/w/index.php?title=Blown_flap&oldid=1110017512

[27] Wikipedia contributors. (2023, April 11). *Aeroelasticity*. Retrieved June 5, 2023, from Wikipedia, The Free Encyclopedia. https://en.wikipedia.org/w/index.php?title=Aeroelasticity&oldid=1149292169

[28] Wikipedia contributors. (2023, March 19). *High-lift device*. Retrieved June 5, 2023, from Wikipedia, The Free Encyclopedia. https://en.wikipedia.org/w/index.php?title=High-lift_device&oldid=1145555662

[29] Wikipedia contributors. (2023a, February 23). *Krueger flap*. Retrieved June 5, 2023, from Wikipedia, The Free Encyclopedia. https://en.wikipedia.org/w/index.php?title=Krueger_flap&oldid=1141180820

[30] Wikipedia contributors. (2023b, June 2). *Kármán vortex street*. Retrieved June 5, 2023, from Wikipedia, The Free Encyclopedia. https://en.wikipedia.org/w/index.php?title=K%C3%A1rm%C3%A1n_vortex_street&oldid=1158134582

[31] Wikipedia contributors. (2023b, May 23). *Computational fluid dynamics*. Retrieved June 5, 2023, from Wikipedia, The Free Encyclopedia. https://en.wikipedia.org/w/index.php?title=Computational_fluid_dynamics&oldid=1156572754

[32] Yuhui, Y., & Yufei, Z. (2020). Optimization and analysis of a blown flap based on a multielement airfoil. *Journal of Aircraft*, *57*(1), 62–75. Retrieved June 5, 2023, from https://doi.org/10.2514/1.c035514